

AD-A121 287

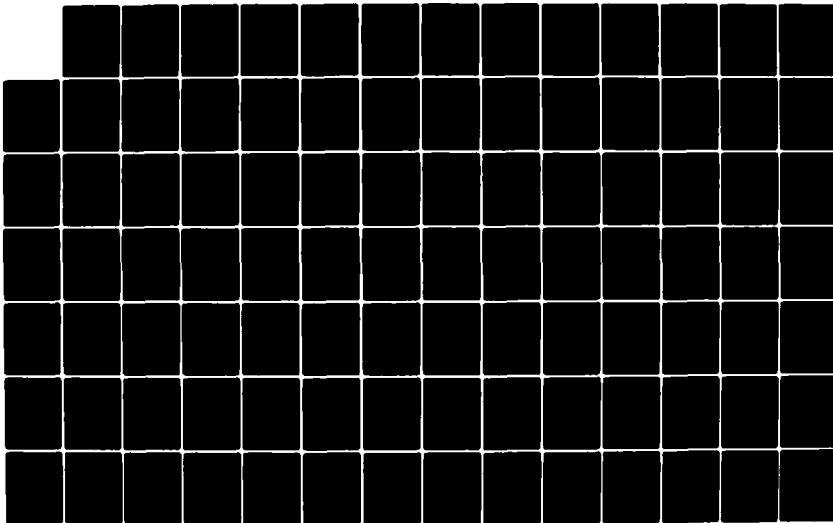
STUDY OF 1/F NOISE IN SOLIDS(U) FLORIDA UNIV
GAINESVILLE DEPT OF ELECTRICAL ENGINEERING
C M VAN VLIET ET AL. JUN 82 AFOSR-TR-82-0958

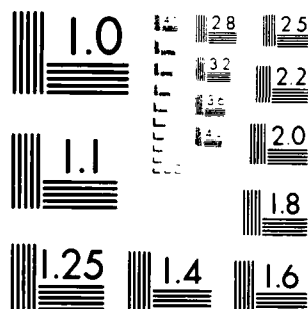
1/2

UNCLASSIFIED

F/G 9/4

NL





MICROCOPY RESOLUTION TEST CHART
NATIONAL BUREAU OF STANDARDS-1963-A

AFOSR-TR- 82 - 0958

12

STUDY OF 1/f NOISE IN SOLIDS

Final Report

to the

Air Force Office of Scientific Research
Bolling Air Force Base, Washington, D.C. 20332

Grant No. AFOSR 80-0050

Period Covered: June 1, 1981 - May 31, 1982

Submitted by

Carel M. van Vliet, Professor and Principal Investigator
E.R. Chenette, Professor and Co-Investigator
G. Bosman, Asst. Professor and Co-Investigator

Department of Electrical Engineering
University of Florida
Gainesville, Florida, 32611

DTIC
ELECTE
NOV 12 1982
S D E

June, 1982

Approved for public release;
distribution unlimited.

AD A121287

FILE COPY

UNCLASSIFIED

SECURITY CLASSIFICATION OF THIS PAGE (When Data Entered)

REPORT DOCUMENTATION PAGE		READ INSTRUCTIONS BEFORE COMPLETING FORM
1. REPORT NUMBER AFOSR-TR-82-0958	2. GOVT ACCESSION NO.	3. RECIPIENT'S CATALOG NUMBER
4. TITLE (and Subtitle) Study of 1/f Noise in Solids		5. TYPE OF REPORT & PERIOD COVERED Final June 1, 1981 - May 31, 1982
		6. PERFORMING ORG. REPORT NUMBER
7. AUTHOR(s) Carel M. van Vliet, Principal Investigator Eugene R. Chenette, Co-Investigator Gijs Bosman, Co-Investigator		8. CONTRACT OR GRANT NUMBER(s) AFOSR 80-0050
9. PERFORMING ORGANIZATION NAME AND ADDRESS Department of Electrical Engineering University of Florida Gainesville, FL 32611		10. PROGRAM ELEMENT, PROJECT, TASK AREA & WORK UNIT NUMBERS 61102F 2305/C1
11. CONTROLLING OFFICE NAME AND ADDRESS Air Force Office of Scientific Research Bolling Air Force Base Washington, D.C. 20332		12. REPORT DATE June, 1982
		13. NUMBER OF PAGES 125
14. MONITORING AGENCY NAME & ADDRESS (if different from Controlling Office) Same as #11.		15. SECURITY CLASS. (of this report) Unclassified
		15a. DECLASSIFICATION/DOWNGRADING SCHEDULE
16. DISTRIBUTION STATEMENT (of this Report) Approved for public release; distribution unlimited.		
17. DISTRIBUTION STATEMENT (of the abstract entered in Block 20, if different from Report) See #16.		
18. SUPPLEMENTARY NOTES		
19. KEY WORDS (Continue on reverse side if necessary and identify by block number) Noise, fluctuations, submicron devices, α -particle counting, gallium arsenide structures		
20. ABSTRACT (Continue on reverse side if necessary and identify by block number) This report is divided into four main parts. In Part A we begin with some introductory remarks on 1/f noise and the impact of the contributions performed during the present grant period. Next we give a survey of 1/f noise theory as it stands today, together with the experimental evidence for the various models. (over)		

DD FORM 1 JAN 73 1473

EDITION OF 1 NOV 65 IS OBSOLETE
S/N 0102-014-6601

UNCLASSIFIED

SECURITY CLASSIFICATION OF THIS PAGE (When Data Entered)

UNCLASSIFIED

SECURITY CLASSIFICATION OF THIS PAGE(When Data Entered)

20. Abstract (Cont'd)

In Part B the experimental work performed under the grant is described. This entails the work on gold films, transistor noise source identification, α -particle counting experiments, and noise in n^+n^+ and n^+pn^+ near-ballistic diodes. The noise in these structures is very low, indicating definitely that mobility fluctuations are at the origin of $1/f$ noise.

In Part C we describe various theoretical contributions of work performed under the grant. In particular, the Allan variance transform theorem throws a new light on the existence of spectra of the form $1/f^\alpha$, $-1 < \alpha < 3$.

UNCLASSIFIED

SECURITY CLASSIFICATION OF THIS PAGE(When Data Entered)

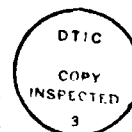
Abstract

This progress report is divided into four main parts. In Part A we begin with some introductory remarks on $1/f$ noise and the impact of the contributions performed during the present grant period. Next we give a survey of $1/f$ noise theory as it stands today, together with the experimental evidence for the various models.

In Part B the experimental work performed under the grant is described. This entails the work on gold films, transistor noise source identification, α -particle counting experiments, and noise in n^+nn^+ and n^+pn^+ near-ballistic diodes. The noise in these structures is very low, indicating definitely that mobility fluctuations are at the origin of $1/f$ noise.

In Part C we describe various theoretical contributions of work performed under the grant. In particular, the Allan variance transform theorem throws a new light on the existence of spectra of the form $1/f^\alpha$, $-1 < \alpha < 3$.

Accession For	
NTIS GRA&I	<input checked="" type="checkbox"/>
DTIC TAB	<input type="checkbox"/>
Unannounced	<input type="checkbox"/>
Justification	
By	
Distribution/	
Availability Codes	
Dist	Avail and/or Special
A	





AIR FORCE OFFICE OF SCIENTIFIC RESEARCH (AFSC)
 NOTICE OF TRANSMITTAL TO DTIC
 This technical report has been reviewed and is
 approved for public release IAW AFR 190-12.
 Distribution is unlimited.
 MATTHEW J. KERPER
 Chief, Technical Information Division

Table of Contents

	<u>Page</u>
Abstract	2
List of Figures	4
A. Introduction	
I. Summary	6
II. Survey of 1/f Noise	8
B. Experimental Work	
I. Gold Films Project (J. Kilmer)	32
II. Presence of Mobility-Fluctuation 1/f Noise Identified in P ⁺ NP Transistors (J. Kilmer, A. van der Ziel, and G. Bosman)	34
III. High Frequency Amplifier and Noise Diode (J. Andrian)	44
IV. 1/f Fluctuations in Radioactive Decay (Jeng Gong)	44
V. Noise in Near-Ballistic n ⁺ nn ⁺ and n ⁺ pn ⁺ Gallium Arsenide Submicron Diodes (R.R. Schmidt, G. Bosman, C.M. van Vliet, L.F. Eastman, and M. Hollis)	47
C. Theory Developed under the Grant	
I. Proposed Discrimination between 1/f Noise Sources in in Transistors (A. van der Ziel)	59
II. On Mobility Fluctuations in 1/f Noise (C.M. van Vliet and R.J.J. Zijlstra)	66
III. Mobility Fluctuation 1/f Noise in Nonuniform Nonlinear Samples and in Mesa Structures (A. van der Ziel and C.M. van Vliet)	70
IV. A New Transform Theorem for Stochastic Processes with Special Application to Counting Statistics (C.M. van Vliet and P.H. Handel)	73
D. Papers Published under grant	91
E. Figures	93

List of Figures

1. Thin gold film resistor configuration.
2. Equivalent common base circuit with noise sources.
3. Equivalent common base circuit.
4. Circuit with high source impedance.
5. Measurement of high-source impedance spectra (S_{HR_s}) and low-source impedance spectra (S_{LR_s}). The base currents are 6 μ A, 3 μ A, 1 μ A.
6. Circuit for low-source impedance data.
7. High-frequency preamplifier.
8. a) One stage of the amplifier
b) Output stage
9. Standard noise source.
10. Block diagram of the counting system.
11. α -decay counting: $R(T)$ vs. $1/T$ (here $R(T)$ is relative Allan variance, T is counting time).
12. $R(T)$ vs. N , where N is the number of samples of duration T .
 $T = 100$ minutes.
13. $R(T)$ vs. N ; $T = 1$ minute.
14. $R(T)$ vs. N ; $T = 3$ minutes.
15. Averaged $R(T)$ vs. $1/T$. The straight line is Poissonian noise; the deviation is due to $1/f$ noise.
16. The variance ($\sigma_{M_T}^2$) and the Allan variance ($\sigma_{M_T}^{A^2}$) vs. T .
17. P-type near-ballistic mesa structure.
18. Equivalent circuit of n^+nn^+ structure, showing parasitic elements.
19. Correlation measurement setup.
20. I-V characteristic n^+nn^+ device.
21. A.C. resistance of n^+nn^+ device versus frequency.

22. I-V characteristic of $n^+ p n^+$ device.
23. Noise spectra for $n^+ n n^+$ device.
24. Thermal (-like) noise for $n^+ n n^+$ device.
25. Plot of thermal (-like) noise of $n^+ n n^+$ diode versus diode current.
26. $1/f$ noise of $n^+ n n^+$ diode versus current.
27. Noise spectra for $n^+ p n^+$ device
28. Noise at 100 hz of $n^+ p n^+$ device versus current. (The ** points are obtained from  and  points if the abscissa denotes only the punch-through current.)
29. a) Current flow in a $p-n-p$ transistor.
b) Equivalent circuit for the fluctuating current generators.
30. Plumb-Chenette schematics for discriminating between i_{f1} and i_{f2} .
31. Splitting $\overline{v^2}$ into component parts representing the effects of i_{f1} , i_{f2} and of shot and thermal noise.
32. Contour integration for inverse Mellin transforms. Shaded area is domain of analyticity for the transformed equation (4.7).
Case $\tau_o < \sigma_o$.
33. Contour integration for inverse Mellin transform. Shaded area is area of existence for $\phi(p)$. Case $\sigma_o < \tau_o$.

A. INTRODUCTION

I. Summary

Research on $1/f$ noise covers a period of 55 years. In that time many theories and models have been put forward to explain this enigmatic phenomenon. We believe that the following types of noise theory have survived:

1. The universal theories
2. Transport theories
3. Specific noise model theories
4. The van der Ziel-Bernamont-du Pre-McWhorter theories; distribution of time constants.
5. The mobility-fluctuation bulk model: phonon effects.
6. The mobility-fluctuation bulk model: quantum $1/f$ noise (Handel)

Under the Air Force grant we have performed both experimental and theoretical work to try to really get at the origin of the $1/f$ noise. Mr. Kilmer's experiments on films are designed to confirm or reject theories of type 2. Most indications to date are, however, pointing in the direction of models 5 and 6. In this report we discuss Kilmer's experiments in transistors, which definitively show that the noise, both of collector and base sources, is due to mobility fluctuations. The older findings, which supported surface effects (theory 4) seem no longer applicable in modern devices. Mr. Schmidt's measurements on near-ballistic gallium arsenide mesa diodes also strongly point to the validity of the mobility-fluctuation model 5 or 6. Further evidence for this is being gathered by Mr. Andrian, who will consider the noise as a function of ratio d/ℓ , where d is the thickness of the structure and ℓ the phonon mean free path. Finally, Mr. Jeng Gong's experiments indicate that Handel's theory (model 6) might explain $1/f$ fluctuations in radioactive

decay. We believe, therefore, that great progress has been made during this grant period to identify the cause of $1/f$ noise in devices and in entirely different phenomena, like α -particle emission.

The various experiments are described in part B. Finally, the extensive theoretical analyses which have been made in conjunction with the experiments are described in part C.

First, in this part, Section II, we present a survey paper on $1/f$ noise, which elaborates the introductory remarks made here; this survey paper (invited) was presented at the October 1981 Rome conference on noise.

II. Survey of 1/f Noise (C.M. van Vliet)

a. Introduction, History, and Extant Theories

Whereas many noise phenomena, like shot noise, thermal noise and generation-recombination noise are well understood, 1/f noise remains an enigma. This noise has been observed in all semiconductors, metal films and semiconductor devices. But it is more universal than that: 1/f noise occurs in a host of phenomena: traffic flow, variations in the rotation around the earth's axis, in music, in hourglass flow, and in many biomedical phenomena such as eyeball movement. Therefore, some investigators believe that there must be some universal phenomenon operative in all these manifestations, like scale invariance. Others believe that we should confine ourselves to a class of phenomena, like electrical 1/f noise. Still others believe that there are many types of electrical 1/f noise; it can further be said that each theory has its device, but not every device has yet its proper theory!

Research on 1/f noise covers a period of 55 years. It started with the discovery of the effect by J.B. Johnson in 1925 [1] in barium oxide cathode vacuum tubes. The first theory was given by Schottky [2], attributing the noise to creation and destruction of emission centers on the cathode due to ion migration; unfortunately, Schottky's theory, like so many others, resulted in Lorentzian noise, $S(\omega) = Ka/(a^2 + \omega^2)$. Since Schottky's theory, perhaps another fifty theories have seen the daylight, some specific, some very general, some sober, and some fantastic. Many theories contained unverifiable parameters, and others which did, like the temperature-fluctuation model, have shown by and large not to work. We believe that the following six types of theories have survived.

1. The "universal" theories. Since no characteristic turnover frequencies have generally been found, the problem is attributed to scale invariance (Machlup [3]). A variation along these lines was proposed by Handel et al [3a], who attribute the noise to a non-linear manifestation. The argument is briefly as follows: Let

$$L[y(t)] + f(y) = h(t) \quad (1.1)$$

be a Langevin equation, where L is a linear operator, while $f(y)$ is non-linear in y . Expanding in a Taylor series $f(y) = \sum a_n y^n$, and making a Fourier analysis on a sample $y_T(t)$ of duration T , one obtains

$$L[\tilde{y}_T(\omega)] + a_1 \tilde{y}_T(\omega) + a_2 \int_{-\infty}^{\infty} \tilde{y}_T(\omega_1) \tilde{y}_T(\omega - \omega') \frac{d\omega'}{2\pi} + \dots = \tilde{h}_T(\omega) \quad (1.2)$$

the second (quadratic) term stems from the nonlinearity. This term indicates that \tilde{y}_T is dimensionless, so y_T has the dimension of time. Since $S_y \propto T^{-1} \langle \tilde{y}_T^2 \rangle$, we see that S_y has the dimension of time. The question is which physical phenomenon can account for this. If there are no characteristic times (scale invariance) then the only dimensional correct quantity is f^{-1} . Hence $S_y(f) = C/f$. Obviously, the quantity C cannot be identified and one learns little from this type of argument.

2. Transport theories. We have seen in lecture II that transport theories of the type

$$L[y(\underline{r}, t)] = \frac{\partial}{\partial t} + \Lambda_r[y(\underline{r}, t)] = \xi(\underline{r}, t), \quad (1.3)$$

where Λ_r is a spatial linear operator such as $-D\nabla^2$, lead to spectra of the form (II, eq. (1.31)):

$$S_y(\underline{r}, \underline{r}', \omega) = \sum_k \int_V d^3r'' F_k(\underline{r}, \underline{r}', \underline{r}'') \frac{1}{\lambda_k + i\omega} \approx \int_{k\text{-space}} d^3k \int_V d^3r'' C(k) F_k(\underline{r}, \underline{r}', \underline{r}'') \frac{1}{\lambda(k) + i\omega} \quad (1.4)$$

So basically, we obtain an infinite sum of Lorentzians. Equation (3.4) is an integral over a distribution of relaxation times $\tau(k) = 1/\text{Re}\lambda(k)$. Can we find a weighting function F_k that does the trick so that the result is $1/f$ noise? So far, one has not been successful, neither for diffusion, nor for heat or temperature-fluctuation phenomena, as we saw in lecture II. The only exception is the surface g-r noise model in MOSFETs. Yet, attempts to work with (3.4) keep appearing in the literature. The first theories of this nature were due to MacFarlane [4], Richardson [5], and Burgess [6]. See also van Vliet and van der Ziel [7].

3. Specific model noise theories. Under this label we gather noise theories based on such specific models, that we can see with almost certainty that the models cannot account for data in many dissimilar devices and solids. For example Leon Bess in the fifties [8] devised a model where atoms were diffusing up and down pipes of edge dislocations. At that time there were many measurements, e.g. by Brophy [9] showing that $1/f$ noise strongly increased in deformed solids. Moreover, the noise went as I^4 , contrary to all modern observations (which find an I^2 dependence). Thus, even if Bess' theory might have been reasonable for the $1/f$ noise in Ge observed at that time, it certainly has no bearing on noise in Ge and Si samples of today, since dislocation-type $1/f$ noise, together with the I^4 dependence, has been eliminated. A similar fate may await recent theories by Min [10] and Pelligrini [11]. In Min's theory there is the assumption that there are regions in a semiconductor, in which interband scattering dominates intraband scattering. Making in addition the assumption that

the scattering rate has a very special (unobserved) dependence on energy, he arrives at a fairly exact $1/f$ spectrum. The problem is that he must postulate the occurrence of such specific impurity regions, requiring an inhomogeneity which is highly unreasonable for modern pure silicon samples. The same objection applies to Pelligrini's island theory.

4. The van der Ziel - Bernamont - duPré - McWhorter theories
distribution of time constants. Bernamont [12] was the first person to note that the distribution $g(\tau) = A/\tau$ will convert a sum of Lorentzians into a $1/f$ spectrum. For

$$S_y(f) = \int_{\tau_1}^{\tau_2} d\tau \frac{1}{\log(\tau_2/\tau_1)} \frac{1}{1+\omega^2\tau^2} = \frac{4\Delta y^2}{2\log(\tau_2/\tau_1)} \frac{\omega\tau_2}{\tau_1} \frac{dx}{1+x^2}$$

$$= \frac{4\Delta y^2\tau_2/\log(\tau_2/\tau_1)}{\Delta y^2/f \log(\tau_2/\tau_1)}, \quad f < 1/2\pi\tau_2$$

$$= \frac{4\Delta y^2\tau_2/\log(\tau_2/\tau_1)}{\Delta y^2/f \log(\tau_2/\tau_1)}, \quad 1/2\pi\tau_2 < f < 1/2\pi\tau_1 \quad (1.5)$$

$$= \frac{4\Delta y^2\tau_2^2/\log(\tau_2/\tau_1)}{\Delta y^2/f^2\tau_1^2 \log(\tau_2/\tau_1)}, \quad 1/2\pi\tau_1 < f.$$

We thus obtain a $1/f$ spectrum over a wide range. In view of the experimental situations ($1/f$ noise has been observed from 10^{-7} Hz [Baker [16], Firle and Winston [17], Rollins and Templeton [18]] up to 10^7 Hz [van Vliet et al [19]]), τ_2/τ_1 must be at least 10^{14} . Two types of theories have been given to explain such a distribution of time constants. (i) A uniform spread in activation energies (van der Ziel, du Pré). Thus let $\tau = \tau_0 \exp(qE/kT)$. Then if $q(E) = 1/(E_2 - E_1)$ for $E_1 \leq E \leq E_2$ and $g(E) = 0$ elsewhere, we have

$$g(\tau) = g(E) \frac{dE}{d\tau} = \frac{kT}{q} \frac{1}{E_2 - E_1} \frac{1}{\tau} \quad (1.6)$$

Now $\log_{10}(\tau_1) = (E_2 - E_1) / qkT$ in accord with (35). We notice that the noise in the 1/f range becomes proportional to T_1 in contrast to recent detailed experimental observations by Horn, Dutta, and Eberhard [20] on metal films in the range 4K-300K. This theory can therefore be laid to rest. (ii) A uniform spread in tunnel distances; this is the basis of MacWhorter's theory and similar theories. We then have the tunnel times $\tau = \tau_0 \exp(\alpha w)$ where w is the tunnel distance and α is a quantum mechanical constant. One easily sees that this also gives a $1/\tau$ distribution. In MOSFETs, MacWhorter's model, with the various modifications by van der Ziel [21], Christenson et al [22], Leventhal [23], Berc [24], Hsu [25], and Fu and Sah [26] may still be applicable to MOSFETs, in which there is a large oxide layer. The idea is that carriers reach the "slow" surface states in these oxide layers by tunnelling, either directly from the conduction band or valence band, or by elastic scattering via the "fast" recombination states at the conductor-oxide interface. Tunnel distances from 0-50Å can easily account for the wide distribution of time constants. This remains therefore a viable model. Also, it could not be that all experiments prior to Hooge's bold "bulk hypothesis" (see below) which indicated a surface mechanism, were wrong. It is possible, however, that technology has improved so much over recent years, that, indeed, presently observed 1/f noise is due to a basic bulk mechanism, whereas the surface 1/f noise has only survived in MOSFETs, which devices are notorious for high 1/f noise. Hooge, Kleinpenning and van Hamme, in a very recent survey article [27], came to the conclusion that in MOSFETs

the bulk and the surface type theories can equally well account for the observed noise characteristics. More experiments in this area are needed.

5. The mobility bulk model: phonon effects. Hooge, in 1969 [28], undertook a survey of much experimental data on semiconductors and metal films. Putting aside such experiments as Krophy's dislocation data, he found that many of the observed measurements could be fitted by the empirical law

$$\frac{S_i(f)}{I^2} = \frac{a}{F_N}, \quad (1.7)$$

where N was the number of carriers in the entire sample (providing this was homogeneous) and a is a constant of order 2×10^{-5} . We refer to it as the Hooge parameter. He also laid to rest the then prevailing notion that $1/f$ noise is often - if not always - caused by poor internal or external contacts; the term contact noise had been dubbed for years after the experiments on single carbon contacts by Christenson and Pearson [29] showed large $1/f$ noise (of the form (1.7), however!, see their article). Van Damme showed [30] that (1.7) "quantitatively" applied (given perhaps an order of magnitude leeway for a from the above given value) if the contact was considered as a distributed resistance. One must then apply (3.7) to small layers and integrate taking into account the hemispherical geometry of a contact. We believe that these experiments and computations put for the first time the bulk hypothesis - vs the older contact and surface hypotheses - on a firm footing. For a hemispherical contact van Damme finds that (2.7) takes the form

$$\frac{S_I(f)}{I^2} = \frac{\alpha^2}{5n\rho^3 f} R^3 \quad (1.8)$$

where n is the carrier density, ρ is the resistivity and R is the measured resistance.

After the bulk hypothesis Hooge, Kleinpenning, and van Damme put forth impressive evidence that the noise is caused by mobility fluctuations. We discuss this in section 2.

The final step in modern developments involved two modifications of the Hooge parameter. First, Hooge and van Damme showed that α decreases if the mobility is due to other components than the lattice mobility [31], [32]. The observed relation was

$$\frac{S_I(f)}{I^2} = \frac{\alpha'}{fN}, \quad \alpha' = \left(\frac{\mu}{\mu_\ell}\right)^2 \alpha. \quad (1.9)$$

Here μ is the observed mobility and μ_ℓ is the lattice-scattering mobility. This relationship was found for very impure samples, where μ (observed) is due to impurity scattering and in very thin samples, where μ (observed) is due to surface scattering. The derivation of (1.9) is straightforward.

Let

$$\frac{1}{\mu} = \frac{1}{\mu_i} + \frac{1}{\mu_\ell}. \quad (1.10)$$

Then, if μ_i has no noise, we find

$$-\frac{1}{\mu^2} \Delta\mu = -\frac{1}{\mu_\ell^2} \Delta\mu_\ell \quad (1.11)$$

or

$$\frac{\overline{\Delta\mu^2}}{\mu^2} = \left(\frac{\mu}{\mu_\ell}\right)^2 \frac{\overline{\Delta\mu_\ell^2}}{\mu_\ell^2} \quad \text{or} \quad \frac{S_\mu}{\mu^2} = \left(\frac{\mu}{\mu_\ell}\right)^2 \frac{S_{\mu_\ell}}{\mu_\ell^2} \quad (1.12)$$

Since, according to Hooge (for criticism, see below)

$$\frac{S_I(f)}{I^2} = \frac{S_\mu}{\mu^2} \quad \text{and} \quad \frac{S_{\mu_\ell}}{\mu_\ell^2} = \frac{\alpha}{fN} \quad (1.13)$$

eq. (1.9) follows.

Secondly, Bosman, Zijlstra, and van Rheezen [33] and later Kleinpenning [34] showed that the Hooge parameter is effected by hot electron effects. They found

$$\frac{S_I(f)}{I^2} = \frac{\alpha''}{fN}, \quad \alpha'' = \frac{\alpha}{1+(E/E_0)^2} \quad (\text{Bosman}) \quad (1.14)$$

or

$$\alpha'' = \frac{\alpha}{(1+E/E_0)^2} \quad (\text{Kleinpenning}) \quad (1.15)$$

Kleinpenning's result is easily explained. For n-type silicon one often has a relation of the form

$$\mu(E) = \frac{\mu_0}{1+\mu_0 E/v_s} \quad (1.16)$$

where v_s is the saturation drift velocity for $v_d = \mu E$ if $E \rightarrow \infty$.

Assuming that the fluctuations are due to only the low field mobility μ_0 , we find

$$\Delta\mu = \frac{\Delta\mu_0 (1+\mu_0 E/v_s) - (\mu_0 E/v_s) \Delta\mu_0}{(1+\mu_0 E/v_s)^2} \quad (1.17)$$

or

$$\frac{\Delta\mu}{\mu} = \frac{\Delta\mu_0}{\mu_0} \frac{1}{1+\mu_0 E/v_s} \quad (1.18)$$

or

$$\frac{S_\mu}{\mu^2} = \frac{S_{\mu_0}}{\mu_0^2} \frac{1}{(1+\mu_0 E/v_s)^2} \quad (1.19)$$

With the same Hooge et al state went as before (viz. $S_I/I^2 = S_{\mu}/\mu^2$), (1.15) follows. The statement that the fluctuations are due to those in the low field mobility can well be defended. For, computation shows that the lattice scattering mean free path for hot electrons (see Yamashita and Watanabe, lecture I) is the same as that for thermal electrons (as found in Wilson's book).

Since many things now point to fluctuations in the lattice mobility as cause for $1/f$ noise, we must now look for mechanisms that lead to such $1/f$ noise. So far, the only reasonable advanced theory is due to Jindal and van der Ziel [35]. They show that phonon creation and annihilation processes lead to a distribution of phonon lifetimes commensurate with $1/f$ noise. There is, however, a problem in that for very long relaxation times very low q -values are necessary. This writer has pointed out to Jindal that the lowest q -value in the Brillouin zone is given by π/aN where N is the number of linear atoms and a the lattice constant. This spoils the argument of an otherwise attractive theory.

6. The mobility-fluctuation model: quantum $1/f$ noise. Several years before the experimental evidence pointed conclusively to mobility or carrier scattering fluctuations, Handel gave a theory of $1/f$ noise based on self interference of the wave packet of a carrier upon scattering with an obstacle [36]. A full account of this was published in 1980 [37], and another version of the theory based on wave interaction in 1981 [38]. Before we mention the essential tenets of this theory, we must point out the connection between mobility fluctuations and scattering

of individual electrons (or holes). In all the literature up to now the argument was first of all that the proportionality with I^2 indicates that $1/f$ noise is due to resistance fluctuations being there already in equilibrium; the current merely serves as a probe to measure these fluctuations (see section 4). Since $R = \text{constant times } \sigma$, one has undoubtedly for linear devices

$$\frac{S_I}{I^2} = \frac{S_R}{R^2} = \frac{S_V}{V^2} = \frac{S_\sigma}{\sigma^2} \quad (1.20)$$

$$\text{Now } \sigma = e\mu n, \quad \Delta\sigma = e\mu\Delta n + en\Delta\mu; \quad (1.21)$$

if $\Delta n = 0$ (no number fluctuations since we are not interested in g-r noise) the reasoning goes $\sigma = en\Delta\mu$, hence

$$S_\sigma/\sigma^2 = S_\mu/\mu^2 = \alpha/fN \quad (1.22)$$

This is, however, wrong as was recently shown by van Vliet and Zijlstra. The point is that differential relationships like: if $y = f(x)$, $\Delta y = (dy/dx)\Delta x$ are not valid stochastically if f is a statistical function! (Relationships of this type have been very often misused in the noise literature). The correct argument is as follows [39].

Let $v_{d_i} = \langle v_i \rangle$ be the drift velocity of the i th electron in a volume ΔV centered on r . Then the $1/f$ noise source is written as

$$H(\underline{r}, t) = \frac{-q}{\Delta V} \sum_{i=1}^{N(\underline{r}, t)} \Delta v_i(t) \quad (1.23)$$

where $N = n(\underline{r}, t)\Delta V$. Since we not consider g-r or diffusion noise, $n(\underline{r}, t) = n_0(\underline{r})$ is constant. However, to all likelihood the electrons in V are scattered independently. Thus from (1.23)

$$S_H(\underline{r}, \underline{r}', f) = \frac{q^2 N(\underline{r})}{(\Delta V)^2} S_{\Delta V}(\underline{r})(f) \quad (1.24)$$

where $S_{\Delta V}(\underline{r})(f)$ is the drift velocity noise of any electron in the neighborhood of \underline{r} . The cross-correlation for different volumes ΔV centered on \underline{r} and \underline{r}' is zero, since, as we saw, the velocity fluctuations are most likely uncorrelated. Thus, replacing $1/\Delta V$ by $\delta(\underline{r}-\underline{r}')$, we also have

$$S_H(\underline{r}, \underline{r}', f) = q^2 n_0(\underline{r}) \delta(\underline{r}-\underline{r}') S_{\Delta V}(\underline{r})(f) \quad (1.25)$$

Now Hooke's relation, when translated to a noise source of a volume ΔV , reads with $H \equiv \Delta J_{\text{stoch}}$.

$$S_H(\underline{r}, \underline{r}', f) = \alpha [J_0(\underline{r})]^2 \delta(\underline{r}-\underline{r}') / f n_0(\underline{r}) \quad (1.26)$$

(note that double integration over $d^3 r d^3 r'$ leads to (1.7)); or also

$$S_\sigma(\underline{r}, \underline{r}', f) = \alpha [\sigma_0(\underline{r})]^2 \delta(\underline{r}-\underline{r}') / f n_0(\underline{r}). \quad (1.27)$$

Comparison of (1.25) and (1.26) yields

$$\begin{aligned} S_{\Delta V}(\underline{r})(f) &= \alpha [J_0(\underline{r})]^2 / e^2 [n_0(\underline{r})]^2 f \\ &= \alpha [\mu_0(\underline{r}) E_0(\underline{r})]^2 / f \end{aligned} \quad (1.28)$$

Since $\underline{v} = \mu \underline{E}_0$, this gives the mobility fluctuation noise

$$S_{\Delta \mu}(\underline{r})(f) = \alpha [\mu_0(\underline{r})]^2 / f. \quad (1.29)$$

In the absence of hot electron effects μ does not usually depend on positions, while also α is then independent of \underline{E}_0 ; then

$$S_{\Delta \mu}(f) = \alpha \mu_0^2 / f \quad (1.30)$$

This is the proper Hooge form for mobility $1/f$ noise. An extension of this derivation was given by van der Ziel and van Vliet [40]. Notice: (a) mobility fluctuations are not correlated in space, i.e. $S_{\Delta\mu}(\mathbf{r}, \mathbf{r}', f)$ as used by Kleinpenning is meaningless; (b) the factor N is missing, since mobility, fluctuations refer to individual scattering effects.

It is here that Handel's theory comes in. This is exactly the model that he considers. He shows that individual scattering has an inelastic component due to the excitation of quantum field modes of the vacuum state involving infrared divergencies. These excitations may involve phonons, photons, electron-hole pairs on the Fermi surface, nuclear spin magnons, or perhaps even largely unknown "correlated states" as described by Ngai [41]. We consider Ngai's theory to be a variation of Handel's general quantum $1/f$ noise mechanism. We briefly describe Handel's theory in section 3.

As we notice, Handel's theory describes individual scattering and leads to the expression (1.30), even though many details (such as the role of lattice scattering versus impurity scattering) still have to be filled in. Following the inverse route of eqs. (1.23) to (1.30), we are thus led to Hooge's relation (1.26)-(1.7).

In closing this section, we mention that presently there are three excellent extensive review papers on $1/f$ noise, viz by van der Ziel in Advances in Electron Physics [21], by Dutta and Horn in Review of Modern Physics [20], and by Hooge, Kleinpenning and van Damme in Reports on Progress in Physics [27]. No serious investigation of $1/f$ noise can do without these surveys!

b. More on the Experimental Evidence

1. α -values

Hooge et al [27] give the following table:

material	n_0 or p_0 from Hall effect	α	T(k)
n-InSb	1.6×10^{14}	1.3×10^{-3}	77
	1.6×10^{16}	3.4×10^{-3}	300
p-InSb	1.2×10^{16}	7×10^{-3}	77
p-GaAs	1.5×10^{17}	2×10^{-3}	77
		3×10^{-3}	300
n-GaAs	2.3×10^{16}	6×10^{-3}	300
p-GaAs	2.3×10^{16}	3.4×10^{-3}	300
n-GaP	2.9×10^{16}	9×10^{-3}	300

Values for elemental semiconductors and metal films were published before [28].

2. The distinguishability problem

Hooge et al investigated the problem of how to distinguish between mobility noise and carrier density noise. Suppose a quantity X depends on μ and on N : $X = X(\mu, N)$. Then their argument is (op cit p.506)

$$\Delta X_N = (dX/dN)_0 \Delta N \rightarrow S_{X_N} [N_0 (dX/dN)_0]^2 S_N / N^2 \quad (2.1)$$

$$\Delta X_\mu = (dX/d\mu)_0 \Delta \mu \rightarrow S_{X_\mu} = [N_0 (dX/d\mu)_0]^2 S_\mu / \mu^2. \quad (2.2)$$

Now, not knowing the cause of $1/f$ noise, it is either

$$S_N / N^2 = \alpha / fN \quad (a)$$

or

$$S_\mu / \mu^2 = \alpha / fN. \quad (b)$$

In order to find different results in S_X , we must thus have a quantity X for which $N dX/dN \neq \mu dX/d\mu$. Obviously, if X is the conductance $\sigma = eN$, the above inequality is not satisfied. Thus conductance fluctuation cannot distinguish between mobility or density fluctuations.

In view of what we said in the last section, this argument is incorrect, since (2.2) does not hold. However, the conclusion remains correct. For $X = \sigma$, (2.1) gives $S_{\sigma_N} = \sigma^2 S_N / N^2$ while (2.2) now reads: $S_{\sigma_\mu} = (\sigma^2 / N) S_\mu / \mu^2$. Instead of (a) and (b) we now have $S_N / N^2 = \alpha / fN$ and $S_\mu / \mu^2 = \alpha / f$. Thus the same ambiguity occurs: $S_{\sigma_N} = S_{\sigma_\mu}$.

For quantities other than σ the argument needs reexamination, since a relationship of the form (2.2) does not exist. In the examples which follow, the argument should be repeated to avoid the erroneous equation (b). We have looked through the examples in some detail. It appears to us that Kleinpenning would not at all have to resort to eq. (b). Instead, most of his arguments need only the true relation for the current noise (1.7) or (1.26), or for the conductivity noise, (1.27).

3. Seebeck fluctuations [42]

The thermal voltage in a temperature gradient $\Delta T/L$ is given by

$$V_{th} = (\varepsilon_F + \varepsilon_k) \Delta T / qT \quad (2.4)$$

Here ε_k is the "mean conduction level"

$$\varepsilon_k = \int_0^\infty \varepsilon G(\varepsilon) d\varepsilon / \int_0^\infty G(\varepsilon) d\varepsilon \quad (2.5)$$

where $G(\varepsilon)d\varepsilon$ is the conductivity $qn(\varepsilon)\mu(\varepsilon)d\varepsilon$ of electrons in the conduction with energies between ε and $\varepsilon+d\varepsilon$. We also have *

$$\Delta \varepsilon_k = \int_0^\infty (\varepsilon - \langle \varepsilon_k \rangle) \Delta G(\varepsilon) d\varepsilon / C \quad (2.6)$$

Now we must interpret (1.27) as a consequence of fluctuations $G(\varepsilon)$ in individual subbands. Here the physics comes in. If the noise is due to mobility fluctuations, there is delta function correlation between the subbands since carriers scatter independently, as we saw before. Thus if (1.27) is due to mobility noise, it has a substratum the microscopic source

$$S_{G(\varepsilon), G(\varepsilon')} = [G(\varepsilon)]^2 \frac{c}{fn(\varepsilon)} \delta(\varepsilon - \varepsilon') \quad (2.7)$$

Carrier fluctuations give $\Delta n(\varepsilon) \propto n(\varepsilon)$, which when substituted in (2.6) yields $S_{\varepsilon_k} = 0$. We now substitute (2.7) into the expression for S_{ε_k}

* The correction $-\langle \varepsilon_k \rangle$ stems from the canonical constraint. We feel this constraint could better have been incorporated into (2.7) by replacing $\delta(\varepsilon - \varepsilon')$ by $\delta(\varepsilon - \varepsilon') - 1/\xi$.

derivable from (2.6). Thus,

$$\begin{aligned}
 S_{\epsilon_k} &= \frac{\alpha}{fG^2} \int_0^\infty \int_0^\infty [\epsilon - \langle \epsilon_k \rangle][\epsilon' - \langle \epsilon_k \rangle] \frac{[G(\epsilon)]^2}{n(\epsilon)} \delta(\epsilon - \epsilon') d\epsilon d\epsilon' \\
 &= \frac{\alpha}{fG^2} \int_0^\infty d\epsilon [\epsilon - \langle \epsilon_k \rangle]^2 [G(\epsilon)]^2 / n(\epsilon)
 \end{aligned}
 \tag{2.8}$$

which is the result used by Kleinpenning. For number fluctuations, $S_{\epsilon_k} = 0$, but $S_{\epsilon_F} = (kT)^2 S_N / N_0^2$ for which we may use relation (a). We thus obtain different results, in particular if we impress an external voltage in addition to ΔT .

4. Other effects

Kleinpenning also showed that different results occur in the Hall effect and in the noise of SCL diodes, depending as to whether the noise is caused by mobility or number fluctuations. Again a warning is in order: the arguments should be repeated, without using the erroneous formula (b).

5. Lattice scattering versus other scattering

The fact that the noise clearly depends on the type of scattering is in our opinion the strongest argument for mobility fluctuation as the cause for $1/f$ noise. The reduction of α for impurity scattering is shown in Ref. [42]. Both results are due to Hooge and van Damme.

c. Handel's Theory

We present here the derivation based on the picture of wave interaction noise, given in a previous paper [38] Handel's theory leads to noise whenever particles undergo scattering. The theory is equally well applicable to the problem of emission of α -particles (see lecture IV) or to scattering with lattice vibrations. We consider the wave function for a particle undergoing small energy losses in scattering in a period T

$$\psi(\underline{r}, t) = a e^{\frac{i}{\hbar}(\underline{p} \cdot \underline{r} - \epsilon t)} [1 + \int_0^{\Lambda} d\epsilon b_T(\epsilon) e^{i\epsilon t/\hbar}] \quad (3.1)$$

where Λ is of order ϵ . For the mean square amplitude one thus finds

$$\langle |\psi|^2 \rangle = |a|^2 (1 + \int_0^{\Lambda} \int_0^{\Lambda} d\epsilon d\epsilon' \langle b_T^*(\epsilon) b_T(\epsilon') \rangle e^{i(\epsilon - \epsilon')t/\hbar}) \quad (3.2)$$

For $T \rightarrow \infty$,

$$\langle b_T^*(\epsilon) b_T(\epsilon') \rangle \rightarrow |b(\epsilon)|^2 \delta(\epsilon - \epsilon'). \quad (3.3)$$

Clearly $b(\epsilon)$ is the crosssection for energy losses; in case these energy losses lead to emission of (very low energy) photons, we speak of bremsstrahlung. However, the energy losses may involve excitations other than of the photon fields, e.g. in correlated states. For small energy losses $|b(\epsilon)|^2$ represents infrared divergencies, and always goes as $(\epsilon/\epsilon_0)^{\alpha A}$ ($\alpha A/\epsilon$). Here αA is due to infrared corrections; as a rule $\alpha A \ll 1$ and

$$|b(\epsilon)|^2 \propto \alpha A/\epsilon. \quad (3.4)$$

For bremsstrahlung

$$\alpha A = \frac{4e^2 (\Delta v)^2}{3c^3 \hbar} = \frac{4}{3} \alpha_f \frac{\Delta v^2}{c^2} \quad (3.5)$$

where α_f is the fine structure constant ($1/137$), Δv is the velocity change and c is the speed of light. For other processes A is different but (3.4) remains correct. Substituting (3.4) and (3.3) in (3.2) we obtain

$$\langle |\psi|^2 \rangle = \alpha^2 (1 + \frac{A}{\epsilon_0} \int_0^\infty d\epsilon \frac{\epsilon A}{\epsilon}) = \int_0^\infty S_{\psi+}(\epsilon) d\epsilon. \quad (3.6)$$

For the analytic signal $S_{\psi+}(\epsilon)$ we thus have upon normalization, denoted by λ , for the spectrum

$$\hat{S}_{\psi+}(\epsilon) = \frac{\delta(\epsilon) + 2\alpha A \epsilon^{-1}}{1 + 2\alpha A \int_0^\infty \epsilon^{-1} d\epsilon} \approx \delta(\epsilon) + \frac{2\alpha A}{\epsilon}. \quad (3.7)$$

Now let $\mathcal{I} = |\psi|^2$ be the intensity of the particle wave, then for $\hat{S}_{\mathcal{I}}$ we have by the convolution theorem if $\epsilon = h\nu$

$$\hat{S}_{\mathcal{I}}(f) = \int_{-\infty}^{\infty} \hat{S}_{\psi+}(\nu) \hat{S}_{\psi+}(f-\nu) d\nu \quad (3.8)$$

This leads to

$$\hat{S}_{\mathcal{I}}(f) = \delta(f) + 2\alpha A f^{-1} \theta(f-f_0) \quad (3.9)$$

where θ is the unit step function; $f_0 = \epsilon_0/h$ is an arbitrarily low frequency of the experimental set-up; we neglected the quadratic term which represents noise of noise. The $\delta(f)$ term stems from the d.c. intensity. Thus

$$\hat{S}_{\Delta\mathcal{I}}(f) = 2\alpha A f^{-1} \theta(f-f_0) \quad (3.10)$$

Since $\Delta\mathcal{I} \propto \Delta\sigma_c \propto \Delta\mu$, where $\Delta\sigma_c$ is the cross section fluctuation, and $\Delta\mu$ the mobility fluctuation resulting from this scattering, we have

$$S_{\Delta\mu} = S_{\Delta\mathcal{I}}/\mu^2 = 2\alpha A/f \quad (f > 0). \quad (3.11)$$

Thus Hooge's α_H is, upon comparison with (1.30)

$$\alpha_H = 2\alpha A. \quad (3.12)$$

For bremsstrahlung, αA turns out to be much too low since $4\pi/c$ for electrons is extremely small. However, there are other loss mechanisms for which αA is much larger. The pinpointing of these loss mechanisms remains the largest challenge for this theory. However, the form (1.30) is easily accounted for by this approach. Presently, Handel and the author are studying the explicit application of these ideas to impurity scattering and lattice scattering.

d. Other Basic Questions

1. 1/f noise an equilibrium property?

In 1976 Voss and Clarke performed an extremely interesting experiment [43]. They measured the Johnson noise of a resistor, over a large bandwidth, with incomplete averaging, i.e. the averaging time was finite. Then the noise of the resistor is

$$S_V(\omega, t) \Delta f = 4kTR(t)p(\omega) \Delta f. \quad (4.1)$$

They now measured the noise of the noise. If $R(t)$ fluctuates in the absence of a current probe with a $1/f$ spectrum, the noise of $S_V(\omega, t)$ must go as $1/f$. This was indeed observed. Beck and Spruit [44]

reported similar measurements. We therefore now know that the current is not driving the $1/f$ noise, but that it serves only as a probe to measure the resistance, i.e. mobility fluctuations. Yet, can one say that $1/f$ noise is an equilibrium phenomenon? Not really, if Handel's

theory applies. For in that case the noise is there under quiescent conditions since scattering (and inverse scattering because of detailed balance) occurs in equilibrium; however, the $1/f$ fluctuations do not stem from the thermal motion of the carriers but from the quantum mechanical nature of the scattering; the noise would be there even if only one carrier underwent collisions. Since quantum $1/f$ noise is not an equilibrium property, we do not have to look for the existence of a fluctuation-dissipation theorem which will yield $1/f$ noise. Such would be the case, however, if Jindal's theory applies (just as carrier g-r noise can be explained by the fluctuation-dissipation theorem - van Vliet 1958 [45]).

2. Is $1/f$ noise stationary?

First we note that the divergence of the variance at the low frequency end really does not matter much. Hooge et al remarked that 10^{-6} Hz corresponds to about 1 month measuring time. But even if one measured a century, the addition to the variance would amount to only 20%! Dutta and Horn noted that $1/f$ noise cannot go on to $f=0$, for then, according to them, the specific heat contribution

$$C_V = \int_0^\infty f S_{AV}(f) df/f = \infty. \quad (4.2)$$

However, the limit 0 is artificial and for high frequencies there are always mechanisms to shunt the noise. More important, we will show in lecture IV that neither the variance, nor the correlation function needs to exist for $1/f$ noise. These concepts are simply meaningless for $1/f$ noise.

The spectrum is always defined by $S = \lim_{T \rightarrow \infty} 2T \langle a^*(\omega_n) a(\omega_n) \rangle$ where a is the Fourier coefficient (Fourier series for truncated time sample); the statistical Allan variance turns out to be stationary, see Lecture IV.

3. Is the 1/f noise mechanism nonlinear?

In Handel's theory: yes, because of the radioactive corrections due to "feedback" of the infra field to the particle wave field. However, these corrections are very small and the deviations from Gaussianity are minute [46]. Brophy [47] and others found that the short time average of the 1/f noise power showed statistical fluctuations larger than expected for stationary signals. On the contrary, Stoisiak and Wolf [48] found the noise to have a stationary Gaussian character.

e. Conclusions

Taking all the 1/f data from the discovery of the effect in 1925 up to now, one must first of all notice that there is conflicting evidence on basic questions such as surface effect or bulk effect, temperature dependence etc. However, this is resolved if one assumes that there were various types of 1/f noise, such as surface 1/f noise, dislocation 1/f noise, etc., most of which disappeared, however, with improved technology. The surface idea mainly remains, in conjunction with McWhorter's theory for MOSFETs. The remaining 1/f noise in present day solids and devices seems to be caused by bulk fluctuations. There is also considerable evidence that the bulk conductance fluctuations, being present

without the passage of current, are due to mobility fluctuations. The most prominent theories are those due to Jindal and van der Ziel, dealing with acoustical phonon fluctuations, and due to Handel dealing with quantum $1/f$ noise. We presented Hooge's result for the conductance fluctuations in the form of a modified mobility noise, eq.(1.30); this is the basic equation. Handel's theory goes a long way in explaining such a relation though many details require more work. The temperature fluctuation hypothesis is practically laid to rest, except for fluctuations near the superconducting transition. More experiments should be done which have a bearing on the current ideas,^{as} set forth in this paper.

REFERENCES

1. J.B.Johnson, Phys.Rev.26, 70 (1925)
2. W.Shottky, Phys.Rev. 28, 74 (1926)
3. S.Machlup, Proc.2nd Conf. $1/f$ noise, Orlando Florida 1980, p.556.
- 3a. P.H.Handel et al, Phys.Lett., submitted.
4. G.G.McFarlane, Proc.Phys.Soc. [B] 65, 807 (1950).
5. J.M.Richardson, Bell.Syst.Tech.J. 29, 117 (1950).
6. R.E.Burgess, Proc.Phys.Soc. [B] 66, 334 (1953)
7. K.M. van Vliet and A. van der Ziel, Physica 24, 415 (1958).
8. L.Bess, Phys.Rev. 103, 72 (1956).
9. J.J.Brophy, J.Appl.Phys. 27, 1383 (1956).
10. H.S.Min, Solid State Electronics (1979).
11. B.Pelligrini, Phys.Rev. B22, 4684 (1980).
12. J.Bernamont, Ann.de Physique, 7, 71 (1957).

13. A. van der Ziel, Phys. 16, 359 (1950).
14. F. du Pré (1950)
15. A.L.McWhorter in "Semiconductor Surface Physics" (R.H.Kingston,ed.)
Univ. of Pennsylvania Press 1957 p.207.
16. Baker
17. T.E.Firle and H.Winston, J.Appl.Phys. 26, 716 (1955).
18. B.V.Rollin and I.M.Templeton, Proc.Phys.Soc. [B] 67, 271 (1954)
19. K.M.van Vliet et al, Physica 20, 481 (1954)
20. P.Dutta and P.M.Horn, Revs Mod.Physics. 53, 497 (1981)
21. A. van der Ziel, Adv. in Electronics and Electron Physics 49,
225 (1979)
22. S.Christenson et al. Solid State Electr. 11, 797 (1968).
23. E.A.Leventhal, Solid State Electr. 11, 621 (1968)
24. F.Berz, Solid State Electr. 13, 621 (1970).
25. S.T.Hsu, Solid State Electr. 13, 1451 (1970).
26. H.S.Fu and C.T.Sah, IEEE Trans, El.Dev. ED-19, 273 (1972).
27. F.N.Hooge, T.G.M.Kleinpenning, and L.K.J. van Damme, Rep. Progress
in Physics 44, 479 (1981).
28. F.N.Hooge, Phys.Lett. 29A, 139 (1969)
29. C.J.Christenson and G.L.Pearson, Bell Syst.Tech.J. 15, 197 (1936)
30. L.K.J. van Damme, Appl.Phys. 11, 89 (1976)
31. F.N.Hooge and L.K.J. van Damme, Phys.Lett. 66A, 315 (1978)
32. F.N.Hooge and L.K.J. van Damme, J.Appl.Phys. 50, 8087 (1979)
33. G.Bosman, R.J.J.Zijlstra and van Rheenen, Phys.Lett. 78A, 385
(1980); *ibid*, 80A, 57 (1980)

34. T.G.M. Kleinpenning, Physica B,C 103, 340 (1981)
35. J.P.Jindal and A.van der Ziel, J.Appl.Phys. 1980
36. P.H.Handel, Phys.Rev.Lett. 34, 1492 (1975)
37. P.H.Handel, Phys. Rev.A22, 745 (1980)
38. K.M.van Vliet, P.H.Handel and A.van der Ziel, Physica, in press.
39. K.M. van Vliet, and R.J.J.Zijlstra, Physica, in press.
40. A. van der Ziel and K.M. van Vliet, Physica, in press.
41. K.L.Ngai, Phys.Rev. B22, 2066 (1980)
42. T.G.M.Kleinpenning, Physica 77, 78 (1974)
43. R.F.Voss and J.Clarke, Phys.Rev. B13, 556 (1976)
44. H.G.E.Beck and W.P.Spruit, J.Appl.Phys. 49, 3384 (1978)
45. K.M. van Vliet, Phys.Rev. 110, 50 (1958)
46. P.H.Handel and D.Wolf, Proc.Second Int.Symp. on i/f Noise, Orlando, University of Florida, 1980, p.56.
47. J.J.Brophy, Phys.Rev. 166, 827 (1968); J.Appl.Phys. 40, 567 (1969); ibid, 41, 2913 (1970)
48. M.Stoisiek and D.Wolf, J.Appl.Phys. 47, 362 (1976)

B. EXPERIMENTAL WORK

I. Gold Thin Films Project (J. Kilmer)

Due to the theoretical possibility of $1/f$ noise stemming from surface heat sources [1] and the possible strong temperature dependence of noise sources in metal thin films [2-4], an investigation of noise correlation over a full ambient temperature range is to be performed. We have received from the National Research & Resource Facility for Submicron Structures at Cornell under Dr. E. Wolf and R.A. Buhrman, closely spaced configurations of gold thin film resistors designed by Dr. van Vliet. The configurations, see Figure 1, consist of 2000 \AA thick gold films deposited on top of a 200 \AA chromium layer adhering to a standard silicon substrate. The standard configuration of three resistors is repeated for varying widths and spacings of $.5 \text{ \mu m}$, 1 \mu m , and 2 \mu m . Each resistor has two 100 \mu m square gold bonding pads and were delivered unbonded so we could decide how to make electrical contact to them when they are in the cryostat. The cryostat, to be ordered in June, is the Cryosystems Model 21 closed-cycle cryogenic refrigerator, capable of maintaining a constant temperature (as low as 10° K) determined by a thermostat setting. The extra data needed at 4° K will be obtained by directly submerging the sample in liquid helium. We have decided to dice the substrate so that a standard group of three resistors is contained on a single silicon chip. The chip is silver epoxy glued (for thermal conductivity) to a six-lead T05 can and the pads are gold wire bonded to the T05 can posts by an ultrasonic bonder. The cryostat comes equipped with a T05 can cold chamber mount and a six-lead feedthrough. We need electrical contact to three resistors in the same thermal environment so that one element can be biased as a "heater" and the correlation between the responses in the other two "sensors" can be observed. The so-called "three-element experiment" is described in Joyce Kilmer's master's thesis [5]

for case of thermally coupled transistors. Once the characteristics of the resistors' thermal coupling are determined, the $1/f$ noise will be measured using the low-noise amplifier designed by Robert Schmidt and the HP3582A FFT spectrum analyzer. The Hooge parameter will be checked to see if it is inversely proportional to the volume (or width in thin films) for a bulk effect. Finally, the correlation of the resistor $1/f$ noise spectra will be measured at cryogenic temperatures. Presently, the linear V/I characteristics of a resistor have been confirmed over a few decades of current in the Cornell devices, and the $1/f$ noise is being measured at room temperature.

References

- [1] C.M. van Vliet, A. van der Ziel, and R.R. Schmidt, "Temperature Fluctuation Noise of Thin Films Supported by a Substrate," *Journal of Applied Physics* 51, 2947, 1980.
- [2] J.W. Eberhard and P.M. Horn, "Temperature Dependence of $1/f$ Noise in Ag and Cu," *Physical Review Letters* 39, 643, 1977.
- [3] P. Dutta, J.W. Eberhard, and P.M. Horn, " $1/f$ Noise in Metal Films: The Role of the Substrate," *Solid State Communications* 27, 1389, 1978.
- [4] P. Dutta, P. Dimon, and P.M. Horn, "Energy Scales for Noise Processes in Metals," *Physical Review Letters* 43, 646, 1979.
- [5] J. Kilmer, "Quest for the Presence of Temperature Fluctuations in Flicker Noise Correlation Experiments," Master's Thesis, University of Florida, 1981.

II. Presence of Mobility-Fluctuation 1/f Noise Identified in Silicon P⁺NP Transistors (J. Kilmer, A. van der Ziel, and G. Bosman)

a. Abstract

The magnitude and location of mobility-fluctuation 1/f noise sources have been identified by means of biasing a PNP transistor in a common emitter configuration with first a high and then a low source resistance. Comparison of the two noise spectra at the same base currents shows the low source resistor bias isolates the collector noise sources, and the high source resistance isolates base noise sources. The magnitude of the observed collector 1/f noise gives an $\alpha \simeq 2 \times 10^{-6}$ from Kleinpenning's mobility-fluctuation theory. The base 1/f noise gives an $\alpha \simeq 10^{-7}$ due to an impurity mobility reduction factor of about 100.

b. Introduction

To date, three causes regarding the origin of 1/f noise in transistors prevail.

1) Fluctuating occupancy of electrons in oxide surface traps (or dislocations) in the base or emitter space-charge region modulates the (surface) recombination velocity. 1/f noise due to fluctuating recombination velocity is represented as a recombination current I_R flowing from emitter to base [1].

2) Mobility fluctuations due to holes interacting with phonons cause 1/f noise in the hole current I_{Ep} diffusing from the emitter to the collector.

3) Mobility fluctuations due to the electron current I_{En} injected from the base into the emitter may also cause 1/f noise.

1/f noise due to a fluctuating series base resistance r_b we do not consider since I_B is small in a high β transistor. The three possible causes are represented as current sources δI_R , δI_{En} , and δI_{Ep} in an equivalent circuit for a PNP transistor first drawn by Plumb and Chenette [2] and later modified

by van der Ziel (see Figure 2). Here we combine the two base current sources into an equivalent base 1/f noise source, i_{fb} , where $i_{fb} = -\delta I_R - \delta I_{En}$ and rename the collector current source, i_{fc} , where $i_{fc} = -\delta I_{Ep}$.

In older transistors the predominant 1/f noise source was the recombination current because those devices had large surface recombination velocities. The purpose of our present investigation is to determine whether 1/f noise due to mobility fluctuations, as presented first by Hooge [3] and recently by Kleinpenning [4], is present in contemporary devices with small surface recombination velocities.

Van der Ziel's appended derivation [5] of Kleinpenning's expression for the noise spectrum due to mobility fluctuations of emitter-collector hole diffusion in P^+NP transistors shows,

$$S_{I_{Ep}}(f) = 2qI_{Ep} \frac{\alpha_p}{4f\tau_{dp}} \ln \left[\frac{P(0)}{P(w_B)} \right] \quad (1)$$

where α_p is the Hooge parameter associated with hole current, $\tau_{dp} = w_B^2/2D_p$ is the diffusion time for holes through the base region, w_B the base width and $P(0)$ and $P(w_B)$ are the hole concentrations for unit length at the emitter side and the collector side of the base, respectively. We see the magnitude of $S_{I_{Ep}}$ is inversely proportional to τ_{dp} , which means that $S_{I_{Ep}}$ is proportional to f_T since

$$f_T = \frac{1}{2\pi\tau_{dp}} \quad (2)$$

Therefore, the hole mobility fluctuation 1/f noise source is larger in transistors with a large f_T (e.g., microwave transistors).

Also for electron injection from base to emitter, we have, due to mobility fluctuations [5,eq.(4)],

$$S_{I_{En}}(f) = 2qI_{En} \frac{\alpha_n}{4f\tau_{dn}} \ln \left[\frac{N(0)}{N(w_E)} \right] \quad (3)$$

where $\tau_{dn} = w_E^2/2D_n$, w_E the width of the emitter region, D_n the electron diffusion constant in the emitter region, whereas $N(0)$ and $N(w_E)$ are the electron concentrations for unit length at the base side of the emitter and at the emitter contact, respectively.

c. Experiment to discriminate between the main noise sources

In the Plumb-Chenette [2] experiment, we can discriminate between i_{fb} and i_{fc} by placing the transistor in a common-base configuration and monitoring the emitter-base noise. The disadvantage of this approach is that the emitter-base noise requires preamplification making this a "less-clean" experiment, since the input impedance of the preamplifier is in parallel with the most sensitive part of the equivalent noise circuit.

A "cleaner" way to observe the base noise is by employing the natural amplification of the device and measuring collector noise. With the transistor in a common-emitter configuration, the noise at the collector will be an amplified version of the base noise provided we limit the collector current to a few milliamps so that the collector shot-noise level lies below the amplified base shot-noise level. Redrawing Figure 2 into a common-emitter configuration and squaring the noise sources so they represent spectral contributors (see Figure 3), we see $(R_s + r_b)$ is now in parallel to the input (base) equivalent circuit of the transistor. Also in Figure 3, the collector noise current sources have been referred to the input equivalent circuit as noise voltage sources by multiplying by $1/g_m = r_\pi/\beta$ (valid if $r_\pi \gg r_b$).

An HP3582A FFT spectrum analyzer measures the spectral density of the collector noise, $M^2/\Delta f$. Calculations from Figure 3 reveal

$$\frac{M^2}{\Delta f} = A^2 \left\{ \left(S_{R_s} + S_{r_b} \right) \left[\frac{r_\pi}{R_s + r_b + r_\pi} \right]^2 + 2kT r_\pi \left[\frac{r_b + R_s}{R_s + r_b + r_\pi} \right]^2 + S_{ifb} \frac{(r_b + R_s)^2 r_\pi^2}{(R_s + r_b + r_\pi)^2} + \frac{2kT}{g_m} + \frac{S_{ifc}}{g_m^2} \right\}. \quad (4)$$

If we use that $r_\pi \gg r_b$ and $\beta \gg 1$, then equation (4) can be rewritten so that we obtain

$$\frac{M^2}{\Delta f} = A^2 \left[\frac{r_\pi}{R_s + r_b + r_\pi} \right]^2 \left\{ \left[2kT(2r_b + 1/g_m) + \frac{S_{ifc}}{g_m^2} + S_{ifb} r_b^2 \right] + R_s \left[4kT + 2 \frac{S_{ifc} r_\pi}{\beta^2} + 2S_{ifb} r_b \right] + R_s^2 \left[\frac{2kT}{r_\pi} + \frac{S_{ifc}}{\beta^2} + S_{ifb} \right] \right\}. \quad (5)$$

We see that there are three regions to the magnitude of the measured noise versus R_s --an independent, a linear, and a quadratic regime.

Ideally, the mobility-fluctuation 1/f noise measurements should be made on microwave transistors biased with low currents for both high and low R_s . Unfortunately, microwave transistors usually do not have a high DC β . So the experiment was performed on low-noise PNP transistors (GE 82 185) with $\beta \approx 350$ typically. A simple biasing scheme was used for the high R_s experiment (see Figure 4) and the noise was measured for three different I_B 's. From equation (5) and for the case of high R_s , we see that we measure with the spectrum analyzer,

$$\frac{M_{HI}^2}{\Delta f} = \beta^2 R_L^2 \left[2eI_B + S_{ifb} + \frac{S_{ifc}}{\beta^2} \right], \quad (6)$$

where we have neglected the small r_b and r_π compared to a high R_s and the terms independent of and proportional with R_s . The measured high R_s noise

spectra. $M_{HI}^2 / \Delta f$, is now scaled down by $1/R_L^2$ so that the noise plotted in Figure 5 (curves IV, V, VI) represents the absolute magnitude of the physical noise sources (in $\text{amp}^2 \text{ sec}$) referred back to the (base) input,

$$S_{HR_S} = \frac{M_{HI}^2}{\Delta f} \left[\frac{1}{R_L^2} \right] = 2eI_B + S_{ifb} + \frac{S_{ifc}}{g_m^2} . \quad (7)$$

The high frequency roll-off, which each of the plots indicates, is attributed to the Miller effect of the capacitance C_T in the equivalent circuit (see Figure 3) where

$$C_T = C_{beo} + C_{bco}(1 + |A_v|) . \quad (8)$$

Since I_B is small, r_π is large, and the $f_m = 1/C_T r_\pi$, Miller cut-off frequency, is low $\sim 2\text{KHz}$. Shot noise, low-pass filtered across the parallel combination of r_π and C_T , gives at sufficiently high frequencies,

$$S_{HR_S} = \frac{2eI_B}{1 + \omega^2 C_T^2 r_\pi^2} , \quad (9)$$

the observed $1/f^2$ roll-off.

To bias the transistor with a low R_S , the voltage divider circuit shown in Figure 6 was used. In this situation we neglect the terms in eq. (5), which are proportional with R_S and R_S^2 . Using $g_m = \beta/r_\pi$ and neglecting R_S and r_b with respect to r_π , we see that we can plot (again in $\text{amp}^2 \text{ sec}$).

$$S_{LR_S} = \frac{M^2}{\Delta f} \left[\frac{1}{R_L^2} \right] = 2eI_C + 4kT r_b g_m^2 + S_{ifc} + S_{ifb} r_b^2 g_m^2 . \quad (10)$$

This was done in Figure 5 (Curves I, II, III) at the same three I_B 's used in the high R_S experiment in order that the high and low R_S spectra can be quantitatively compared.

It should be noted that eq. (10) is only valid for $R_s \ll r_b$. In practice, however, R_s was of the same order of magnitude as r_b at low I_E ($R_s \approx 50$). As a consequence, the thermal noise generated by R_s cannot be neglected and has to be incorporated in eq. (10). The expression for S_{LR_s} becomes

$$S_{LR_s} = 2eI_c + 4kT(r_b + R_s)g_m^2 + S_{ifc} + S_{ifb}r_b^2g_m^2. \quad (11)$$

The observed white noise levels of the low R_s spectra were extrapolated by subtracting out the $1/f$ component and were found to lie above the shot-noise levels. We note from equation (11) that there are two contributors to the observed white-noise level, that due to I_c and that due to $(r_b + R_s)$. The difference between the observed white-noise level, $(S_{LR_s})_W$, and the collector shot noise ($2eI_c$) is attributed to $(r_b + R_s)$. Therefore, we have a way to calculate r_b since

$$\begin{aligned} \left(S_{LR_s} \right)_W - 2eI_c &= 4kT(r_b + R_s)g_m^2, \\ r_b &= \left[\left(S_{LR_s} \right)_W - 2eI_c \right] \frac{kT}{(2eI_c)^2} - R_s. \end{aligned} \quad (12)$$

The calculated values of r_b are indicated in the data table below. We notice that the base resistance decreases with increasing emitter current as it should for increasing injection, see van Vliet and Min [9] (the dependence is roughly as $1/I_E$; see also Spenke [10]).

Table of Data Obtained

Bias	Low R_s Data					High R_s Data			
	Curve	I_E	β	r_b	$(a)_{P\text{ MIN}}$	Curve	I_P	β	$(a)_{P\text{ MIN}}$
$I_B \approx 6\mu A$	I	2.25mA	340	4 Ω	1.72×10^{-6}	IV	6.7 μA	362	1.2×10^{-7}
$I_B \approx 3\mu A$	II	1.3mA	420	9 Ω	2.17×10^{-6}	V	3 μA	363	6.6×10^{-8}
$I_B \approx 1\mu A$	III	505 μA	413	20 Ω	1.86×10^{-6}	VI	1.2 μA	307	9.2×10^{-8}

To calculate the magnitudes of S_{ifc} and S_{ifb} , we look only at the $1/f$ portion of our spectra (i.e., at $f < 100$ Hz) where we are above the shot-noise level and can write, at low f ,

$$S_{LR_s} = S_{ifb}(r_b^2 g_m^2) + S_{ifc}, \quad (13)$$

and

$$S_{HR_s} = S_{ifb} + \frac{S_{ifc}}{\beta^2}. \quad (14)$$

Having two equations involving the two unknowns S_{ifc} and S_{ifb} , we solve for S_{ifc} and find

$$S_{ifc} = \frac{S_{LR_s} \left[\frac{1}{r_b g_m} \right]^2 - S_{HR_s}}{\left[\frac{1}{r_b g_m} \right]^2 - \frac{1}{\beta^2}}. \quad (15)$$

Now from inspection of Figure 5, we see $S_{HR_s} \ll S_{LR_s}$ at 1 Hz, and since

$$\left[\frac{1}{r_b g_m} \right]^2 = \left[\frac{r_\pi}{\beta r_b} \right]^2 \sim 1,$$

we can neglect $1/\epsilon^2$ and (15) simplifies to

$$S_{LR_s} = S_{ifc} \quad (16)$$

We see at low frequencies the low R_s bias configuration isolates S_{ifc} .

Solving S_{ifb} we find

$$S_{ifb} = S_{HR_s} - \frac{S_{LR_s}}{\epsilon^2} \quad (17)$$

From our data, S_{LR_s} is a factor of ten less than S_{HR_s} at 1 Hz, and we see the high R_s configuration essentially isolates S_{ifb} .

Now that the noise sources have been identified, we must apply the results of the fluctuation theory equations (1) and (2) to calculate the value of the noise parameter α . Since the low R_s experiment isolated collector noise, we have

$$S_{LR_s} = S_{ifc} \approx S_{I_{Ep}} \quad (18)$$

Solving for α_p and using equation 2, we have

$$\alpha_p = \frac{S_{LR_s} f}{\pi f_T q I_E \ln \left[\frac{P(0)}{P(w_B)} \right]} \quad (19)$$

To estimate the ratio $P(0)/P(w_B)$ according to Kleinpenning [5, eq. (A7)], we have the inequality

$$P(0)/P(w) \leq w v_s / D_p \quad (20)$$

where v_s is the saturated drift velocity. Using this permits us to calculate

a minimum value for α . Further, we know

$$w_B = \sqrt{\frac{D_P}{\pi f_T}}. \quad (21)$$

For our silicon PNP with $f_T = 200$ MHz, $w_B = 1.35$ μm . Using $v_s \approx 10^7$ cm s^{-1} , we calculate $\ln[P(0)/P(w_B)] \leq 4.75$. This value, used in eq. (19), gives the minimum values of α_p tabulated in the data table for S_{LR_s} evaluated at 1.Hz. Values of $\alpha_p \approx 10^{-6}$ are small but typical of silicon at room temperature according to Bosman et al. [6, Fig.5].

For the case of base 1/f noise, we have

$$S_{HR_s} \approx S_{ifb} \approx S_{I_{En}}, \quad (22)$$

and using the base to emitter expression (3) we have, for α_n ,

$$\alpha_n = \frac{S_{HR_s} f^{2\tau_{dn}}}{q I_B \ln \left[\frac{N(0)}{N(w_E)} \right]}, \quad (23)$$

since $I_{En} = I_B$ in a P^+NP transistor. We saw for the case of holes the \ln term in the denominator did not significantly affect the order of magnitude of α , and we expect a similar case for electrons. We take $\ln[N(0)/N(w_E)] \leq 5$. since we expect the ratio of electrons in the emitter to be a few orders of magnitude greater than the ratio of holes in the base due to the high recombination of electrons in the heavily doped emitter. Using this and the approximation that $\tau_{dn} \approx \tau_{dp}$ suggested by van der Ziel [5], we calculated the minimum values of α_n which are tabulated in the table for S_{HR_s} evaluated at 1 Hz. Here we see the values of α_n are one or two orders of magnitude lower than α_p , which at first glance seems to imply that recombination current fluctuations, Cause 1, still account for base 1/f noise. However, we realize that we have a P^+NP

device where the emitter is heavily doped and our observed α_n is diminished by an impurity mobility reduction factor. We have, according to Hooge et al. [7, eq.(8.10)],

$$\alpha_{\text{observed}} = \left[\frac{\mu_{\text{imp}}}{\mu_{\text{latt}}} \right]^2 \alpha_{\text{true}} \quad (24)$$

From the study by Jacoboni et al. [8, Fig.5], we see, for an impurity concentration $\approx 7 \times 10^{18} \text{ cm}^{-3}$, the ratio of $\mu_{\text{imp}}/\mu_{\text{latt}} \approx 1/10$. Using eq. (24), we obtain a minimum value of $\approx 10^{-5}$ for $(\alpha_n)_{\text{true}}$.

Bosman et al. report α values ranging between 10^{-5} and 10^{-3} for electrons in n-type silicon. Hence we conclude that the $1/f$ noise in the base of transistors can also be attributed to a mobility-fluctuation mechanism, similar to the one causing the collector $1/f$ noise.

References

- [1] W.H. Fonger, Transistors I, R.C.A. Laboratories, N.J. (1956).
- [2] J.L. Plumb and E.R. Chenette, I.E.E.E. Trans. ED-10, 304 (1963).
- [3] F.N. Hooge, Physica 60, 130 (1972); Physica 83B, 14 (1976).
- [4] T.G.M. Kleinpenning, Physica 98B, 289 (1980).
- [5] A. van der Ziel, Solid State Electronics 25, 141 (1982).
- [6] G. Bosman, R.J.J. Zijlstra, and A. van Rheenen, Physica 112B, 193 (1982).
- [7] F.N. Hooge, T.G.M. Kleinpenning, and L.K.J. Vandamme, Reports on Progress in Physics 44, 515 (1981).
- [8] C. Jacoboni, C. Canali, G. Ottaviani, and A. Alberigi Quaranta, Solid State Electronics 20, 82 (1977).
- [9] K.M. van Vliet and H.S. Min, Solid State Electronics 17, 267 (1974).
- [10] E. Spenke, Z. Angewandte Physik 10, 65 (1958).

III. High Frequency Amplifier and Noise Diode (J. Andrian)

a. Amplifier

We need a standard noise source and high-frequency amplifier to perform noise measurements in the high-frequency range. We can have that by using 5 dual gate amplifiers in parallel with a common source as output, see Fig. 7.

We give one stage in Fig. 8a. This configuration has a very good performance at high frequencies.

The output stage is necessary to match impedance, see Fig. 8b.

b. Standard noise source

The idea is to have a flexible noise source using a noise diode (5722). The circuit used to build that noise source is given in Fig. 9.

IV. 1/f Fluctuations in Radioactive Decay Rate (Jeng Gong)

The block diagram of the counting system being used to investigate 1/f fluctuations in α -particle emission rate is shown in Figure 10. The source is ${}_{95}\text{Am}^{241}$, which decays with a half-life of $T_{1/2} = 458$ years with the emission of 5.48 MeV α -particles into ${}_{93}\text{Np}^{237}$. The detector, a silicon surface barrier detector, is reverse-biased at 80 volts, and the dead time of the Analog to Digital Converter and Multi-Channel Analyzer are 6 n-seconds and 6 μ -seconds respectively. Therefore, no dead-time correction is necessary, as long as the counting rate is kept lower than 1000 counts per second (or the averaged time elapse between two counts is higher than 1000 μ -seconds).

Based on van Vliet and Handel's Allan variance transform theory (see section C), the Allan variance, $\sigma_{M_T}^2$, for Poissonian shot noise with spectrum $S_m(\omega) = 2m_0$, equals $m_0 T$. Where m_0 is the average counting rate in the

time interval $(t, t+T)$, and $m_0 T$ is the averaged total counts for a time interval T . For $1/f$ noise with a spectrum of $S_m(\omega) = 2\pi C/|\omega|$, the Allan variance is $2CT^2 \ln 2$.

For suppose that the radioactive decay is composed of white noise, i.e., $\sigma_{M_T}^2 = m_0 T + 2CT^2 \ln 2$; recall that $\langle M_T \rangle = m_0 T$, then a measurement of $R(T) = \sigma_{M_T}^2 / \langle M_T \rangle^2$ yields $R(T) = 1/m_0 T + 2C' \ln 2$, where $C' = C/m_0^2$ is a constant in the order of 10^{-6} . For short time intervals the term $1/m_0 T$ is dominant; hence $R(T)$ is proportional to $1/T$. When T is long enough, $2C' \ln 2$ becomes dominant; $R(T)$ is, therefore, a constant.

The measured $R(T)$ versus $1/T$ is shown in Figure 11. It shows clearly that for T small $R(T)$ is proportional to $1/T$, for T large $R(T)$ becomes independent of T . The 200-minute measurement, $R(200)$, is 53% higher than Poissonian noise, which indicates that $1/f$ noise becomes comparable to shot noise at this frequency ($1/200$ minutes = 8.3×10^{-4} Hz). A measurement of $R(400)$ gives a value very close to that of $R(200)$'s, which is strong evidence that $1/f$ fluctuations do exist in α -particle emission rate, since we expect $R(T)$ to be a constant for $1/f$ noise, when T is long enough.

The points in Figure 11 don't fall on the line very well; this is due to small sampling size (only seven sets of data were acquired for 400-minute measurements). In order to determine the minimum number of intervals needed for an accurate measurement, we then plot $R(T)$ versus the number of intervals, N , for different T 's. These figures show that when N is small, $R(T)$ is spread over a wide range; when N is increased, $R(T)$ is converged, and finally reaches a stable value.

For example: Figure 12 shows that for $T=100$ minutes, 21 sets of measurement give $R(T) = (7.09 \pm 3.94) \times 10^{-7}$; for $N=24$, $R(T) = (7.23 \pm 2.14) \times 10^{-7}$; for $N=27$, $R(T) = (7.13 \pm 1.85) \times 10^{-7}$. Here $R(T)$ is given in the

form of (mean value \pm standard deviation). From Figure 13 we know that for $T=1$ minute at least 70 sets of measurements are necessary for a reliable value of $R(T)$. Figure 14 shows that for $T=3$ minutes we need $N \geq 50$.

According to the above analysis, we then measured $R(T)$ several times, with sufficient number of intervals contained in each measurement. The averaged values of $R(T)$ are shown in Figure 15, which is much more reliable than the results shown in Figure 11. From Figure 15 we see that 400 minutes is still not long enough to obtain a constant $R(T)$; longer time measurements are necessary.

In Figure 16 we show the comparison of Allan variance and normally defined variance,

$$\sigma^2 = \frac{1}{N-1} \sum_{i=1}^N (M_i - \langle M \rangle)^2,$$

from which we see that for T small $\sigma_{M_T}^2$ is proportional to T , for T large it shows the tendency of T^2 . The normal variance shows similar behavior; however, it does not behave so well as the Allan variance does. Hence the Allan variance is the better tool to investigate $1/f$ fluctuations in counting experiments.

V. Noise in Near-Ballistic n^+nn^+ and n^+pn^+

Gallium Arsenide Submicron Diodes

(R.R. Schmidt, G. Bosman, C.M. van Vliet; L.F. Eastman
and M. Hollis, Cornell University, Ithaca, N.Y.)

a. Abstract

D.c. characteristics and noise measurements in the range 1 hz - 25 khz are reported for n^+nn^+ and n^+pn^+ near-ballistic devices, with n regions (p regions) of $0.4\ \mu\text{m}$ ($0.45\ \mu\text{m}$), fabricated by molecular beam epitaxy at Cornell. The n^+nn^+ mesa structures show very low $1/f$ noise, indicating a Hooge parameter $\alpha_H = 2 \times 10^{-8}$. This very low noise is attributed to the near absence of phonon collisions. The thermal (-like) noise above 1 khz is equal to Nyquist noise at the lowest currents, rising to slightly above Nyquist noise for high currents, indicating the presence of carrier drag effects. The n^+pn^+ noise, on the contrary, is quite high. It seems to be associated with the current which is present below punch-through. The spectral shape indicates a diffusion origin. The importance of noise measurements for discriminating between the various existing d.c. current treatments is discussed.

b. Introduction

Submicron gallium arsenide structures are of great current interest, since they permit ballistic or near-ballistic electron flow, which in turn leads to carrier velocities that far exceed the saturation velocity in collision-dominated conduction, thus enabling the design of picosecond switching devices and other novel applications. The fabrication of submicron devices has been made possible by modern MBE techniques, electron lithography, etc. For GaAs near-ballistic behavior requires that the distance to be traveled by the injected electrons is less than or of the order of $0.7\ \mu\text{m}$. Eastman et al. report¹⁾ that the mean free path for phonon emission into optical polar modes at room temperature is $0.1\ \mu\text{m}$ for electrons of 0.05 eV, and

0.2 μm for electrons of 0.5 eV. Phonon absorption has a longer mean free path and can be neglected for the devices reported here, having thicknesses of 0.4 μm (thickness of n layer in n^+nn^+ devices) and 0.45 μm (thickness of p layer in n^+pn^+ devices). At higher electron energy intervalley scattering becomes important, thus limiting the near-ballistic range to about 0.5 eV of electron energy. In a sample of 0.4 μm thickness about two phonon emissions may occur. These involve, however, small angle deflections only ($5^\circ - 10^\circ$) and have little effect on the d.c. carrier characteristics, according to Ref. 1.

The theory for "pure" ballistic behavior (no collisions suffered whatsoever) was developed by Shur and Eastman in 1979 in a basic paper on this topic²⁾. They solve Poisson's equation, allowing for space charge of both fixed ionized donors (or acceptors) and injected carriers. Employing boundary conditions which neglect the initial thermal energy of the electrons injected from the n^+ into the n layer (or p layer after punch-through), they find the solid state analog of Child's law in vacuum tubes. For sufficiently small voltages there is a domain in which the current I goes as $V^{1/2}$; when the injected space charge exceeds the fixed charge due to the ionized donors or acceptors, the characteristic changes, however, to the familiar $V^{3/2}$ form. In Ref. 1 measurements are presented which fairly well support these predictions, providing the nonparabolicity of the bands and the onset of intervalley scattering at higher voltages are taken into account. In a later theory, Shur³⁾ and Shur and Eastman⁴⁾ extended the theory to that for "near-ballistic" devices, in which few collisions can occur. Since the Boltzmann equation would be inappropriate for that regime, the collisions are taken into account by adding momentum and energy "drag terms" to the otherwise

ballistic equations of motion. In this way, the transition from Child's law ($\tau \rightarrow \infty$, where τ is the collision time) to the Mott and Gurney law, $I \propto V^2$ (finite τ) is covered by this approach.

Two modifications have been proposed by others, which may have a bearing on the present paper. First, Rosenberg, Yoffa and Nathan⁵⁾ discuss the effects of "spillover" of carriers at the n^+n high-low junction. This means, in essence, that the boundary conditions must be changed to account for the depletion of n^+ regions and spillover into the adjacent Debye lengths. As a result, the effective width of the n region is smaller and the current is higher than that computed in Ref. 2. Secondly, Cook and Jeffrey⁶⁾ have indicated that the energy or velocity distribution of the electrons cannot be neglected. The velocity dispersion is accounted for by the introduction of an electron temperature gradient term in the momentum balance equation (op cit eq. (8)). Though they argue that this leads to the occurrence of a potential minimum somewhere beyond the "cathode"--rather than at the cathode--similar to Langmuir's treatment of vacuum diodes, we have great reservations about their treatment, as we discuss in section 5. Undoubtedly, however, the inclusion of the velocity dispersion is essential, if not for the d.c. characteristic, yet certainly for the velocity-fluctuation noise.

In this paper we will describe both low-frequency and high-frequency noise measurements on near-ballistic devices. These measurements are preliminary, in that a full-scale investigation, involving a variation of dimensions, temperature, and magnetic field, is still underway. However, definite results at room temperature for n^+nn^+ and n^+pn^+ devices of $0.4 \mu m$ and $0.45 \mu m$, respectively, will be reported. Such measurements serve a threefold purpose. First, from a practical point of view, noise data reveal the practical performance limitations of the novel high-speed devices. As we will indicate--

the noise of the n^+nn^+ devices is extremely low; the n^+pn^+ devices, however, fare much worse. Secondly, noise measurements at audio and subaudio frequencies shed much light on the $1/f$ noise problem. According to most recent theories, such noise is thought to be caused by mobility fluctuations (see, e.g., Hooge et al.⁷⁾ and van der Ziel⁸⁾. If collisions in the near-ballistic regime are rare, one expects the $1/f$ noise to be very low and ultimately, in "pure" ballistic devices, to be absent. Our preliminary work in n^+nn^+ devices indicates that this could be correct. Third, and not least, we believe that the high-frequency noise (thermal, velocity-fluctuation, or diffusion noise) will shed much light on the mode of operation of near-ballistic devices. To date, no full-fledged theory for such noise exists; we only have some preliminary computations by van der Ziel and Bosman⁹⁾¹⁰⁾. However, once this noise is understood, we will have a powerful means of substantiating or amending the various theories mentioned in this introduction. We come back to this in the discussion of the results, section f.

c. Experimental

The near-ballistic diode (NBD) is a sandwiched mesa structure of five lightly doped p or n layers, alternating with heavily doped n^+ layers, see Fig. 17. The doping densities of the various regions are 10^{18} cm^{-3} for the n^+ regions, approximately $2 \times 10^{15} \text{ cm}^{-3}$ for the n regions and approximately $6 \times 10^{14} \text{ cm}^{-3}$ for the p regions. The diameter of the mesas is $100 \mu\text{m}$. The devices were manufactured by molecular beam epitaxy at the Cornell University Submicron Research Facility. The mesas were provided with very low ohmic Au-Ge contacts. A low-frequency equivalent circuit of the n^+nn^+ device is given in Fig. 18. The main element (n regions) has a resistance of order 0.75Ω . For the n^+pn^+ devices the p layers gave a resistance of order 90Ω at 1 mA ; the parasitic resistances in this case were negligible.

The characteristics of the two types of devices are quite different. The noise measurement of the n NBD's, in particular, was a challenge. To do this we used the setup shown in Fig. 19. A Hewlett Packard 3582 spectrum analyzer, featuring a dual channel fast Fourier transform method, was employed. By measuring the coherence (square of the correlation) between the two channels, noise levels significantly below the noise level of the preamplifier could be detected. For the preamplifiers we used five common emitter transistors GE82 in parallel. This resulted in a 7Ω noise resistance for frequencies above 20 hz. The equivalent noise resistance of the cross-correlation setup is not known at this moment, but is believed to be a few tenths of an ohm, thus enabling us to measure the thermal noise of the 0.75Ω devices.

The d.c. I-V characteristic of an n-type device is shown in Fig. 20. In contrast to the device reported in Ref. 1, there is no clear \sqrt{V} region; however, the slope seems to be less than one for very low currents. As in Ref. 1, the $V^{3/2}$ region is never reached for reasons indicated in the introduction. In the range of interest for the noise measurements, the characteristic was essentially linear with $R_x = 0.75\Omega$. This is also confirmed by the a.c. resistance measurements in Fig. 21.

The d.c. I-V characteristic of a p-type device is shown in Fig. 22. The device is linear up to a current level of 1 mA, corresponding to about $R_x = 90\Omega$. The slope then increases to a value of about 3 in the 10 to 100 mA range. Finally, at very high currents the slope becomes less, perhaps approaching three-halves and the slope falls off. The a.c. resistances are again flat for all measured frequencies (up to 25 khz).

d. Noise of n^+nn^+ device

The magnitude of the noise current spectrum for four different currents, in the frequency range 1 hz - 25 khz, is shown in Fig. 23. Thermal levels and

excess $1/f$ noise are seen. To determine the thermal (\sim like) noise levels, the $1/f$ components are subtracted. The results are shown in Fig. 24. The levels are averaged over the frequencies for which there is a plateau (1 kHz - 25 kHz; the 75 mA curve may, however, show some g-r noise from 1 kHz - 7 kHz; the thermal-like noise occurs for 7 kHz and higher). The ratio of these averages to $4 kT/0.75$ is plotted versus bias current in Fig. 25. We note that there is an indication that the noise exceeds the true thermal noise $4 kT/R_x$ at the higher bias currents.

The $1/f$ slope of the noise for the higher current levels is clearly seen, and straight-line approximations are made to the data. The values so obtained at 10 Hz are plotted versus bias current in Fig. 26. We note that the expected behavior for $1/f$ noise, $S_I \propto I^2$ is well satisfied.

e. Noise of n^+pn^+ device

The noise current spectrum versus frequency for several bias currents of an n^+pn^+ device is shown in Fig. 27. The excess low frequency noise of this device is orders of magnitude larger than for the n-type device. Another notable feature is the frequency dependence, which shows a slope of $f^{-0.7}$ to $f^{-0.8}$. Extrapolating to the corner frequency above which thermal noise dominates gives a value of over 100 MHz for even the lowest (100 μ A) bias current.

The dependence of the noise current at 100 Hz on bias current is displayed in Fig. 28. There is an I^2 dependence up to about 1 mA. At higher currents the noise increases less fast.

f. Discussion of n^+pn^+ results

The I-V characteristic is not very pronounced in its deviation from strict linearity, yet it may represent near-ballistic behavior¹⁾.

1. 1/f noise

In 1969 Hooge developed the following empirical formula for 1/f noise:

$$S_{\Delta I}(f)/I^2 = \alpha_H/fN \quad (5.1)$$

where f is the frequency, N the total number of carriers in the sample contributing to the noise, and α_H is Hooge's parameter. Initially, α_H was thought to be a constant, of order 2×10^{-3} . Later on, it was found that material variations for α_H do occur, whereas, in addition, α_H decreases as $(\mu/\mu_L)^2$ if impurity scattering dominates over lattice scattering (μ_L); Bosman, Zijlstra, and van Rheenen¹¹⁾ also found that α_H decreases due to carrier heating. In a nonhomogeneous sample in which the carrier density is a function of position, $n(x)$, such as occurs in our mesas due to spillover (section 1) and injection, eq. (5.1) must be modified. It is easily shown (van der Ziel and van Vliet¹²⁾) that in that case (5.1) is to be replaced by

$$S_{\Delta I}(f)/I^2 = (\alpha_H/fAL^2m) \int_0^L \frac{dx}{n(x)} \quad (\text{ballistic case}) \quad (5.2)$$

where m is the number of n layers in series, L the width of one n layer, and A the cross section. Whereas the detailed profile $n(x)$ is complex, we see from Ref. 2, Fig. 3, that for most of the layer $n(x) \approx 0.7n_0$, where n_0 is the doping density. With this estimate we obtain for α_H from Fig. 26. $\alpha_H = 2.2 \times 10^{-8}$. If, on the other hand, the diode is not ballistic but collision limited, we proved in Ref. 12,

$$S_{\Delta I}(f)/I^2 = \alpha_H(9\mu R_x)/L_{\text{tot}}^2 f \quad (\text{collision limited}) \quad (5.3)$$

where $L_{\text{tot}} = mL$ is the total width of the n layers and R_x is the total

observed resistance, while μ is the lattice mobility. Taking for the latter 8,500 cm²/V sec, we obtain: $\alpha_H = 6.2 \times 10^{-8}$.

While the value of α_H for bulk GaAs is not known at present, we may surmise that it is of the same order as for other semiconductors in which lattice scattering dominates, say 10^{-5} . Thus, whatever model is used, the above values for α_H are extremely low, thus confirming that collisions are mainly absent in this device. Moreover, if Handel's theory of 1/f noise is valid¹³⁾, very low noise can be expected from those collisions which still occur, involving polar phonon emission. As we noticed, the deflection angle θ for such processes is very small, whereas in Handel's theory of quantum 1/f noise, the magnitude goes as $\sin^2 \frac{1}{2} \theta$. Measurements on 0.24 μ devices are in the planning stage. It is hoped that for these devices α_H shows a continued decrease. So far, the results are the best confirmation yet that 1/f noise is caused by lattice phonon collisions.

2. Thermal noise

The designation "thermal noise" is used here for the thermal-like noise observed at high frequencies. In a collision-limited device this noise is due to the diffusion-noise source, which by Einstein's relation transforms to a thermal-noise source for cold electrons. In the space-charge limited injection operation (Mott Gurney law), the noise becomes then $8 kT/R_x$, see ¹⁰⁾¹⁴⁾. In a "pure" ballistic device, on the other hand, this noise is due to shot noise. However, the vacuum case shows that the noise is distinctly governed by the velocity distribution of the omitted particles. Thus, a treatment as the Child's law analog of Ref. 2 will not suffice to obtain the noise; the latter must be patterned after Langmuir's derivation of the d.c. characteristic; see in particular the noise treatment by D.O. North¹⁵⁾ and Schottky and Spenke¹⁶⁾. Lacking a detailed theory, van der Ziel and Bosman⁹⁾ indicated, nevertheless, that subthermal noise,

$0.4kT/R_x$ with $\theta < 1$, can be expected. This is not corroborated by the results of Fig. 25. While it is very unlikely that the collision-limited case applies--in view of the low $1/f$ noise reported above--it is likely that carrier drag effects, such as considered in Refs. 3, 4, and 6, take place. These effects should be considered, by considering a Langevin equation patterned after the momentum and energy balance equations of Shur and Eastman³⁾⁴⁾, but with velocity dispersion at $x = 0$. The approach of Cook and Frey, on the other hand, which includes collective velocity dispersion effects in the momentum balance equation of a single electron, seems highly inappropriate; noise theory in vacuum tubes tells us that, in the space-charge suppressed ballistic case, the carriers in different velocity groups fluctuate independently. For the near-ballistic regime with corner drag effects, the same independence can be expected. Thus, as stated in the introduction, the development of a complete noise theory for near-ballistic devices may aid considerably in discriminating between the various existing approaches employed for the d.c. behavior.

g. Discussion of n^+pn^+

These devices showed large excess noise. The noise is not very close to $1/f$. If, nevertheless, we apply Hooge's formula, at 10 Hz and 100 μA , we obtain $\alpha_H \approx 3 \times 10^{-3}$.

For $V \geq 200$ mV, the I-V characteristic of Fig. 22 is in reasonable agreement with the theoretical predictions and previously reported result¹⁾. The current below the punch-through voltage (≈ 150 mV) is not well understood.

It is significant to note, however, that the character of the noise, in particular its spectral shape, does not change when we pass the punch-through voltage, see Fig. 27; only, above the punch-through voltage, the noise magnitude starts to decline, going no longer as I^2 , see Fig. 12. This

can be explained if the current above punch-through is composed of two parts, I (punch-through) and I (normal). Extrapolating the data below 150 mV to higher voltages (see dashed line in Fig. 22), we can replot the noise versus I (punch-through) rather than versus the total current. Thus, if the abscissa in Fig. 28 is interpreted as I (punch-through) only, all points (see the *) fall now on the line for I^2 (punch-through).

Altogether, it seems to us highly doubtful that the low-frequency noise is mobility-fluctuation $1/f$ noise of the Hooge type. Rather, it seems that the spectra represent a one-dimensional diffusion process (for low frequencies such a process goes as $f^{-0.5}$,¹⁷⁾). If the diffusion is due to ambipolar hole-electron motion in the floating base of the n^+pn^+ device, the effect should be determined by $D_p \left(\frac{p+n}{n} \right)$ in this case, since the electrons are near-ballistic. The turnover frequency $\approx D_p/2\pi L^2$ lies at 10^9 Hz. It is thus reasonable that for audio frequencies, with the effect rising as $\omega^{-0.5}$ or steeper, there is a large low-frequency tail. Whatever the cause of the effect, it seems to be associated with the presence of current (diffusion current?) below punch-through. We finally remark that similar-type spectra, going slower than $1/f$, were observed in $6\mu m$ p^+np^+ punch-through diodes by van de Roer¹⁸⁾.

h. Conclusions

Near-ballistic n^+nn^+ devices exhibit extremely low $1/f$ noise, with a Hooge parameter of 2×10^{-8} . This indicates that the $1/f$ noise is probably caused by lattice scattering (possibly due to polar optical phonon emission), which is rare in the near-ballistic regime. The thermal noise of these devices is slightly higher than Nyquist noise for the highest current levels observed. It indicates a near-ballistic origin, affected by carrier drag effects and by the velocity dispersion of the injected carriers.

Near-ballistic n^+pn^+ devices exhibit very large low-frequency excess noise, probably of a diffusion origin. The noise seems to be associated with the current denoted as I (punch-through), which is present below the punch-through voltage. The noise rises as I^2 (punch-through), the latter being also extrapolated from Fig. 27 above the punch-through voltage. Thermal noise for these devices, requiring measurements above 100 Mhz, have not yet been carried out.

Similar measurements on n^+nn^+ diodes are being reported by Peczalski, van der Ziel, and Hollis¹⁹⁾.

Acknowledgements

We are indebted to Professor A. van der Ziel for discussions and encouragement, and for exchange of preliminary data by the Minnesota group.

References

1. M.S. Shur and L.F. Eastman, Electronics Lts. 16, 522 (1980); also L.F. Eastman, R. Stall, D. Woodard, N. Dandekar, C.E.C. Wood, M.S. Shur, and K. Board, Electronics Lts. 16, 524 (1980).
2. M.S. Shur and L.F. Eastman, IEEE Trans. Electr. Dev. ED-26, 1677 (1979).
3. M.S. Shur, IEEE Trans. Electr. Dev. ED-28, 1120 (1981).
4. M.S. Shur and L.F. Eastman, Solid St. Electr. 24, 11 (1981).
5. J.J. Rosenberg, E.J. Yoffa, and M.I. Nathan, IEEE Trans. Electron Dev. ED-28, 941 (1981).
6. R.K. Cook and J. Frey, IEEE Trans. Electron Dev. ED-28, 951 (1981).
7. F.N. Hooge, T.J.G. Kleinpenning, and L.K. van Damme, Reports Progress in Physics 44, 479 (1981).

8. A. van der Ziel, *Advances in Electronics and Electron Physics* (Martin, ed.) 49, 225 (Academic Press, New York, 1979).
9. A. van der Ziel and G. Bosman, "Near thermal noise in short solid state diodes; I, ballistic regime." Submitted to Physica Status Solidi.
10. A. van der Ziel and G. Bosman, *ibid*; "II, Collision-limited regime." Submitted to Physica Status Solidi.
11. G. Bosman, R.J.J. Zijlstra, and A.D. van Rheezen, *Phys. Ltrs.* 78A, 385 (1980); *ibid*, 80A, 57 (1980).
12. A. van der Ziel and K.M. van Vliet, Physica Status Solidi (submitted).
13. P.H. Handel, *Phys. Rev.* A22, 745 (1980).
14. K.M. van Vliet, A. Friedmann, R.J.J. Zijlstra, A. Gisolf, and A. van der Ziel, *J. Applied Physics* 46, 1804 (1975).
15. D.O. North, *RCA Review* 4, 441 (1940); 5, 106 (1941).
16. W. Schottky and E. Spenke, *Wissenschaftliche Veröffentlichungen aus den Siemens-Werken* 16, 1 (1937).
17. K.M. van Vliet and J.R. Fassett, in Fluctuation Phenomena in Solids (R.E. Burgess, ed.), p. 334 (Academic Press, New York, 1965).
18. Th. G. van de Roer, *Solid State Electr.* 23, 695 (1980).
19. A. Peczalski, A. van der Ziel, and M. Hollis (to be published).

C. THEORY DEVELOPED UNDER THE GRANT

I. Proposed Discrimination between 1/f Noise Sources in Transistors
(A. van der Ziel)

a. Summary

There are four possible 1/f noise sources in transistors; the two most important ones are recombination 1/f noise in the emitter space charge region and mobility fluctuation 1/f noise in the collector current. It is shown that an extension of the Plumb-Chenette procedure can discriminate between these possibilities.

b. 1/f noise sources in transistors

There are four possible 1/f noise sources in p-n-p transistors:

- 1) 1/f noise in the recombination current I_R of the emitter space-charge region, either at the surface or at dislocations. The first is usually attributed to fluctuations in the surface recombination velocity, as first introduced by Fonger¹ and verified by Hsu et al.². For an alternate but less likely interpretation see Kleinpenning³.
- 2) Mobility fluctuation 1/f noise in the hole current I_{Ep} flowing from the emitter to the collector.
- 3) Mobility fluctuation 1/f noise in the electron current I_{En} flowing from the base into the emitter.
- 4) Resistance fluctuation 1/f noise in the base resistance r_b of the transistor. Because the base current I_B is relatively small in a good transistor, this is probably a very small effect.

The mobility fluctuation $1/f$ noise was recently introduced by Kleinpenning³ in his discussion of $1/f$ noise in p^+-n diodes. We shall see that source (3) is small in comparison with source (2), so that the most significant noise sources are (1) and (2).

There is considerable evidence, mostly assembled by Hooge and his coworkers, that $1/f$ noise in semiconductors and semiconductor devices can come from mobility fluctuations⁴. Because of the Einstein relation, fluctuations in the mobility μ_p imply fluctuations in the diffusion constant D_p . For since

$$qD_p = kT\mu_p \text{ we have } q\delta D_p = kT\delta\mu_p \quad (1)$$

and we can write with Kleinpenning³

$$\frac{S_{D_p}(x, x', f)}{D_p^2} = \frac{S_{\mu_p}(x, x', f)}{\mu_p^2} = \frac{\alpha}{fP(x')} \delta(x' - x) \quad (2)$$

where α is the Hooge parameter, f the frequency, $P(x')$ the hole concentration for unit length at x' in the base and $\delta(x'-x)$ the Dirac delta function.

Kleinpenning³ has calculated the hole current noise spectrum in a short p^+-n diode due to mobility fluctuations. Since the base region of a p^+-n-p transistor corresponds to a short p^+-n diode with an infinite recombination velocity at the contact to the n -region, his equation (59) can be applied directly. Assuming negligible recombination in the

base and relatively small injection, we thus obtain for the spectrum of the emitter-collector current I_{Ep}

$$S_{I_{Ep}} = \frac{qD_p I_{Ep}^\alpha}{w^2 f} \ln \left(\frac{P(o)}{P(w)} \right) = 2qI_{Ep} \frac{\alpha}{4f\tau_{dp}} \ln \left(\frac{P(o)}{P(w)} \right) \quad (3)$$

where $\tau_{dp} = w^2/2D_p$ is the diffusion time for holes through the base region, w the base width and $P(o)$ and $P(w)$ are the hole concentrations for unit length at the emitter side and the collector side of the base, respectively.

In the same way we have for the $1/f$ noise of the electron current I_{En} injected from the base into the emitter

$$S_{I_{En}}(f) = 2qI_{En} \frac{\alpha}{4f\tau_{dn}} \ln \left(\frac{N(o)}{N(w_E)} \right) \quad (4)$$

where $\tau_{dn} = w_E^2/2D_n$, w_E the width of the emitter region, D_n the electron diffusion constant in the emitter region, whereas $N(o)$ and $N(w_E)$ are the electron concentrations for unit length at the base side of the emitter and at the emitter contact, respectively.

Since I_{En} is about two orders of magnitude smaller than I_{Ep} in a good p^+-n-p transistor, whereas τ_{dn} and τ_{dp} are of the same order of magnitude, $S_{I_{En}}(f)$ will be about two orders of magnitude smaller than $S_{I_{Ep}}(f)$, so that process (3) is most likely insignificant.

Since the cut-off frequency f_T of the transistor is given by

$$f_T = (2\pi\tau_{dp})^{-1} \quad (5)$$

$S_{I_{Ep}}(f)$ is proportional to f_T , so that it is largest for microwave transistors.

The extension to n^+-p-n transistors is accomplished by interchanging n with p and N with P , respectively.

It will now be shown how one can discriminate between the noise sources of a p^+-n-p transistor. To that end we look at the current flow in the transistor; Fig.29a shows the currents I_{Ep} , I_{En} and I_R . The corresponding equivalent circuit for the noise current generators δI_{Ep} , δI_{En} and δI_R is pictured in Fig.29b. We note that δI_{Ep} is connected between emitter and collector and δI_{En} and δI_R are connected between emitter and base. There are thus two current generators i_{f1} and i_{f2} ; i_{f1} is connected between base and emitter and i_{f2} between collector and emitter. As seen by inspection

$$i_{f1} = -\delta I_R - \delta I_{En} ; i_{f2} = -\delta I_{Ep} \quad (6)$$

Due to this topology and with the help of the Plumb-Chenette approach we can now discriminate between i_{f1} and i_{f2} . In Fig. 30 the emitter resistance R_E is chosen so large that the emitter can be considered as being fed from a constant current source. An external resistance R_b is connected between base and ground and the collector is a.c. connected to ground.

According to Fig. 2 we have for the noise voltage v between emitter and ground, since $i_e = i_{f1} + i_{f2}$,

$$\begin{aligned} v &= (i_{f1} + i_{f2})r_{co} - \alpha_o i_e (R_b + r_b) + i_{f2}(R_b + r_b) \\ &= i_{f1}[r_{co} - \alpha_o(R_b + r_b)] + i_{f2}[r_{co} + (1 - \alpha_o)(R_b + r_b)]. \end{aligned} \quad (7)$$

We now determine $\overline{v^2}$ as a function of R_b . Since the first term in the second half of (7) is zero when

$$r_{co} - \alpha_o(r_b + R_b) = 0, \text{ or } R_b = r_{co}/\alpha_o - r_b, \quad (8)$$

the noise source i_{f1} gives rise to a sharp minimum in $\overline{v^2}$ versus R_b ; from the parabola thus obtained the value of $\overline{i_{f1}^2}$ can be determined. The existence of this parabola is an indication that the current generator i_{f1} is present.

The second term in the second half of (7) depends very slowly upon R_b because $(1 - \alpha_o)$ is a small number. By measuring the spectrum in the minimum of the $\overline{v^2}$ versus R_b curve, one can determine $\overline{i_{f2}^2}$. The reason is that the $1/f$ part of the spectrum comes from i_{f2} , whereas the frequency-independent part must be attributed to thermal noise and shot noise. This situation is pictured in Fig. 31.

If the effect of i_{f2} is extremely small, it may be assumed that δI_{En} is also negligible; the noise is then completely attributable to noise source (1). If the i_{f2} effect is appreciable, one can estimate the effect of $\overline{\delta I_{En}^2}$ and so determine the relative significance of the noise terms (1) - (3). We can then also determine Mooge's parameter from $\overline{i_{f2}^2}$.

We thus see that the discrimination between $1/f$ noise sources in transistors is possible by an extension of the Plumb-Chenette procedure. Experiments are on the way at the University of Florida to carry out this discrimination; we hope to report on these experiments at a later date.

Acknowledgement

The author is indebted to Dr. P.H. Handel, Dr. F.N. Hooge, Dr. T.G.M. Kleinpenning and Dr. L.K.J. Vandamme for helpful discussions and to Dr. Kleinpenning for private correspondence.

Appendix.

Since Kleinpenning's derivation of Eq. (3) is not easily followed, we derive it here with the help of the Klaassen-Prins method⁶. If $P(x)$ is the hole concentration for unit length at x , we have for small injection

$$I_{Ep} = -qD_p dP/dx \quad (A.1)$$

If we have fluctuations $\delta D_p(x, t)$ in D_p , they will drive fluctuations $\delta P(x, t)$ in P , so that $\delta I_{Ep}(t)$ depends on time only, at least if the junctions are a.c. short-circuited. Hence

$$\begin{aligned} \delta I_{Ep}(t) &= -qD_p \frac{d}{dx} [\delta P(x, t)] - q \frac{dP}{dx} \delta D_p(x, t) \\ &= -qD_p \frac{d}{dx} [\delta P(x, t)] + H(x, t) \end{aligned} \quad (A.2)$$

where

$$H(x, t) = -q \frac{dP}{dx} \delta D_p(x, t) = I_{Ep} \delta D_p(x, t) / D_p \quad (A.2a)$$

and

$$S_H(x, x', f) = I_{Ep}^2 S_{D_p}(x, x', f) / D_p^2 = I_{Ep}^2 [\sigma / f P(x')] \delta(x' - x) \quad (A.3)$$

Since $P(0)$ and $P(w)$ do not fluctuate if the junctions are a.c. short-circuited, $\delta P(0)$ and $\delta P(w)$ are zero. Multiplying both sides of (A.3) by dx , integrating over the base length w , and

bearing in mind the boundary conditions for $\delta P(0)$ and $\delta P(w)$, yields

$$\delta I_{Ep}(t) = \frac{1}{w} \int_0^w H(x,t) dx \quad (A.4)$$

Making a Fourier analysis yields

$$S_{I_{Ep}}(f) = \frac{1}{w^2} \int_0^w \int_0^w S_H(x,x',f) dx dx' = \frac{I_{Ep}}{w^2 f} \int_0^w \frac{I_{Ep}}{P(x)} dx \quad (A.5)$$

Substituting for I_{Ep} from (A.1) yields Eq. (3).

The value $P(0)/P(w)$ is easily estimated from the device dimensions and parameters. According to Kleinpenning (private correspondence)

$$I_{Ep} = qD_p P(0)/w \quad \text{and} \quad I_{Ep} \leq qP(w)v_s \quad (A.6)$$

where v_s is the saturation velocity of the carriers. Hence

$$P(0)/P(w) \leq wv_s/D_p \quad (A.7)$$

References.

1. W. H. Fonger, Transistors I, R.C.A. Laboratories, N.J. (1956).
2. S. T. Hsu, D. J. Fitzgerald and A. S. Grove, Appl. Phys. Lett., 12, 287 (1968); S. T. Hsu, Solid State Electron., 13, 843 (1970).
3. T. G. M. Kleinpenning, Physica, 98B, 289 (1980).
4. F. N. Hooge, Physica, 60, 130 (1972), Physica, 83B, 14 (1976); T. G. M. Kleinpenning, Physica, 77, 78 (1974), Physica, 94B, 141 (1978).
5. J. L. Plumb and E. R. Chenette, I.E.E.E. Trans., ED-10, 304 (1964).
6. F. M. Klaassen and J. Prins, Philips Research Repts. 22, 505 (1967).

II. On Mobility Fluctuations in 1/f Noise (C.M. van Vliet and R.J.J. Zijlstra, Physics Laboratory, State University Utrecht, The Netherlands)

a. Abstract

If 1/f noise, as expressed by Hooge's formula, is attributed to mobility-fluctuations noise, then the latter can be represented by a source $S_{\Delta\mu}/\mu_0^2 = \alpha_H/f$; there is no factor N in the denominator and there is no cross-correlation source, as claimed in the literature.

b. Introduction

The current opinion is that flicker or 1/f noise in metal films on semiconductors and devices is to be interpreted as a bulk effect; for a homogeneous sample with N current carriers subject to a mean current I_0 ; the current-fluctuation noise is expressed by Hooge's formula¹⁾

$$S_{\Delta I} = \alpha_H I_0^2 / fN \quad , \quad (1)$$

where α_H is Hooge's parameter, which supposedly can depend on the electrical field E_0 ²⁾ (often but not always of order 2×10^{-3}) and f is the frequency. Zijlstra²⁾ has shown that in nonhomogeneous samples or devices (1) is to be replaced by the noise of a current density source $H(\underline{r}, t)$, such that

$$\Delta J_{\underline{r}} = (\Delta J)_{\text{phen.}} + H(\underline{r}, t) + \eta(\underline{r}, t) \quad (2)$$

where $(\Delta J)_{\text{phen.}}$ is the current density fluctuation of the phenomenological laws, $\eta(\underline{r}, t)$ is the diffusion source (of no interest to us here), $H(\underline{r}, t)$ is the 1/f noise source with the cross correlation spectrum for $\overline{H(\underline{r}, t)H(\underline{r}', t)}$ being given by the tensor spectrum

$$S_{H(\underline{r}, \underline{r}', f)} = \alpha_H J_0(\underline{r}) J_0(\underline{r}') \delta(\underline{r} - \underline{r}') / f n_0(\underline{r}) \quad , \quad (3)$$

where $J_0(\underline{r})$ is the steady state current density and $n_0(\underline{r})$ the steady state local carrier density (here assumed to be electrons). For a homogeneous

sample integration of (3) over the sample leads to (1). If $\underline{\hat{J}}(\underline{r})$ is a curvilinear unit vector in the direction of $\underline{J}_0(\underline{r})$ and $\underline{\hat{J}} \underline{\hat{J}}$ the unit tensor, we also write $\underline{J}_0 = \underline{\hat{J}}_0 \underline{\hat{J}}$, $\underline{S} = S \underline{\hat{J}} \underline{\hat{J}}$, so that

$$S_{\underline{\hat{J}}}(\underline{r}, \underline{r}', f) = \alpha_H [J_0(\underline{r})]^2 \delta(\underline{r} - \underline{r}') / f n_0(\underline{r}) \quad . \quad (4)$$

It is now customary to write S_H in terms of conductivity-fluctuation noise S_σ . Since $\underline{J} = \sigma \underline{E}$, we have for the source in σ (σ is assumed to be a scalar), noticing that S_H represents a Norton source ($E = E_0$ is kept constant), $\Delta\sigma/\sigma_0 = \Delta J/J_0$; hence $\Delta\sigma = (\Delta\sigma)_{\text{phen.}} + \xi_\sigma$, with $\xi_\sigma/\sigma_0 = H/J_0$; this gives as spectrum

$$S_{\xi_\sigma}(\underline{r}, \underline{r}', f) = \alpha_H [\sigma_0(\underline{r})]^2 \delta(\underline{r} - \underline{r}') / f n_0(\underline{r}) \quad . \quad (5)$$

When now the conductivity-fluctuation noise is attributed to mobility fluctuation noise, it is further argued that (see Kleinpenning³⁾, van der Ziel⁴⁾), since $\sigma = e n \mu$, one has for fixed $n = n_0$: $\Delta\mu = (\Delta\mu)_{\text{phen.}} + \xi_\mu$, with $\xi_\mu/\mu_0 = \xi_\sigma/\sigma_0$; this gives a spectrum

$$S_{\xi_\mu}(\underline{r}, \underline{r}', f) = \alpha_H [\mu_0(\underline{r})]^2 \delta(\underline{r} - \underline{r}') / f n_0(\underline{r}) \quad . \quad (6)$$

However, even though $n(\underline{r})$ does not contribute to $1/f$ noise, this density remains a statistical quantity. Therefore, $\xi_\mu/\mu_0 \neq \xi_\sigma/\sigma_0$, so that (6) is incorrect.

c. Drift-velocity noise

A different view as to the connection with mobility-fluctuation noise was in principle already given by Zijlstra⁵⁾. Let $\underline{v}_{d_i} = \langle \underline{v}_i \rangle$ be the

drift velocity of the i th electron in a volume ΔV , centered on \underline{r} . Then

$$H(\underline{r}, t) = -\frac{e}{\Delta V} \sum_{i=1}^{N(\underline{r}, t)} \Delta v_i(t) \quad , \quad (7)$$

where $N(\underline{r}, t) = n(\underline{r}, t) \Delta V$. Since we do not consider g-r or diffusion noise, we may consider $n(\underline{r}, t) = n_0(\underline{r})$ is constant. However, to all likelihood the electrons in ΔV are scattered independently. Thus

$$S_H(\underline{r}, \underline{r}', f) = \frac{e^2 N(\underline{r})}{(\Delta V)^2} S_{\Delta v}(\underline{r}) (f) \quad (8a)$$

where $S_{\Delta v}(\underline{r})$ is the drift-velocity noise of any electron in the neighbourhood of \underline{r} . The cross correlation for different volumes ΔV centered on \underline{r} and \underline{r}' is zero since the velocity fluctuations are uncorrelated. Thus replacing in (8a) $1/\Delta V$ by $\delta(\underline{r} - \underline{r}')$ we also have

$$S_H(\underline{r}, \underline{r}', f) = e^2 n_0(\underline{r}) \delta(\underline{r} - \underline{r}') S_{\Delta v}(\underline{r}) (f) \quad . \quad (8b)$$

Comparison with (4) yields

$$S_{\Delta v}(\underline{r}) = \alpha_H [J_0(\underline{r})]^2 / e^2 [n_0(\underline{r})]^2 f = \alpha_H [\mu_0(\underline{r}) E_0(\underline{r})]^2 / f \quad . \quad (9)$$

With $v = \mu E_0$, this gives the mobility fluctuation noise

$$S_{\Delta \mu}(\underline{r}) = \alpha_H [\mu_0(\underline{r})]^2 / f \quad . \quad (10)$$

In the absence of hot electron effects μ does usually not depend on position, while also α_H is then independent of E_0 ; then

$$S_{\Delta \mu} = \alpha_H \mu_0^2 / f \quad . \quad (11)$$

Theories for $1/f$ noise caused by mobility fluctuations should therefore aim at explaining the simple relation (11) rather than the erroneous representation (6). We note, however, that for device applications it suffices to apply the current noise source (4); the origin of this source in terms of $S_{\xi_{\sigma}}$, $S_{\xi_{\mu}}$, or $S_{\Delta v_{\nu}}$ is immaterial. Where in the past the erroneous source spectrum (6) has been used, revision may be necessary.

References

1. F.N. Hooge, Physics Letters 29A (1969) 139.
2. R.J.J. Zijlstra, Noise in Physical Systems, Ed. D. Wolf, Springer, Berlin 1978, p. 90.
3. T.G.M. Kleinpenning, Physica 94B+C (1978) 141.
4. A. van der Ziel, Flicker Noise in Electronic Devices, in "Advances in Electronics and Electron Physics, Vol. 49, L. Marton and C. Marton, Eds., Academic Press, New York 1979, p. 225.
5. R.J.J. Zijlstra, Proc. Second International Symposium on $1/f$ Noise, K.M. van Vliet, Ed., University of Florida, Gainesville, Florida 1980, p. 405.

III. Mobility-Fluctuation 1/f Noise in Nonuniform Nonlinear Samples and in Mesa Structures (A. van der Ziel and C.M. van Vliet)

In a uniform sample mobility-fluctuation 1/f noise is described by the Hooge formula [1][2]

$$S_{\Delta I}(f) = \alpha_H I_0^2 / fN \quad (1)$$

where I_0 is the d.c. current, f the frequency, N the total number of carriers in the sample contributing to the noise, and α_H is the Hooge parameter. For nonhomogeneous samples or for mesa structures this result must be modified. Van Vliet and Zijlstra [3] showed that for a nonhomogeneous sample of constant cross section we should use the noise source $H(x,t)$ defined by

$$\Delta I = (\Delta I)_{\text{phen.}} + H(x,t) , \quad (2)$$

with

$$S_H(x,x',f) = \alpha_H(x) I_0^2 \delta(x-x') / f n_0(x) A \quad (3)$$

where the first term to the right is the phenomenological current, $n_0(x)$ is the carrier density at x , and A is the cross-sectional area. As a consequence, one finds for a nonuniform and possibly nonlinear sample, of length L , instead of (1)

$$S_{\Delta I}(f) = \frac{I_0^2}{fL^2} \int_0^L \frac{\alpha_H(x) dx}{A n_0(x)} . \quad (4)$$

The proof is simple. Explicitly, (2) reads

$$\Delta I(t) = d[g(v)\Delta v(x)] / dx + H(x,t) \quad (5)$$

where $g(v)$ is the conductance per unit length at $v = v(x)$, and $\Delta v(x)$ is the fluctuation of v at x . Multiplying with dx and integrating over the length of the sample yields

$$\Delta I(t)L = [g(v)\Delta v(x)]_0^L + \int_0^L H(x,t) dx . \quad (6)$$

For the noise Norton generator $\Delta v(L) = \Delta v(0) = 0$, so that

$$S_{\Delta I}(t) = \frac{1}{L^2} \int_0^L \int_0^L S_H(x, x', f) dx dx' . \quad (7)$$

Substitution of (3) yields (4). This result is general, even if the sample is a nonlinear near-ballistic device.

For a collision-limited sample with conduction determined by a constant mobility, we now note that the current due to drift and diffusion can always be written as [4],

$$I = q\mu n_o(x) A d\psi(x)/dx \quad (8)$$

where $\psi(x)$ is the quasi-Fermi voltage or electrochemical potential at position x . Thus, also

$$\frac{I}{q\mu n_o(x) A} dx = d\psi(x) , \quad (9)$$

or, by integration, noticing once more that the current is solenoidal,

$$\frac{I}{q\mu A} \int_0^L \frac{dx}{n_o(x)} = \psi(L) - \psi(0) = V , \quad (10)$$

where V is the applied voltage. Hence, for the d.c. resistance:

$$R = \frac{V}{I} = \frac{1}{q\mu A} \int_0^L \frac{dx}{n_o(x)} . \quad (11)$$

Note that this expression holds in a nonuniform device even if part of the current is not carried by drift. Combining (4) and (2) we have, if we may suppose that the Hooge parameter does not depend on x (or if α_H is a weighted Hooge parameter over the device),

$$S_{\Delta I}(f) = \frac{\alpha_H I_o^2}{f L^2} (q\mu R) . \quad (12)$$

In collision-limited diodes of structure n^+nn^+ , this formula is of importance since due to spill-over from the n^+ regions the density $n_0(x)$ in the n-region is not constant; moreover, nonuniformity and nonlinearity can occur due to space-charge injection. Often, for these devices one utilizes mesa structures, consisting of m alternating n^+ and n layers. We assume the n^+ regions are shorts and cause no noise. Let $[S_{\Delta I}(f)\Delta f]^{\frac{1}{2}}$ be the Norton generator in parallel with each n-region; then for the total voltage noise of the mesa structure

$$S_{\Delta V}(f) = m S_{\Delta I}(f) R^2. \quad (13)$$

Hence, for the overall Norton generator of the device, of measured resistance $\rho = mR$, we have

$$S_{\Delta I_{\text{overall}}}(f) = \frac{1}{m} S_{\Delta I}(f). \quad (14)$$

Employing (12) this yields

$$S_{\Delta I_{\text{overall}}}(f) = \frac{\alpha_H I_o^2}{f L_m^2} (q\mu\rho) = \frac{\alpha_H I_o^2}{f L_{\text{total}}^2} (q\mu\rho). \quad (15)$$

This result allows us to determine the Hooge parameter from the measured noise, I_o , L_{total} and ρ .

Acknowledgement

We are indebted to Dr. G. Bosman for discussions on this topic.

References

- [1] F.N. Hooge, Physics Letters 29A, 139 (1969).
- [2] R.P. Jindal and A. van der Ziel, J. Appl. Physics 52, 2884 (1981).
- [3] K.M. van Vliet and R.J.J. Zijlstra, Physica 111B, 321 (1981).
- [4] A.H. Marshak and K.M. van Vliet, Solid State Electr. 21, 417 (1978).

IV. A New Transform Theorem for Stochastic Processes, with Special Application to Counting Statistics and 1/f Noise (C.M. van Vliet & P.H. Handel)

a. Abstract

A new transform is derived which links the Allan variance uniquely to the spectrum and vice versa. This transform pair handles well, besides the usual Lorentzian spectra, the less well behaved spectra $S(\omega) = C\omega^{-\mu}$, $-1 < \mu < 3$. In particular the theorem is useful for 1/f noise, for which the connection with counting statistics is described in detail. Possible measurements to verify Handel's quantum theory of 1/f noise are described.

b. Introduction

In emission phenomena the effects of the statistics can be measured in various ways. Most directly, one can determine the counting statistical distribution $P(M_T, T)$ for the number of counts M_T in a time interval $(t, t+T)$, or the interval distribution between counts $W(T)$; conversely, one can characterize the statistics by the noise of the counting flux as measured by the current in a detector. The latter procedure is the usual procedure if the pulse rate is too high to be separated by a counter. The measurement of photon statistics can be based on both procedures, see e.g. Refs.1,2. For electronic emissions, one usually examines the electrical current noise in the anode current. For radioactive decay, on the other hand, counting techniques are most prevalent.

The connections between counting statistics and particle current noise were pointed out in Ref.1 (especially Section 8). The main link is provided by MacDonald's theorem. We define the following useful quantities:

$m(t)$: instantaneous number of particles detected per second;

$m_T(t)$: time average of $m(t)$ in an interval $(t, t+T)$,

$$m_T(t) = \frac{1}{T} \int_t^{t+T} m(t') dt', \quad (1.1)$$

$M_T(t)$: total number of particles detected in $(t, t+T)$,

$$M_T(t) = \int_t^{t+T} m(t') dt' = T m_T(t); \quad (1.2)$$

$q(t)$: number of arrivals in $(-\infty, t)$

$$q(t) = \int_{-\infty}^t m(t') dt'. \quad (1.3)$$

We also define the variances:

$$\sigma_{m_T}^2 = \langle \Delta m_T^2 \rangle = \frac{1}{T^2} \int_t^{t+T} \int_t^{t+T} \langle \Delta m(t') \Delta m(t'') \rangle dt' dt'' \quad (1.4)$$

$$\sigma_{M_T}^2 = \langle \Delta M_T^2 \rangle = T^2 \sigma_{m_T}^2. \quad (1.5)$$

Notice that $\sigma_{M_T}^2$ is dimensionless, while $\sigma_{m_T}^2$ has the dimension T^{-2} .

For a Poisson process, $\langle \Delta M_T^2 \rangle = \langle M_T \rangle = \langle m \rangle T$; thus, if the process is stationary, i.e., $\langle m \rangle = m_0$ is constant, $\sigma_{M_T}^2$ goes as T while $\sigma_{m_T}^2$ goes as T^{-1} . MacDonald's theorem gives the following transform, linking the second order moments of the counting distribution with the noise spectral density, $S_m(\omega)$, of the flux fluctuations, $\Delta m(t)$ (2)(3):

$$\frac{d}{dT} \langle \Delta M_T^2 \rangle = \frac{1}{\pi} \int_0^\infty S_m(\omega) \omega^{-1} \sin \omega T d\omega \quad (1.6)$$

with inversion

$$S(\omega) = 2\omega \int_0^\infty dT \sin \omega T \frac{d}{dT} \langle \Delta M_T^2 \rangle. \quad (1.7)$$

The theorem is useful for Poissonian statistics. Then

$$\langle \Delta M_T^2 \rangle = \langle M_T \rangle = m_0 T \quad (1.8)$$

and

$$S(\omega) = 2\omega m_0 \int_0^\infty dT \sin \omega T = 2m_0; \quad (1.9)$$

in other words we have full shot noise. Conversely, if there is other noise, like $1/f$ noise or "Schottky flicker noise" (which has a Lorentzian spectrum, see Ref.5), the statistics cannot be Poissonian.

Unfortunately, for 1/f noise eq. (1.6) is not applicable, since the integral diverges. However, a useful concept in this case is the "two sample variance" or "Allan variance". Let $m_T^{(1)}$ be the average counting rate in $(t, t+T)$ and $m_T^{(2)}$ the counting rate in $(t+1, t+2T)$, see eq. (1.1). Then we define the Allan variance by

$$\sigma_{m_T}^{A2} = \frac{1}{2} \langle (m_T^{(1)} - m_T^{(2)})^2 \rangle \quad (1.10)$$

and

$$\sigma_{M_T}^{A2} = \frac{1}{2} \langle (M_T^{(1)} - M_T^{(2)})^2 \rangle = T^2 \sigma_{m_T}^{A2} \quad (1.11)$$

The variance σ^{A2} (which means $(\sigma^A)^2$) turns out to be finite for 1/f noise, in contrast to σ^2 , as was shown by Allan⁶). This variance is also useful for other noise spectra. In section 2 we derive a general transform theorem linking σ^{A2} and $S(\omega)$. In section 4 we present the inversion of this theorem. We thus have a new transform pair, which in many cases is more useful than MacDonald's theorem or the Wiener-Khintchine theorem. In section 3 we discuss the consequences for counting statistics. In section 5 we add a small refinement.

c. The Allan variance transform

The theorem reads

$$\sigma_{M_T}^{A2}(T) = \frac{4}{\pi} \int_0^\infty \frac{d\omega}{\omega^2} S_m(\omega) \sin^4 \frac{\omega T}{2} \quad (2.1)$$

The derivation is straightforward. Let $A_q(\tau)$ be the correlation function of $q(t)$. Then by the Wiener-Khintchine theorem, noting that $S_q = S_m/\omega^2$,

$$A_q(\tau) \equiv \langle q(t)q(t+\tau) \rangle = \int_0^\infty S_q(\omega) \cos \omega \tau \frac{d\omega}{2\pi} = \lim_{\epsilon \rightarrow 0} \int_\epsilon^\infty \frac{S_m(\omega)}{\omega^2} \cos \omega \tau \frac{d\omega}{2\pi} \quad (2.2)$$

where we used (1.3). It should be noted that the limit $\epsilon \rightarrow 0$ may not exist, so it is not carried out at this moment. From the definition of Allan variance, we have noticing (1.1) and (1.3)

$$\begin{aligned}\sigma_{L_T}^{A2} &= \frac{1}{2T^2} \langle [q(T+t) - q(t) - q(2T+t) + q(T+t)]^2 \rangle \\ &= \frac{1}{2T^2} [2A_q(2T) - 8A_q(T) + 6A_q(0)] ,\end{aligned}\quad (2.3)$$

where we assumed the process to be stationary, so that $\langle q(t+2T)q(t+T) \rangle = A_q(T)$, etc. Substituting (2.2) we have

$$\sigma_{m_T}^{A2} = \frac{1}{2T^2} \lim_{\epsilon \rightarrow 0} \int_{\epsilon}^{\infty} \frac{d\omega}{2\pi\omega} S_m(\omega) [2\cos 2\omega T - 8\cos \omega T + 6]. \quad (2.4)$$

The expression is meaningful if the limit $\epsilon \rightarrow 0$ exists for the total right-hand side. We now notice

$$\begin{aligned}2\cos 2\omega T - 8\cos \omega T + 6 &= -2(1 - \cos 2\omega T) + 8(1 - \cos \omega T) = -4\sin^2 \omega T + 16\sin^2 \frac{\omega T}{2} \\ &= -16\sin^2 \frac{\omega T}{2} \cos^2 \frac{\omega T}{2} + 16\sin^2 \frac{\omega T}{2} = 16\sin^4 \frac{\omega T}{2} .\end{aligned}\quad (2.5)$$

Consequently,

$$\sigma_{m_T}^{A2} = \frac{4}{\pi T^2} \lim_{\epsilon \rightarrow 0} \int_{\epsilon}^{\infty} \frac{d\omega}{\omega} S_m(\omega) \sin^4 \frac{\omega T}{2} \quad (2.6)$$

which proves (2.1). For 1/f noise the limit exists, since with $S(\omega) = C/\omega$,

$$8C \int_0^{\infty} \frac{d\omega}{\omega^3 T^2} \sin^4 \frac{\omega T}{2} = 2C \int_0^{\infty} \frac{d\xi}{\xi^3} \sin^4 \xi = 2C \log 2. \quad (2.7)$$

Hence,

$$\sigma_{M_T}^{A2}(T) = 2CT^2 \log 2. \quad (2.8)$$

Since the transforms (2.6) are not always easily performable, we also

give another form. Let $F(s)$ be the Laplace transform of $\sigma_{M_T}^{A2}$,

$$F(s) = \int_0^{\infty} dT e^{-sT} \sigma_{M_T}^{A2}(T); \quad (2.9)$$

the transform of the kernel $\sin^4 \omega T/2$ is easily found by rewriting the argument in the l.h.s. of (2.5); we then obtain

$$F(s) = \frac{6}{\pi} \int_0^{\infty} d\omega \frac{\omega^2}{(s^2 + 4\omega^2)(s^2 + \omega^2)s} S(\omega). \quad (2.10)$$

For spectra which are even and analytic this can be gainfully written as

$$F(s) = \frac{3}{\pi} \oint_C d\omega \frac{\omega^2}{(s^2 + 4\omega^2)(s^2 + \omega^2)s} S(\omega), \quad (2.11)$$

where C is a contour consisting of the real axis and a semicircle in the upper plane, at infinity.

For 1/f noise, (2.11) is not useful since $S(\omega) = 2\pi C/|\omega|$, which is not analytic in the plane. However, using partial fractions, (2.10) is split into elementary integrals; the result is $F(s) = 4C(\log 2)s^{-3}$, which upon inversion yields (2.8).

For white noise, $S(\omega) = 2A$, so (2.11) has upper half plane poles only at $\omega = is$ and $is/2$. We easily find

$$F(s) = A/s^2, \quad \sigma_{M_T}^{A2}(T) = AT. \quad (2.12)$$

Finally we consider Lorentzian flicker noise, of the form

$$S(\omega) = 4B\alpha/(a^2 + \omega^2) = 4B\tau/(1 + \omega^2\tau^2), \quad \tau = \frac{1}{a}. \quad (2.13)$$

There is now an extra pole at $\omega = ia$. From the residue theorem one finds,

$$F(s) = 2B \left[\frac{4a}{s^2(s^2 - 4a^2)} - \frac{2a}{s^2(s^2 - a^2)} - \frac{6a^2}{s(s^2 - 4a^2)(s^2 - a^2)} \right]; \quad (2.14)$$

the inverse transform yields

$$\sigma_{M_T}^{A2}(T) = \frac{B}{a^2} [4e^{-\alpha T} - e^{-2\alpha T} + 2\alpha T - 3]. \quad (2.15)$$

The various results are summarized in Table I.

	$S_m(\omega)$	$F(s)$	$\sigma_{M_T}^{A2}(T)$
Poissonian shot noise	$2m_0$	$2m_0/s^2$	$\langle M_T \rangle = m_0 T$
general shot noise	$2 \langle \Delta m_T^2 \rangle T$	$2 \langle \Delta m_T^2 \rangle T / s^2$	$\langle \Delta M_T^2 \rangle = m_0 T$ \leftarrow
1/f noise	$2\pi C/ \omega $	$4C(\log 2)/s^3$	$2CT^2 \log 2$
Lorentzian flicker noise	$4B \frac{\alpha}{\alpha^2 + \omega^2}$	$2B \left[\frac{4\alpha}{s^2(s^2 - 4\alpha^2)} - \frac{2\alpha}{s^2(s^2 - \alpha^2)} - \frac{6\alpha^2}{s(s^2 - 4\alpha^2)(s^2 - \alpha^2)} \right]$	$\frac{B}{\alpha^2} [4e^{-\alpha T} - e^{-2\alpha T} + 2\alpha T - 3]$
"Pathological noise"	$L/ \omega ^{\lambda-1}$ $0 < \lambda < 4; \lambda \neq 2$	$\frac{L(1-2^{\lambda-2})s^{-\lambda-1}}{\sin(\pi\lambda/2)}$	$\frac{LT^\lambda(1-2^{\lambda-2})}{\sin(\pi\lambda/2)\Gamma(\lambda+1)}$

TABLE I

A few explanatory words about the details are in order. The first column lists the spectral densities, in particular the ω -dependence. The last column gives the T-dependence and the explicit results obtainable from $S_m(\omega)$ via the Allan transform theorem (2.1). For Poissonian shot noise (or "full shot noise") the Allan variance equals the regular variance σ^2 , which equals the mean; note that m_0 is a constant for a stationary process, so $\sigma_{M_T}^{A2}$ goes as T. We also included the case of general shot noise (or non-Poissonian shot noise). In this case the spectrum is given by Milatz' theorem, $S_m = 2(\text{var } m_T)T$, which is a variant of MacDonald's theorem⁴⁾. Though the distribution $P(M_T, T)$ is non-Poissonian, the assumption of white noise indicates that the autocorrelation function is still a delta function $\langle \Delta m(t) \Delta m(t+\delta) \rangle = \langle \Delta m(t)^2 \rangle \delta(\delta)$. The Allan

variance turns out to be equal to the regular variance, as is also found directly, for

$$\begin{aligned}\sigma_{M_T}^{A2} &= \frac{1}{2} \langle (M_T^{(1)} - M_T^{(2)})^2 \rangle = \frac{1}{2} [\langle M_T^{(1)2} \rangle + \langle M_T^{(2)2} \rangle - 2 \langle M_T^{(1)} M_T^{(2)} \rangle] \\ &= \langle M_T^2 \rangle - \langle M_T \rangle^2 = \sigma_{M_T}^2, \quad (2.16)\end{aligned}$$

since the delta function correlation implies $\langle M_T^{(1)} M_T^{(2)} \rangle = \langle M_T^{(1)} \rangle \langle M_T^{(2)} \rangle = \langle M_T \rangle^2$ for $T > 0$. The case of non-Poissonian shot noise occurs e.g. in photon emission when the counting statistics is a compound Poisson distribution which reflects the Bose-Einstein statistics of the photons in a mode ^{1,5}. In that case the super Poisson factor x reflects the Boson factor

$$x = \frac{\langle \Delta M_T^2 \rangle}{\langle M_T \rangle} = 1+B, \quad B = \frac{\langle M_T \rangle}{Z}, \quad (2.17)$$

where Z is the number of modes comprised in a counting time T and solid angle Ω of measurement. We assumed here $\omega \ll \tau_c^{-1}$ where τ_c is the coherence time; for these frequencies the spectrum is white. (Rigorously speaking, if we include $\omega \gg \tau_c^{-1}$, this is a special case of Lorentzian type noise.)

For $1/f$ noise and Lorentzian flicker noise the constants C and B depend on the model. This will be further discussed in section d. In fact, the measurement of $\sigma_{M_T}^{A2}$ should be a very useful tool to discern between the various models, as we discuss there.

For the last entry "pathological noise", we performed the computations from the inverse of the Allan variance theorem, see section e.

d. Counting experiments

The presence of non-white noise in counting statistics can now be determined from a measurement of the Allan variance, as a function of T .

For suppose that the noise is composed of white noise, 1/f noise and Lorentzian flicker noise, i.e.,

$$S_m(\omega) = 2\kappa m_0 + 2\pi C \frac{1}{|\omega|} + 4B \frac{\alpha}{\alpha^2 + \omega^2} ; \quad (3.1)$$

then, a measurement of $R(T) \equiv \frac{\langle M_T^2 \rangle}{\langle M_T \rangle^2}$ yields, noticing again $\langle M_T \rangle = m_0 T$ where m_0 is constant,

$$R(T) \equiv \frac{\langle (M_T^{(1)} - M_T^{(2)})^2 \rangle}{2\langle M_T \rangle^2} = \frac{\kappa}{m_0 T} + 2 \frac{C}{m_0^2} \log 2 + \frac{B}{m_0^2 T^2 \alpha^2} [4e^{-\alpha T} - e^{-2\alpha T} + 2\alpha T - 3] . \quad (3.2)$$

In all flicker noise and 1/f noise theories the extra noise goes with the flux squared. Thus we write $C' = C/m_0^2$, $B' = B/m_0^2$. For $T \gg \alpha^{-1}$, we have then

$$R(T) \approx \frac{\kappa}{m_0 T} + 2C' \log 2 + \frac{2B'}{\alpha T} ; \quad (3.3)$$

for $T \ll \alpha^{-1}$ (very slow Lorentzian flicker noise!) we have

$$R(T) \approx \frac{\kappa}{m_0 T} + 2C' \log 2 + \frac{2B'}{3} \alpha T. \quad (3.4)$$

Thus, a slow Lorentzian reveals a term αT . Fast Lorentzians will not be easily recognized unless B' is very large. The presence of 1/f noise gives the so-called flicker floor⁶⁾: for $T \rightarrow \infty$, there is a remaining term in the relative Allan variance $R(T) \rightarrow 2C' \log 2 \equiv F$. From this the 1/f noise strength can be determined.

The Lorentzian flicker noise occurs if there are $N(t)$ emission centres whose creation and annihilation affects the emission. In Ref.5 we established

$$B' = 4 \frac{\langle N^2 \rangle}{\langle N \rangle^2} , \quad (3.5)$$

with $m_0 = \lambda \langle N \rangle$, λ being the emission rate per centre.

For $1/f$ noise Handel has devised the model of quantum $1/f$ noise, based on self interference of the wave packets of the emitted particles, see 5) and 7)8). In this theory one finds

$$S_m(\omega) = \frac{2\alpha_f A}{|\vec{r}|} m_0^2 \zeta \quad (3.6)$$

so that

$$C' = 2\alpha_f A \zeta; \quad (3.7)$$

hence the flicker floor becomes $F = 4\alpha_f A \log 2$. Here ζ is a coherence factor, α_f is the fine structure constant, $1/137$, and $A = 2(\Delta v)^2/3\pi c^2$, where Δv is the velocity change of the particles in the emission process.

For α -particles we expect ζ to be close to one, while it may be considerably smaller than one for β^+ or β^- emission due to incoherence introduced by the associated neutrino emission. For these particles one easily finds

$$\alpha_f A = 8.32 \times 10^{-7} E \quad (E \text{ in MeV}). \quad (3.8)$$

For many α -emitters, such as ${}_{90}\text{Th}^{230} \rightarrow {}_{88}\text{Ra}^{226}$, ${}_{90}\text{Th}^{232} \rightarrow {}_{88}\text{Ra}^{228}$, ${}_{92}\text{U}^{238} \rightarrow {}_{90}\text{Th}^{234}$, ${}_{95}\text{Am}^{243} \rightarrow {}_{93}\text{Np}^{239}$, one finds that $\alpha_f A \approx 4 \times 10^{-6}$.

Hence the flicker floor becomes $F = 11.2 \times 10^{-6}$. For a 10 micro curie source, the number of disintegrations per second is $3.7 \times 10^5 \text{ sec}^{-1}$.

Assuming an efficiency $\eta \approx 10^{-2}$, which accounts for solid angle and absorption in the source, we arrive at $\langle M_T \rangle \approx 1.3 \times 10^7$ in $T=1$ hr. The Poissonian term in (3.4) ($\alpha=1$) thus becomes $1/\langle M_T \rangle \approx 0.08 \times 10^{-6}$, which is well below the flicker floor. Experiments to verify the theory of quantum $1/f$ noise by α -particle counting statistics are underway at the

University of Florida. It should be noted that Handel's theory also includes contributions to $1/f$ noise from infraparticles other than photons; the resulting αA is the sum of contributions for all types of infraparticles participating in the energy transfer.

e. Inversion of the Allan variance theorem

It is generally believed that a constant relative Allan variance implies the presence of $1/f$ noise; or, more generally, one expects that a given Allan variance determines uniquely the spectrum $S(\omega)$. This will now be shown by inverting the theorem (2.1), which composes a Fredholm integral equation of the first kind.

To this purpose we restate (2.10) in the form

$$F(s) = \frac{6}{\pi} \int_0^\infty \frac{d\omega}{\omega} \frac{1}{(s/\omega) (\frac{s^2}{\omega^2} + 4) (\frac{s^2}{\omega^2} + 1)} X(\omega), \quad (4.1)$$

where $X(\omega) = S(\omega)/\omega^2$. We will take the Mellin transform of this equation, and follow a method discussed by Morse and Feshbach⁹⁾. The transform has to be taken piecewise, since the full transform does not usually exist for the functions $F(s)$ encountered in noise problems. We have seen in all cases (cf Table I) that for

$$\begin{aligned} s \rightarrow 0, \quad F(s) &= O(s^{-\sigma}), \quad \sigma > 0, \\ s \rightarrow \infty, \quad F(s) &= O(s^{-\tau}), \quad \tau > 0. \end{aligned} \quad (4.2)$$

For the various noises the values of σ and τ are given in table II

noise	σ	τ	inversion applies	type of transform
white	2	2	yes	partial
$1/f$	3	3	yes	partial
Lorentzian	2	4	yes	full
$1/f^3$	5	5	no	—

TABLE II

Consequently, let*

$$\Phi_-(p) = \int_0^1 F(s) s^{p-1} ds; \quad \text{exists for } \operatorname{Re} p > \sigma_0; \quad (4.3)$$

$$\Phi_+(p) = \int_1^\infty F(s) s^{p-1} ds; \quad \text{exists for } \operatorname{Re} p < \tau_0. \quad (4.4)$$

Since $\tau_0 = \sigma_0$ for most cases, there is no region in the complex plane where both Φ 's exist together. Only the Lorentzian behaves better; it has a complete Mellin transform $\Phi(p)$. Other cases may occur where $\tau_0 < \sigma_0$.†

We now recall the Mellin transform convolution theorem,

$$\mathcal{M}[\int_0^\infty v(s/\omega) g(\omega) d\omega/\omega] = V(p)G(p), \quad (4.5)$$

where \mathcal{M} denotes the Mellin transform; here capitals refer to the transformed functions. Noticing that (4.1) is of the same form as the expression in the rectangular bracket on the l.h.s. of (4.5), we find that the transformed equation (4.1) is

$V(p)Y(p)$ with, for the transformed kernel

$$V(p) = \frac{6}{\pi} \int_0^\infty ds \frac{s^{p-2}}{(s^2+4)(s^2+1)} = \frac{1-2^{p-3}}{\sin \frac{1}{2}(p-1)\pi}, \quad 1 < \operatorname{Re} p < 5. \quad (4.6)$$

Thus we obtain

$$\Phi_-(p) + \Phi_+(p) = \frac{1-2^{p-3}}{\sin \frac{1}{2}(p-1)\pi} [\gamma_-(p) + \gamma_+(p)]. \quad (4.7)$$

* Usually, for the existence one considers the Lebesgue integral $\int_0^1 |F(s)|^2 s^{2\sigma-1} ds$; if this is finite for $\sigma > \sigma_0$ the transform Φ exists for $\operatorname{Re} p \geq \sigma$. Likewise for Φ_+ .

† The Mellin transform presents a dimensional anomaly since s has the dimension \sec^{-1} . Strictly speaking we should replace ω by $\bar{\omega} = \omega/\omega_c$ and T by $\bar{T} = T/T_c$ where ω_c and T_c are an arbitrary normalizing frequency and time interval. This has consequences for the reverse transform, see later examples.

In order that there is a region in which both $V(p)$ and $\phi_-(p)$ or $\phi_+(p)$ exist, it is necessary that $\tau_0 > 1$ and $\sigma_0 < 5$. The situation is depicted in Fig. 32.

From (4.7) we deduce

$$\phi_-(p) - \chi_-(p) \frac{1-2^{p-3}}{\sin \frac{1}{2}(p-1)\pi} = -\phi_+(p) + \chi_+(p) \frac{1-2^{p-3}}{\sin \frac{1}{2}(p-1)\pi} \quad (4.8)$$

This equality which initially is valid in the shaded area only can be made to hold in the entire plane except at singularities by analytic continuation. Besides this, the integrals over each of the members, going along a line $\text{Re } p = \sigma'$ for the l.h.s. and $\text{Re } p = \tau'$ for the r.h.s., are equal due to the inverted transform equality. Using a theorem of Morse and Feshbach (op cit. p.463) we conclude that each member equals a function $R(p)$ which is analytic in the entire area $1 < \text{Re } p < 5$. We thus obtain by transforming back

$$\begin{aligned} \chi(\omega) &= \mathcal{M}_-^{-1} \chi_-(p) + \mathcal{M}_+^{-1} \chi_+(p) \\ &= -\frac{1}{2\pi i} \int_{-i\infty+\sigma'}^{i\infty+\sigma'} \frac{dp}{\omega^p} \phi_-(p) \frac{\cos p\pi/2}{1-2^{p-3}} - \frac{1}{2\pi i} \int_{-i\infty+\tau'}^{i\infty+\tau'} \frac{dp}{\omega^p} \phi_+(p) \frac{\cos p\pi/2}{1-2^{p-3}} \\ &\quad + \oint_C \frac{dp}{\omega^p} R(p) \frac{\cos p\pi/2}{1-2^{p-3}}, \end{aligned} \quad (4.9)$$

where C is a counterclockwise contour made up of the lines $\text{Re } p = \sigma'$ and $\text{Re } p = \tau'$; the σ' and τ' are in the strips as indicated in Fig. 32. Since $R(p)$ is analytic and the factor following $R(p)$ is regular (at $p=3$, both numerator and denominator are zero, but their ratio is finite) the contour integral is zero; i.e. there are no solutions of

the homogeneous equation. The solution of the inhomogeneous equation is thus unique. The solution (4.9) becomes - reverting to

$$S(\omega) = \chi(\omega)\omega^2;$$

$$S(\omega) = -\frac{1}{2\pi i} \int_{-i\infty+\sigma'}^{i\infty+\sigma'} \frac{dp}{\omega^{p-2}} \frac{\cos \frac{1}{2}p\pi}{1-2^{p-3}} \chi[\sigma_{M_T}^{A2}(T)] \\ - \frac{1}{2\pi i} \int_{-i\infty+\tau'}^{i\infty+\tau'} \frac{dp}{\omega^{p-2}} \frac{\cos \frac{1}{2}p\pi}{1-2^{p-3}} \chi[\sigma_{M_T}^{A2}(T)], \quad \sigma' > \sigma_0, \quad \tau' < \tau_0. \quad (4.10)$$

This is the complete inversion theorem corresponding to the Allan variance theorem (2.1).

For the case $\sigma_0 < \tau_0$ the situation is depicted in Fig. 33. The full transform exists and is analytic for the shaded area. We can now select a line $\text{Re } p = \beta$, $\sigma_0 < \beta < \tau_0$ for the inverse transforms. Thus, adding the two terms of (4.10) (i.e. taking $\sigma' = \beta$, $\tau' = \beta$), we obtain:

$$S(\omega) = -\frac{1}{2\pi i} \int_{-i\infty+\beta}^{i\infty+\beta} \frac{dp}{\omega^{p-2}} \frac{\cos \frac{1}{2}p\pi}{1-2^{p-3}} \chi[\sigma_{M_T}^{A2}(T)], \quad \sigma_0 < \beta < \tau_0. \quad (4.11)$$

If the Mellin and Laplace transforms are interchangeable, then (4.11) allows the simple expression

$$S(\omega) = -\frac{1}{2\pi i} \int_{-i\infty+\beta}^{i\infty+\beta} \frac{dp}{\omega^{p-2}} \frac{\cos \frac{1}{2}p\pi}{1-2^{p-3}} \Gamma(p) \int_0^\infty \frac{dT}{T^p} \sigma_{M_T}^{A2}(T), \quad (4.12)$$

where β is in the domain of analyticity of the expression

$$\Gamma(p) \int_0^\infty dT T^{-p} \sigma_{M_T}^{A2}(T).$$

We will show the application of (4.10) and (4.11) or (4.12) to two general cases. First consider an Allan variance of the form KT^λ , $0 < \lambda < 4$.

Then $F(s) = K\Gamma(\lambda+1)s^{-\lambda-1}$, and

$$\phi_-(p) = \frac{K}{p-\lambda-1} \Gamma(\lambda+1), \quad \text{Re } p > \sigma_0 = 1+\lambda, \quad (4.13)$$

$$\phi_+(p) = -\frac{K}{p-\lambda-1} \Gamma(\lambda+1), \quad \text{Re } p < \tau_0 = 1+\lambda. \quad (4.14)$$

Then Φ 's are substituted into (4.10). We consider first " $\omega \ll 1$ ". In view of what we said in the previous footnote, this means in reality $\bar{\omega} < 1$ or $\omega \ll \omega_c$. Since ω_c can be chosen arbitrarily large, the Φ_- solution alone should cover the entire spectrum! We now close the contours in Fig.1 with large semicircles in the left-hand plane; on these semicircles the integrand goes sufficiently fast to zero. Moreover, since $\Phi_+(p)$ as well as $\cos \frac{1}{2}p\pi / (1-2^{p-3})$ is analytic for $\text{Re } p < \tau$, the contour integral for this part vanishes. We are thus left with

$$S(\omega) = - \frac{1}{2\pi i} \oint_{C_I} \frac{dp}{\omega^{p-2}} \frac{\cos \frac{1}{2}p\pi}{1-2^{p-3}} \frac{K\Gamma(\lambda+1)}{p-\lambda-1}. \quad (4.15)$$

We note that there is only one pole, $p=\lambda+1$ (for $p=3$, the denominator $1-2^{p-3}$ is zero, but so is $\cos \frac{1}{2}p\pi$, their ratio being finite). Hence,

$$S(\omega) = - \frac{K}{\omega^{\lambda-1}} \lim_{p \rightarrow \lambda+1} \frac{\cos \frac{1}{2}p\pi}{1-2^{p-3}} \Gamma(\lambda+1). \quad (4.16)$$

For $\lambda \neq 2$, the limit is straightforward. Then

$$S(\omega) = \frac{K}{\omega^{\lambda-1}} \frac{\sin \lambda\pi/2}{1-2^{\lambda-2}} \Gamma(\lambda+1). \quad (4.17)$$

For white noise, $K = m_0$, $\lambda = 1$ (see Table I), hence $S(\omega) = 2m_0$, as expected. For 1/f noise $K = 2C \log 2$ and $\lambda=2$. Then from (4.16) by de l'Hôpital's rule,

$$S(\omega) = - \frac{4C \log 2}{\omega} \lim_{p \rightarrow 3} \frac{1}{2} \frac{\sin \frac{1}{2}p\pi}{\log 2 \cdot c^{(p-3) \log 2}} = \frac{2\pi C}{\omega}, \quad (4.18)$$

thus confirming the point of departure. We note that, since λ runs from zero to four, spectra from $\omega^{1-\epsilon}$ up to $\omega^{-3+\epsilon}$, (where ϵ is arbitrarily small) can occur for the present pair of transforms (2.1)

and (4.10) to be valid. The flexibility of this transform pair is thus much larger than that of the Wiener Khintchine theorem, which handles only spectra from ω^0 to $\omega^{1-\epsilon}$. Notice also from (4.17), that if we know in advance that the spectrum is $S(\omega) = L/\omega^{\lambda-1}$, then the Allan variance is ($\lambda \neq 2$)

$$\sigma_{M_T}^{A2} = L T^{\lambda} (1-2^{\lambda-2}) / \sin(\lambda\pi/2) \Gamma(\lambda+1) . \quad (4.19)$$

Finally we remark that we can obtain the same results from ϕ_+ . We then take " $\omega > 1$ ", and close the two contours with semicircles in the right-hand half-plane. The contour integral over the ϕ_- -part vanishes. The contour integral over ϕ_+ (clockwise) yields with (4.14) again the result (4.16).

Next, we consider Lorentzian noise. From $F(s)$, see Table II or (2.14), we obtain

$$\Phi(p) = \mathcal{M} F(s) = \frac{2\pi\alpha^{p-3} (1-2^{p-3})}{\sin p \frac{\pi}{2} \cosh p \frac{\pi}{2}} , \quad 2 < \text{Re } p < 4 . \quad (4.20)$$

This is put into (4.11), which yields

$$S(\omega) = \frac{i}{\alpha} \int_{-i\infty+\beta}^{i\infty+\beta} dp \left(\frac{\omega}{\alpha}\right)^{p-2} \frac{1}{\sin(p\pi/2)} . \quad (4.21)$$

This result can also be obtained from (4.12) providing we still use

$\Gamma(p)\Gamma(1-p) = \pi/\sin p\pi$. In order to evaluate the integral over

$\sigma_{M_T}^{A2}$ - which integral is $\mathcal{M}_{1-p} \sigma_{M_T}^{A2}(T)$ - we notice that $\sigma_{M_T}^{A2}$ for $T \rightarrow 0$ is of order T^3 as is found by Taylor expansion. We first compute¹⁰⁾

$\mathcal{M}_- \sigma^{A2}$ and $\mathcal{M}_+ \sigma^{A2}$ for very restricted conditions on p for the four individual terms of σ^{A2} ; on joining the results the conditions on p are then relaxed with \mathcal{M}_- existing for $\text{Re } p < 4$ and \mathcal{M}_+ existing for

$\text{Re } p > 2$. There is now an overlap on $2 < \text{Re } p < 4$; the partial Mellin transform can be added, resulting in (4.21).

In equation (4.21) there are poles at
 $p = 2m, \quad m = 0, \pm 1, \pm 2, \dots$ (4.22)

Consider first $\omega < a$. We then close with a semicircle to the left. From Fig. 33 we notice that we enclose the poles $p = -2m', m' = -1, 0, 1, \dots, \infty$. For the residues we have

$$\text{Res} = \frac{i}{a} \left(\frac{\omega}{a}\right)^{2(m'+1)} \lim_{p \rightarrow -2m'} \frac{p+2m'}{\sin \frac{1}{2} p \pi} = \frac{2}{\pi} \frac{i}{a} \left(\frac{\omega}{a}\right)^{2(m'+1)} (-1)^{m'}. \quad (4.23)$$

Thus the result of (4.21) is the power series

$$S(\omega) = -\frac{4}{a} \sum_{m'=-1}^{\infty} \left(\frac{\omega}{a}\right)^{2(m'+1)} (-1)^{m'} = \frac{4}{a} \sum_{n=0}^{\infty} \left(\frac{\omega}{a}\right)^{2n} (-1)^n = \frac{4a}{a^2 + \omega^2}, \quad (\omega < a). \quad (4.24)$$

Likewise, if $\omega > a$, we enclose with a semicircle to the right. The poles to be included are now at $p = 2m'', m'' = 2, 3, \dots, \infty$. One easily obtains the asymptotic series

$$S(\omega) = \frac{4a}{\omega^2} \sum_{n=0}^{\infty} \left(\frac{a}{\omega}\right)^{2n} (-1)^n = \frac{4a}{a^2 + \omega^2}, \quad (\omega > a). \quad (4.25)$$

f. Nonadjacent sampling

The measurement of the Allan variance necessitates adjacent sampling. This is generally not exactly possible because of the dead time of the registering instrument. We are thus led to define a slight generalization of the Allan variance, which was already foreseen by Allan [6].

Let τ be the dead time between samples. We then define,

$$\sigma_{M_T}^{B2} = \frac{1}{2} \left\langle \left[M_T(T + \tau + t) - M_T(t) \right]^2 \right\rangle, \quad (5.1)$$

Analogous to (2.3) we have,

$$\begin{aligned}\sigma_{M_T}^{B2} &= \frac{1}{2} \langle [q(2T+\tau+t) - q(T+\tau+t) - q(T+t) + q(t)] \rangle \\ &= A_q(2T+\tau) - 2A_q(T+\tau) - 2A_q(T) + A_q(\tau) + 2A_q(0) .\end{aligned}\quad (5.2)$$

We thus find

$$\sigma_{M_T}^{B2} = \int_0^\omega \frac{d\omega}{2\pi} \frac{S_m(\omega)}{\omega^2} [\cos \omega(2T+\tau) - 2\cos \omega(T+\tau) - 2\cos \omega T + \cos \omega \tau + 2] .\quad (5.3)$$

With some trigonometry this yields

$$\sigma_{M_T}^{B2} = \frac{4}{\pi} \int_0^\omega \frac{d\omega}{\omega^2} S_m(\omega) \frac{\sin^2 \omega T}{2} \frac{\sin^2 \omega(T+\tau)}{2} ,\quad (5.4)$$

which is a straightforward extension of (2.1). Again, for any τ , spectra of the form $S(\omega) \propto \omega^{-\mu}$, $-1 < \mu < 3$, as well as regular spectra (Lorentzians, etc.), allow a transform to exist. For the particular case that $\tau = T$ we have

$$\sigma_{M_T}^{B2} = \frac{16}{\pi} \int_0^\omega \frac{d\omega}{\omega^2} S_m(\omega) \sin^4 \frac{\omega T}{2} \cos^2 \frac{\omega T}{2} .\quad (5.5)$$

For 1/f noise, the integral (5.4) is found to yield, using the Laplace transform as in section 2,

$$\sigma_{M_T}^{B2} = \frac{1}{2} C T^2 [(2+r)^2 \log(2+r) - 2(1+r)^2 \log(1+r) + r^2 \log r] ,\quad (5.6)$$

where $r = \tau/T$. This is the correction to be applied to the counting statistics results of section 3 if $r \neq 0$.

Inverses of (5.4) and (5.5) can in principle also be found; however, since these have less fundamental meaning than those of section 4, we refrain from these results.

g. Conclusions

For most realistic noise spectra, eqs. (2.1) and (4.10) through (4.12) provide a new transform pair, similar to MacDonald's and the Wiener-Khintchine theorem, but with wider range of applicability. The theorem is in particular useful for 1/f noise, for which neither the correlation function nor the variance $\sigma_{M_T}^2$ exists. A measurement of the Allan variance may aid in understanding the ubiquitous 1/f noise phenomenon.

References

1. K.M. van Vliet, Physica 83B, (1976) 52.
2. F.C. van Rijswijk and C.Smit, Physica 49 (1970) 549.
3. D.K.C. MacDonald, Reports Progress in Physics 12 (1948) 56.
4. K.M. van Vliet, Physica 86A (1977) 130.
5. K.M. van Vliet, P.H.Handel and A.van der Ziel, Physica, in Press.
6. D.W. Allan, Proc. IEEE 54 (1966) 221.
7. P.H.Handel, Phys.Rev. Lett. 34 (1975) 1492.
8. P.H.Handel, Phys.Rev. A22 (1980) 745.
9. P.M.Morse and H.Feshbach, "Methods of Theoretical Physics vol.I " Section 8.5, McGraw-Hill New York 1953.
10. M.Abramowitz and I.Stegun, "Handbook of Mathematical Functions" Section 6.5, National Bureau of Standards Applied Math.Series 55, Nov. 1964, Washington D.C..

D. PAPERS PUBLISHED UNDER THE GRANT

1. A. van der Ziel, Proposed Discrimination between $1/f$ Noise Sources in Transistors. Solid State Electr. 25, 141 (1982).
2. J. Kilmer, A. van der Ziel, and G. Bosman, Presence of Mobility-Fluctuation $1/f$ Noise Identified in Silicon P^+NP Transistors. Solid State Electr. In press.
3. K.M. van Vliet and R.J.J. Zijlstra, On Mobility Fluctuations in $1/f$ Noise. Physica 111B, 321 (1981).
4. A. van der Ziel and K.M. van Vliet, Extension of Burgess' Variance Theorem to Autocorrelation Functions and Spectra, Physica 113B, 15 (1982).
5. A. van der Ziel and C.M. van Vliet, Mobility-Fluctuation $1/f$ Noise in Non-uniform Nonlinear Samples and in Mesa Structures. Physica Status Solidi(a). Submitted.
6. R.R. Schmidt, G. Bosman, C.M. van Vliet, L. Eastman, and M. Hollis. Noise in Near-Ballistic n^+nn^+ and n^+pn^+ Gallium Arsenide Submicron Diodes. Solid State Electronics. Submitted.
7. C.M. van Vliet and P.H. Handel, A New Transform Theorem for Stochastic Processes with Special Application to Counting Statistics. Physica A. In press.
8. C.M. van Vliet, General Solution Methods for Fredholm Integral Equations with Kernel $K(2,20) = g(220)$ on the Interval $(0,\infty)$. Revue des Sciences Mathematiques de Quebec. In press.
9. A. van der Ziel and G. Bosman, Thermal-Like Noise in Near-Ballistic Diodes: I. The Ballistic Regime. Physica Status Solidi (a). In press.
10. A. van der Ziel and G. Bosman, Thermal-Like Noise in Near-Ballistic Diodes II. The Collision Limited Regime. Physica Status Solidi (a). In press.

11. C.M. van Vliet, 1/f Noise in Solids and Devices: Theories and Experimental Evidence. Proc. Rome Conference on Noise, Rome, Oct. 1981.
(19 pages).
12. C.M. van Vliet, Review of Thermal Noise and Generation-Recombination Noise in Solids and Solid State Devices. Proc. Rome Conference on Noise, Rome, Oct. 1981 (38 pages).

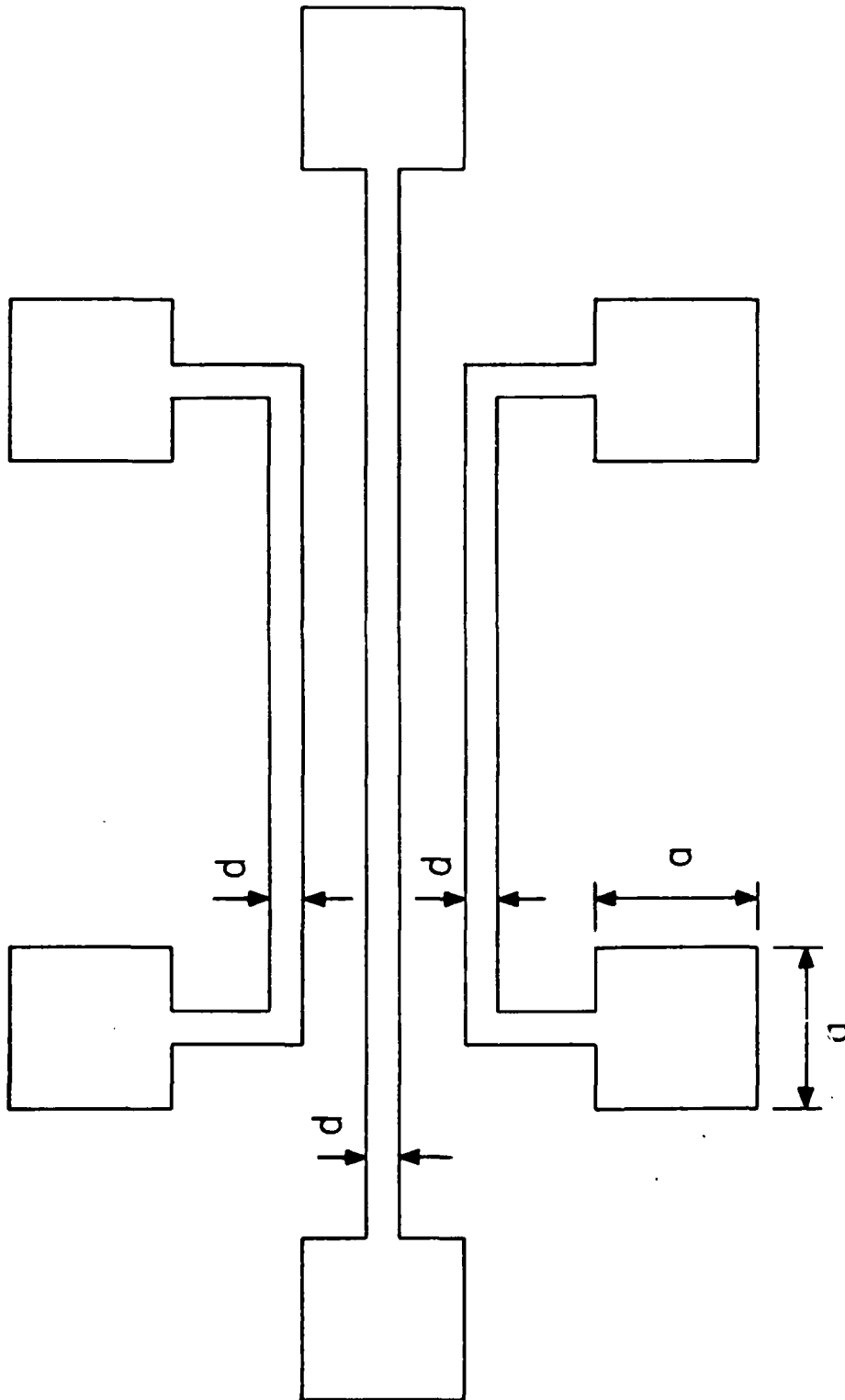


Figure 1. Thin gold film resistor configuration. The size of the bonding pads ($a \times a$) is $100 \times 100 \mu\text{m}^2$. Three film widths ($d = 0.5, 1, 2 \mu\text{m}$) are available.

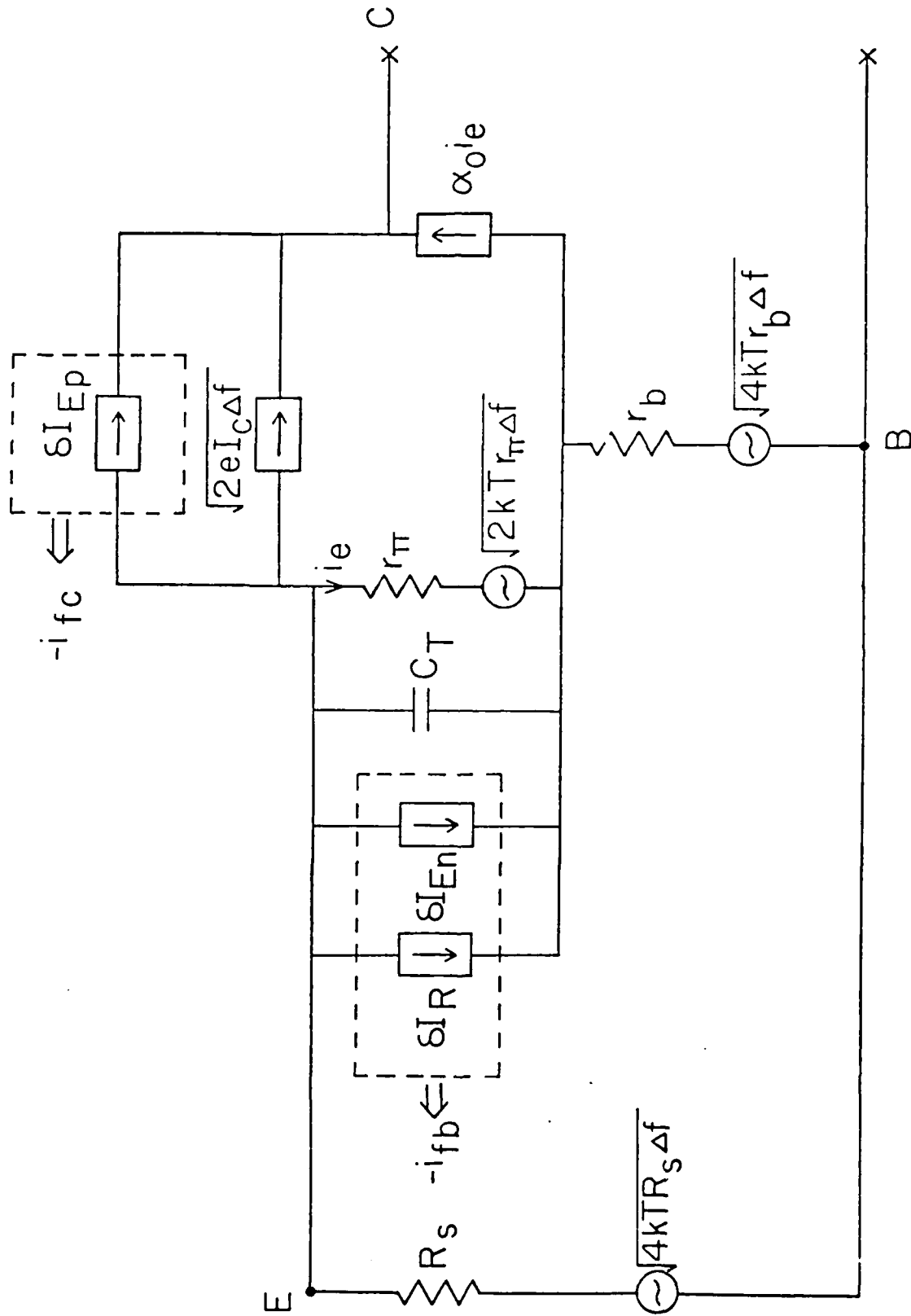


Figure 2. Equivalent common base circuit with noise sources.

AD-A121 287

STUDY OF 1/F NOISE IN SOLIDS(U) FLORIDA UNIV
GAINESVILLE DEPT OF ELECTRICAL ENGINEERING
C M VAN VLIET ET AL. JUN 82 AFOSR-TR-82-0958

2/2

UNCLASSIFIED

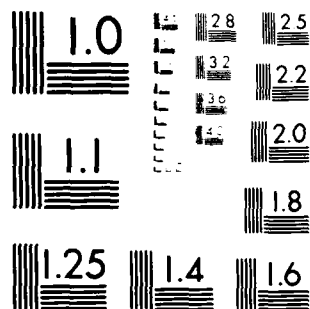
F/G 9/4

NL

END

FILED

DTIC



MICROCOPY RESOLUTION TEST CHART
NATIONAL BUREAU OF STANDARDS-1963-A

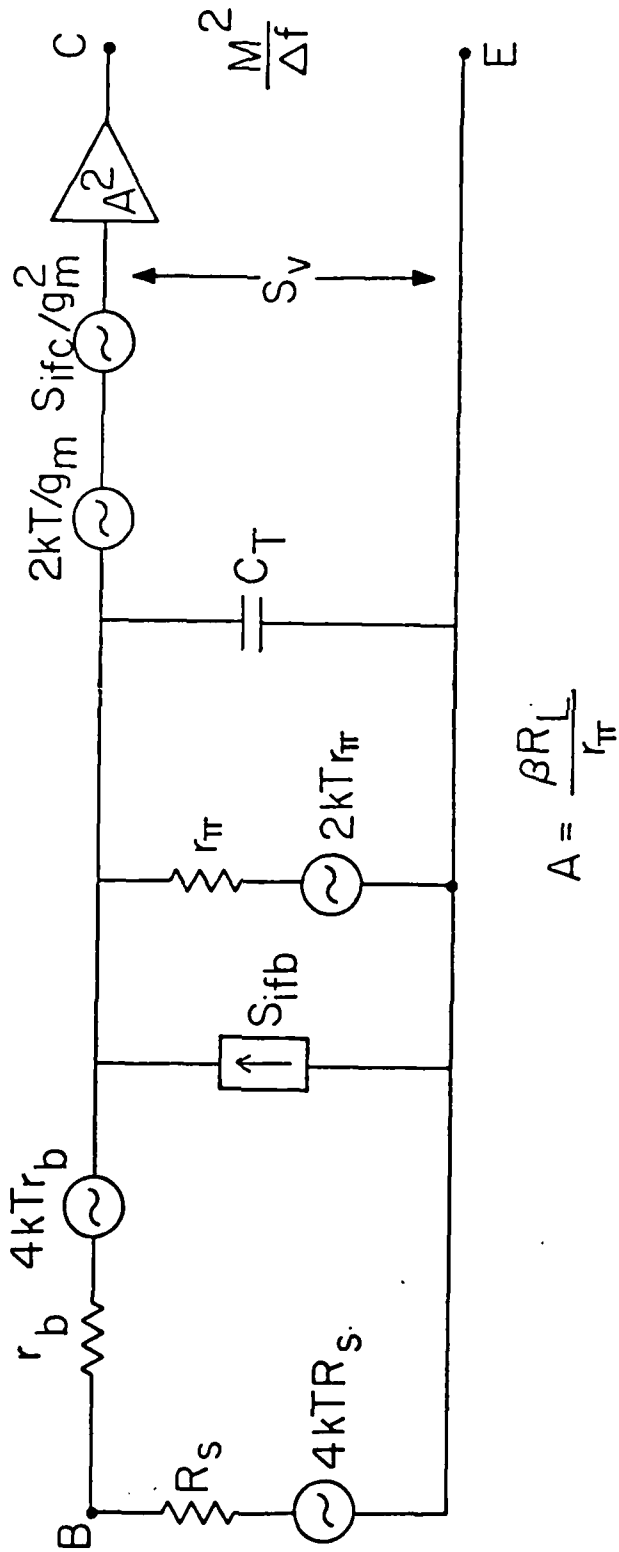


Figure 3. Equivalent common base circuit.

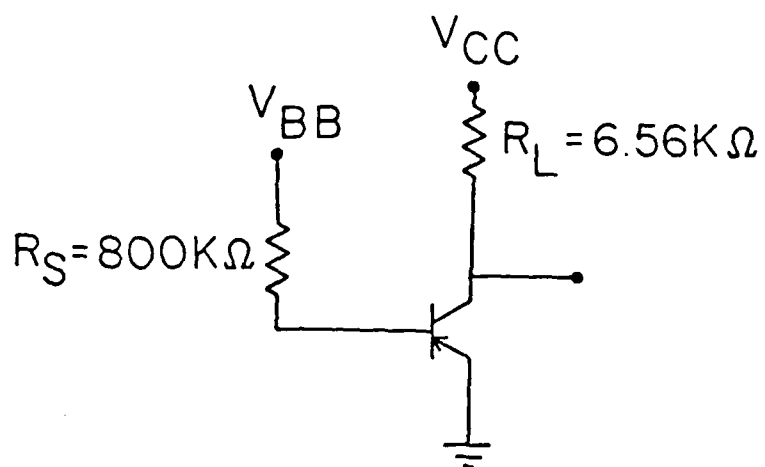


Figure 4. Circuit with high source impedance.

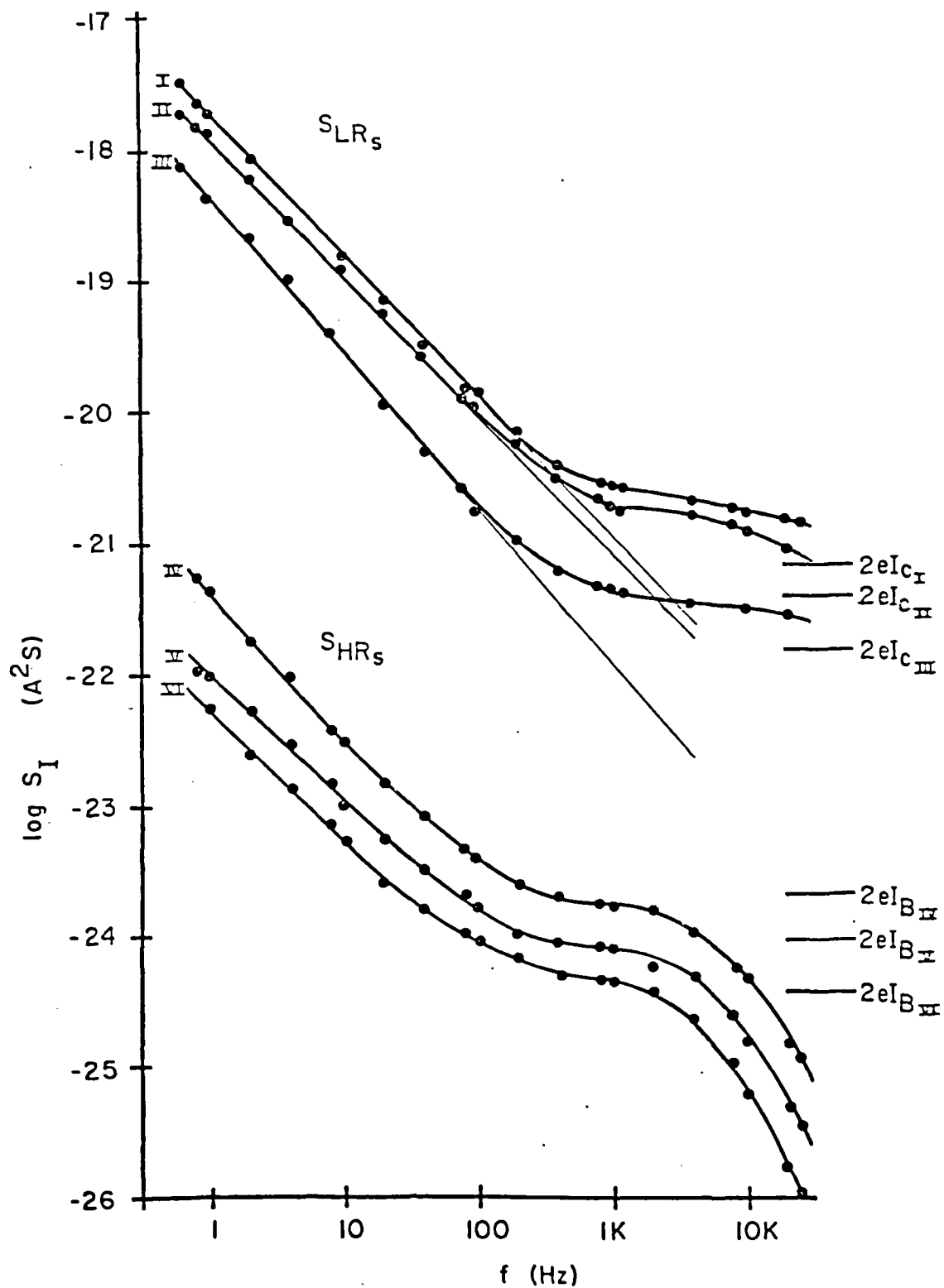


Figure 5. Measurement of high-source impedance spectra (S_{HR_s}) and low-source impedance spectra (S_{LR_s}). The base currents are $6\mu\text{A}$, $3\mu\text{A}$, $1\mu\text{A}$.

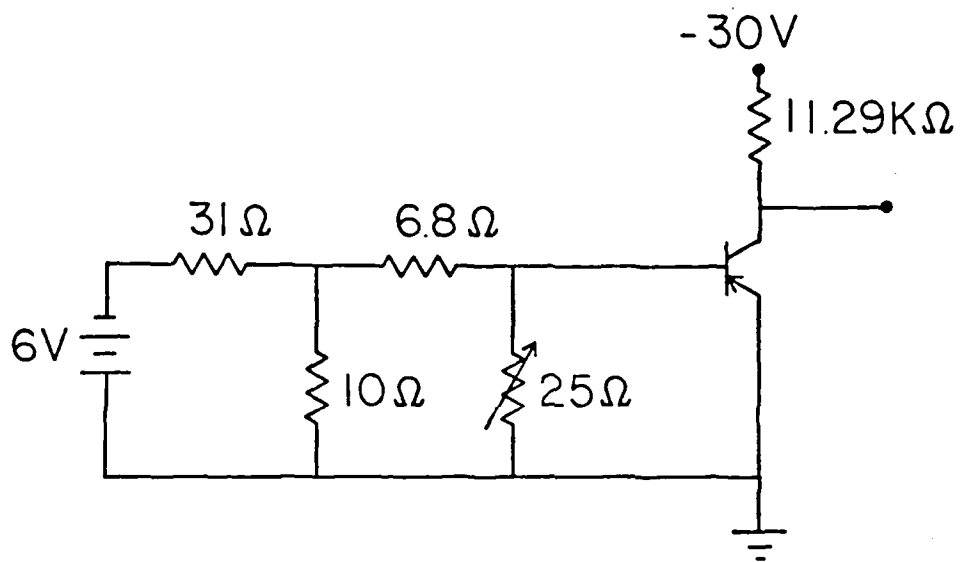


Figure 6. Circuit for low-source impedance data.

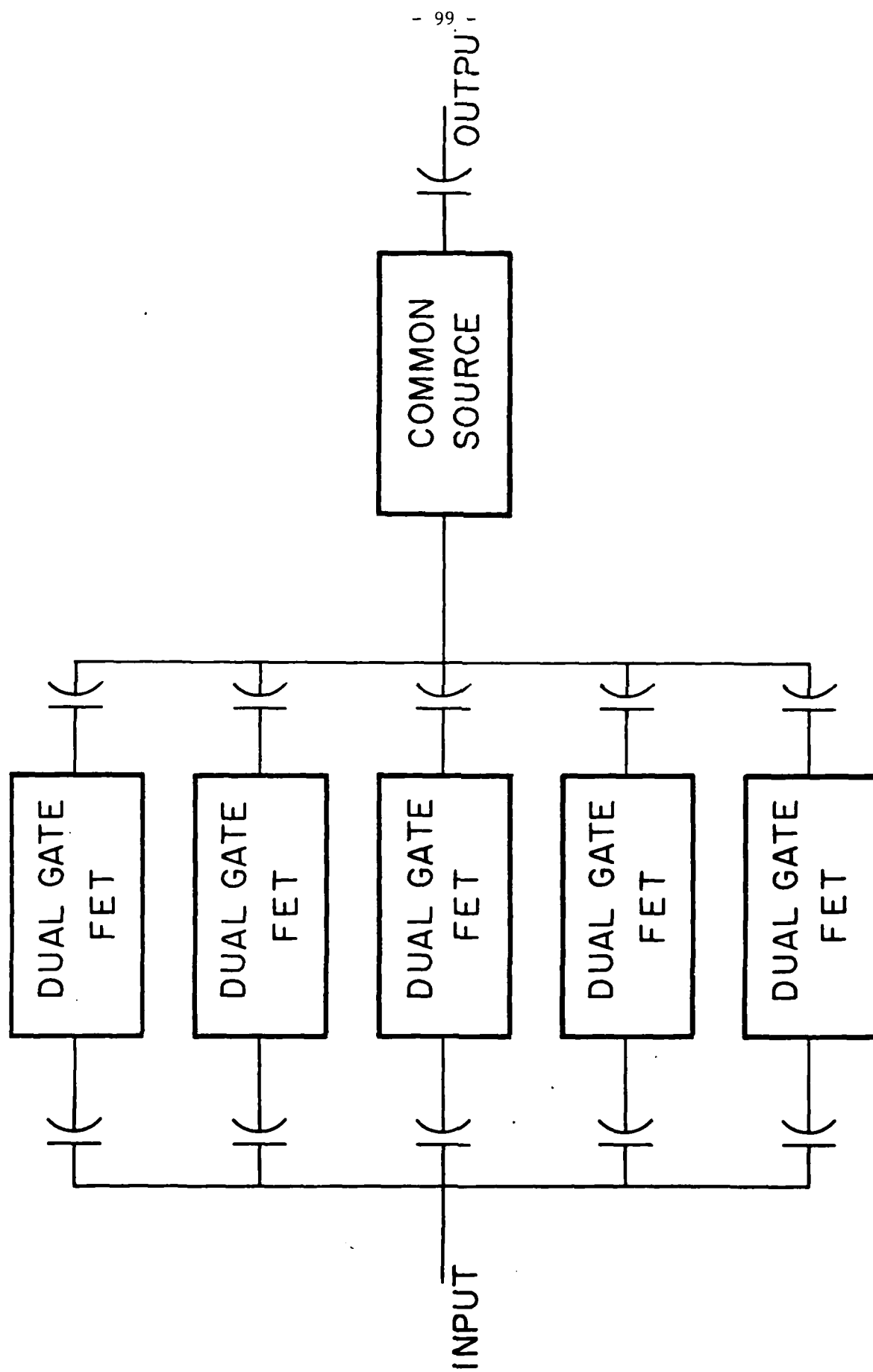


Figure 7. High-frequency preamplifier.

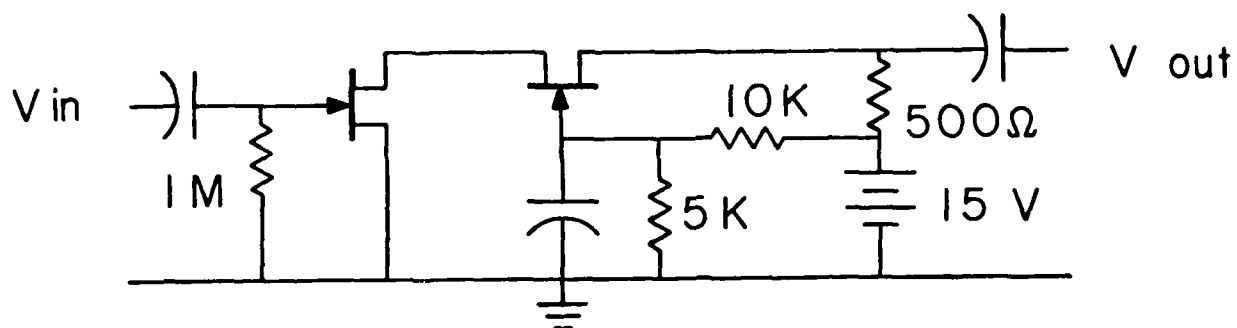


Figure 8. a) One stage of the amplifier.

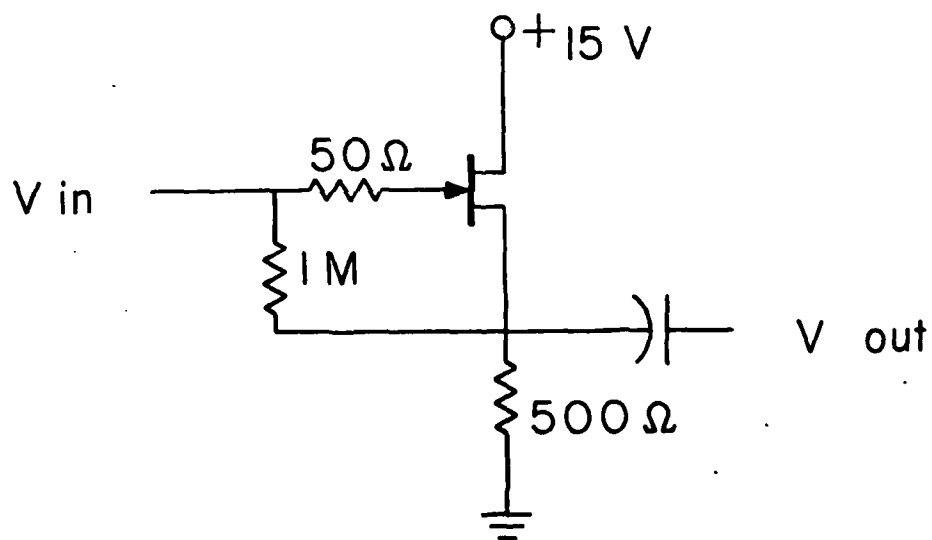


Figure 8. b) Output stage.

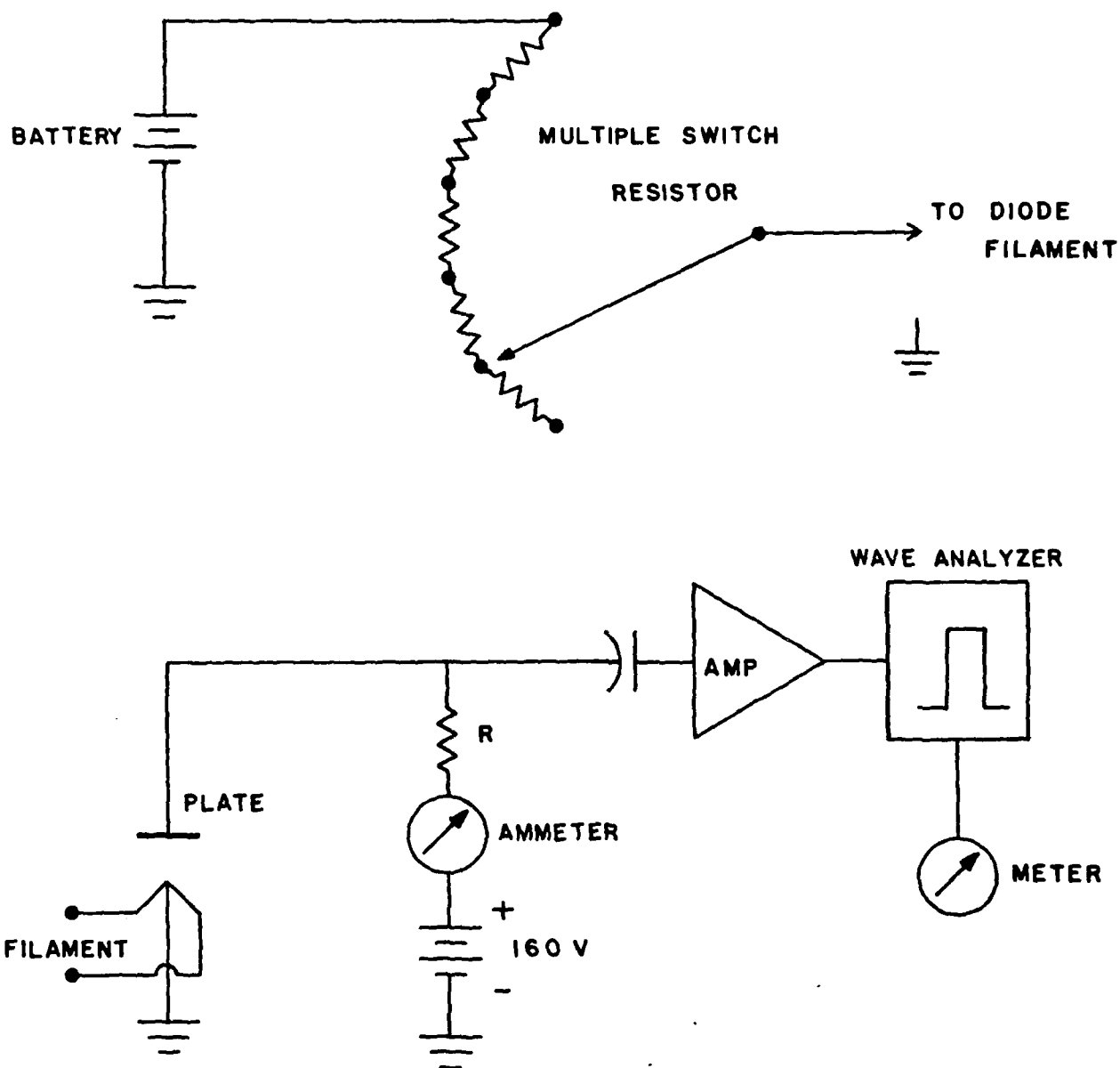


Figure 9. Standard noise source.

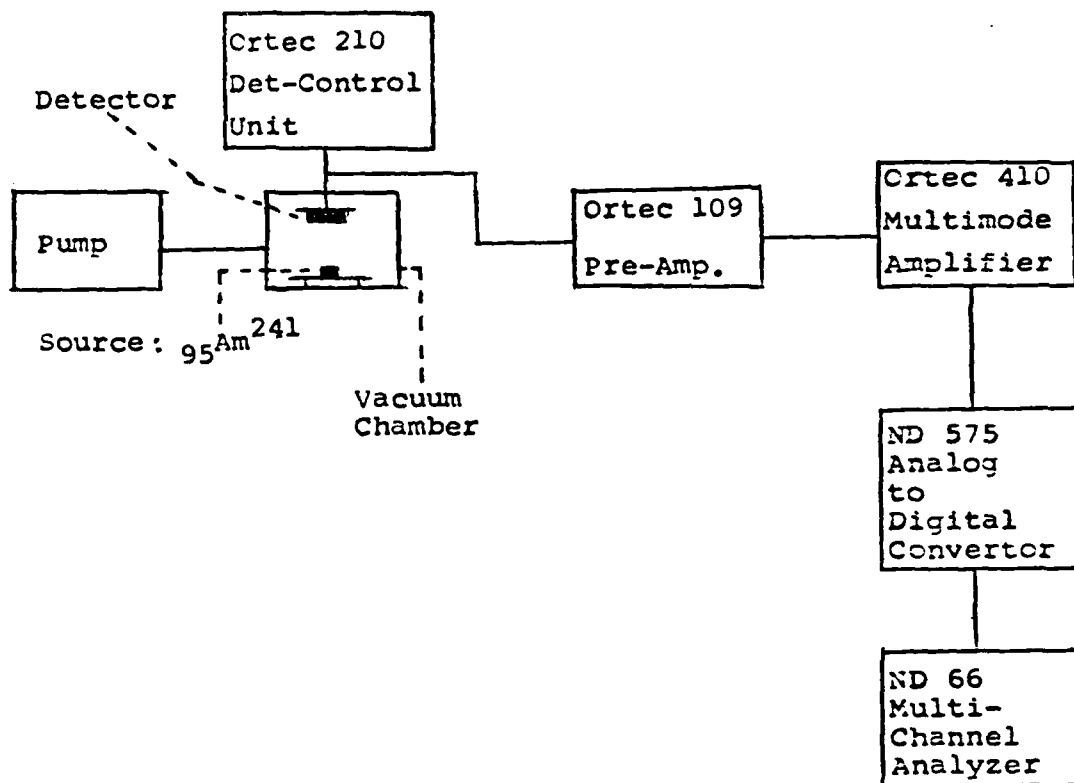


Figure 10. Block diagram of the counting system.

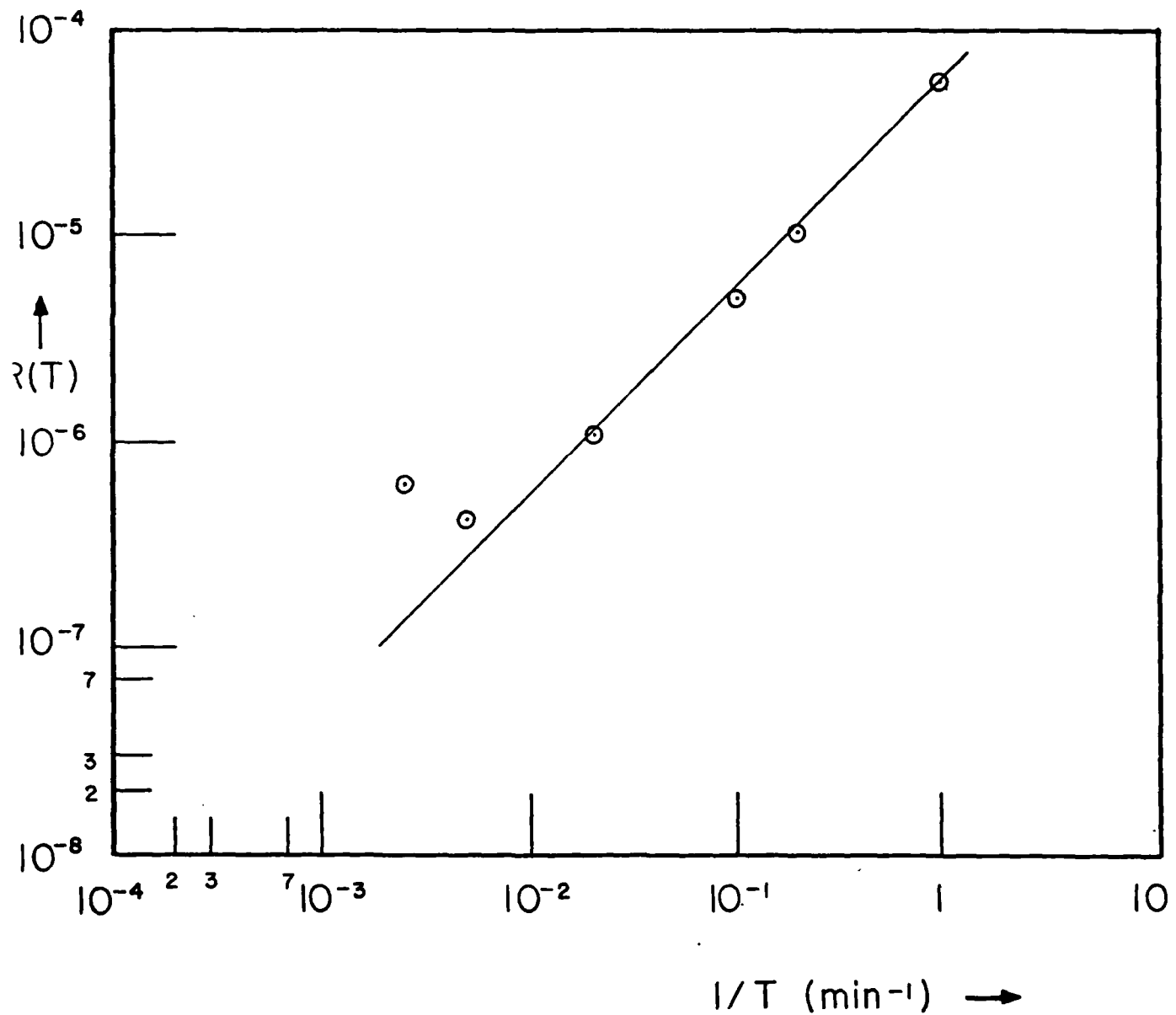


Figure 11. α -decay counting: $R(T)$ vs. $1/T$ (here $R(T)$ is relative Allan variance, T is counting time).

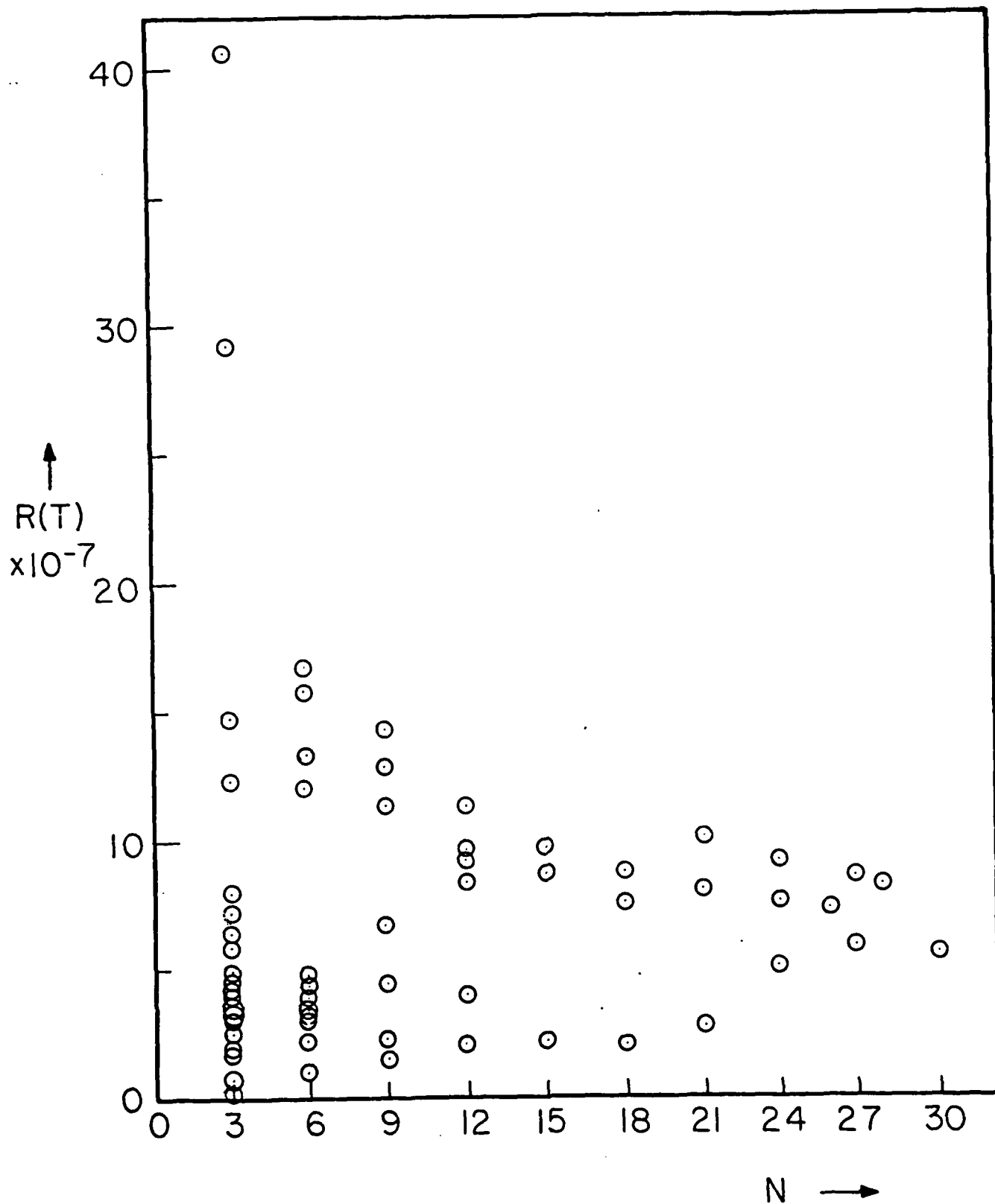


Figure. 12. $R(T)$ vs. N , where N is the number of samples of ρ ratio T $T = 100$ minutes.

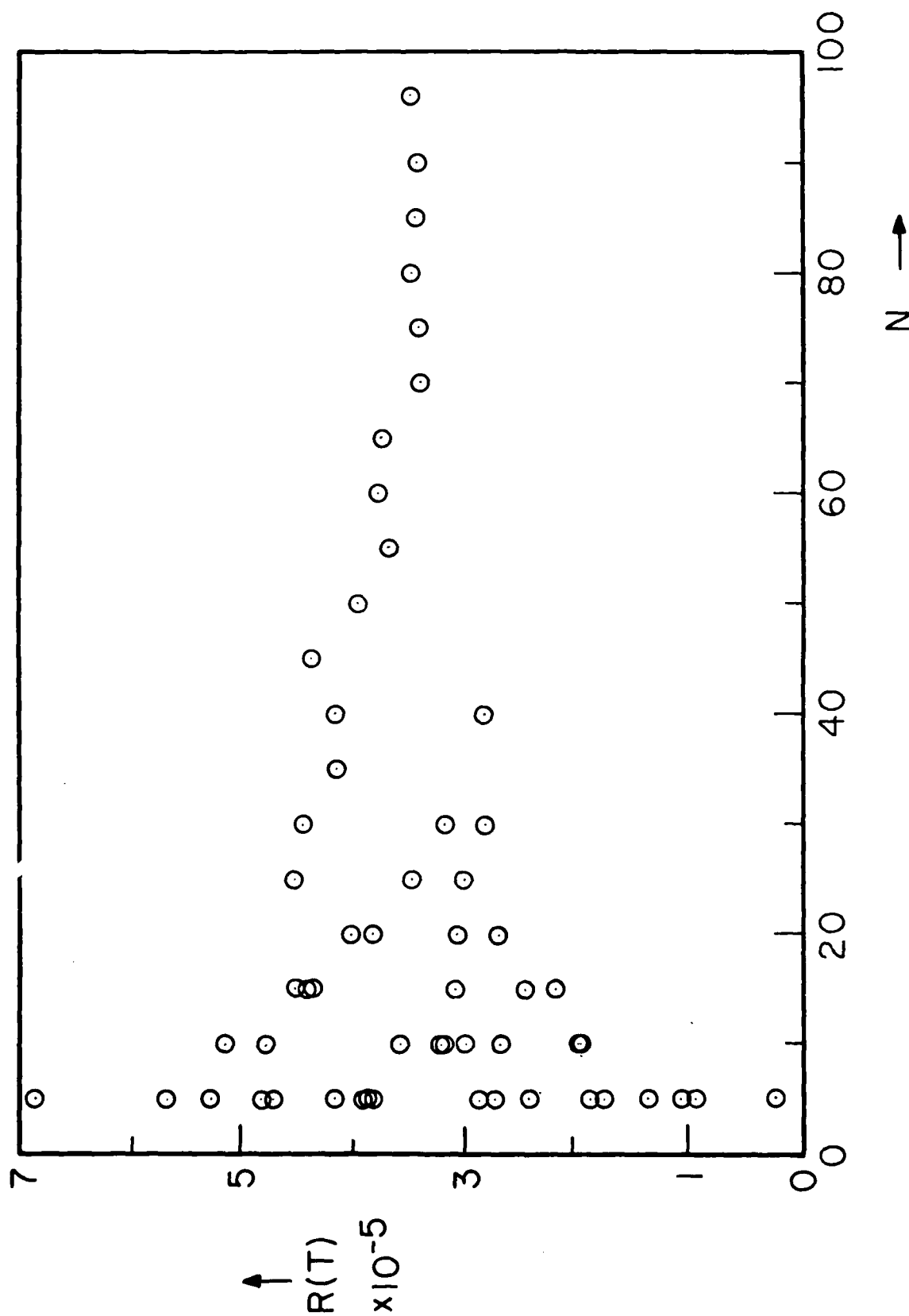


Figure 13. $R(T)$ vs. N ; $T = 1$ minute.

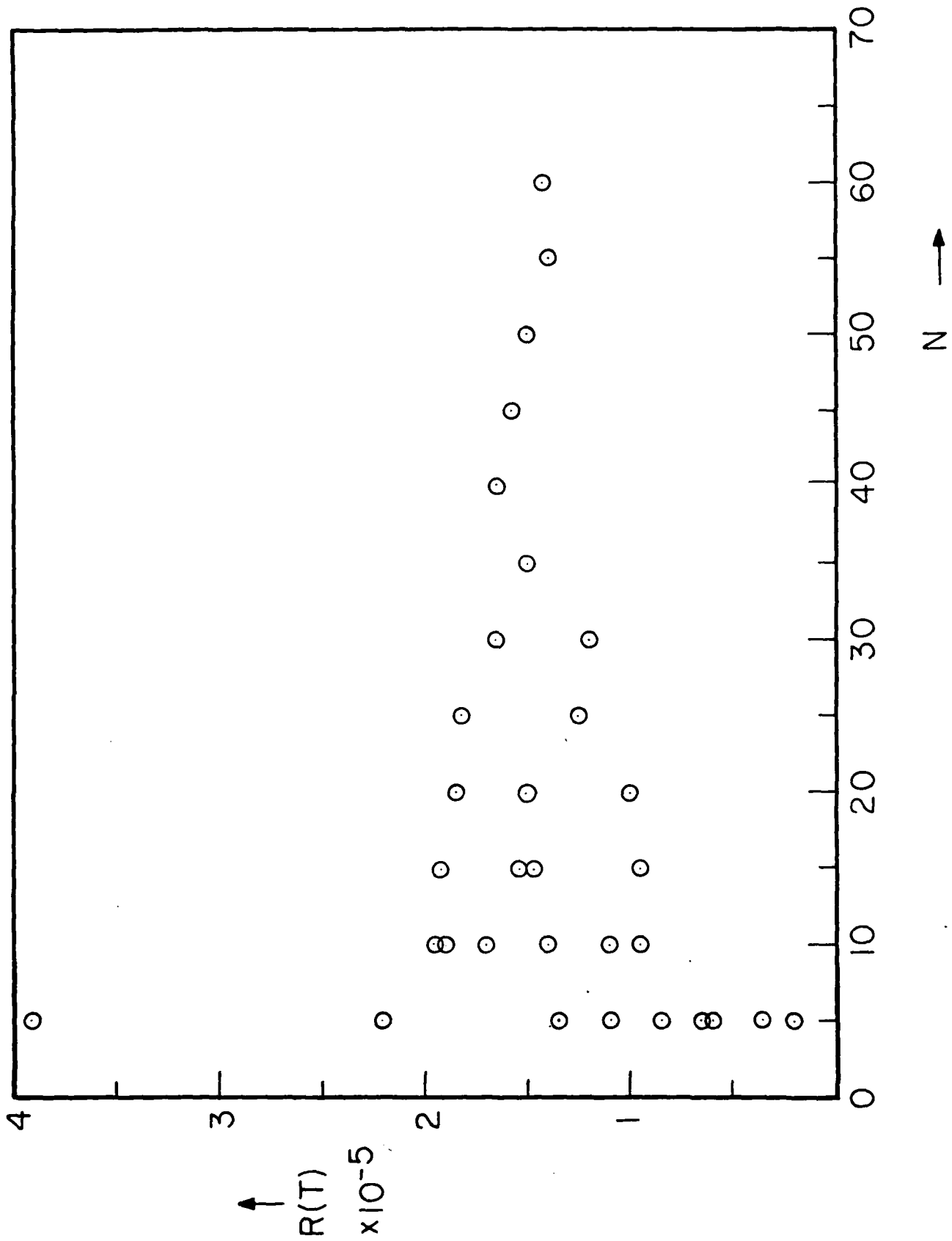


Figure 14. $R(T)$ vs. N ; $T = 3$ minutes.

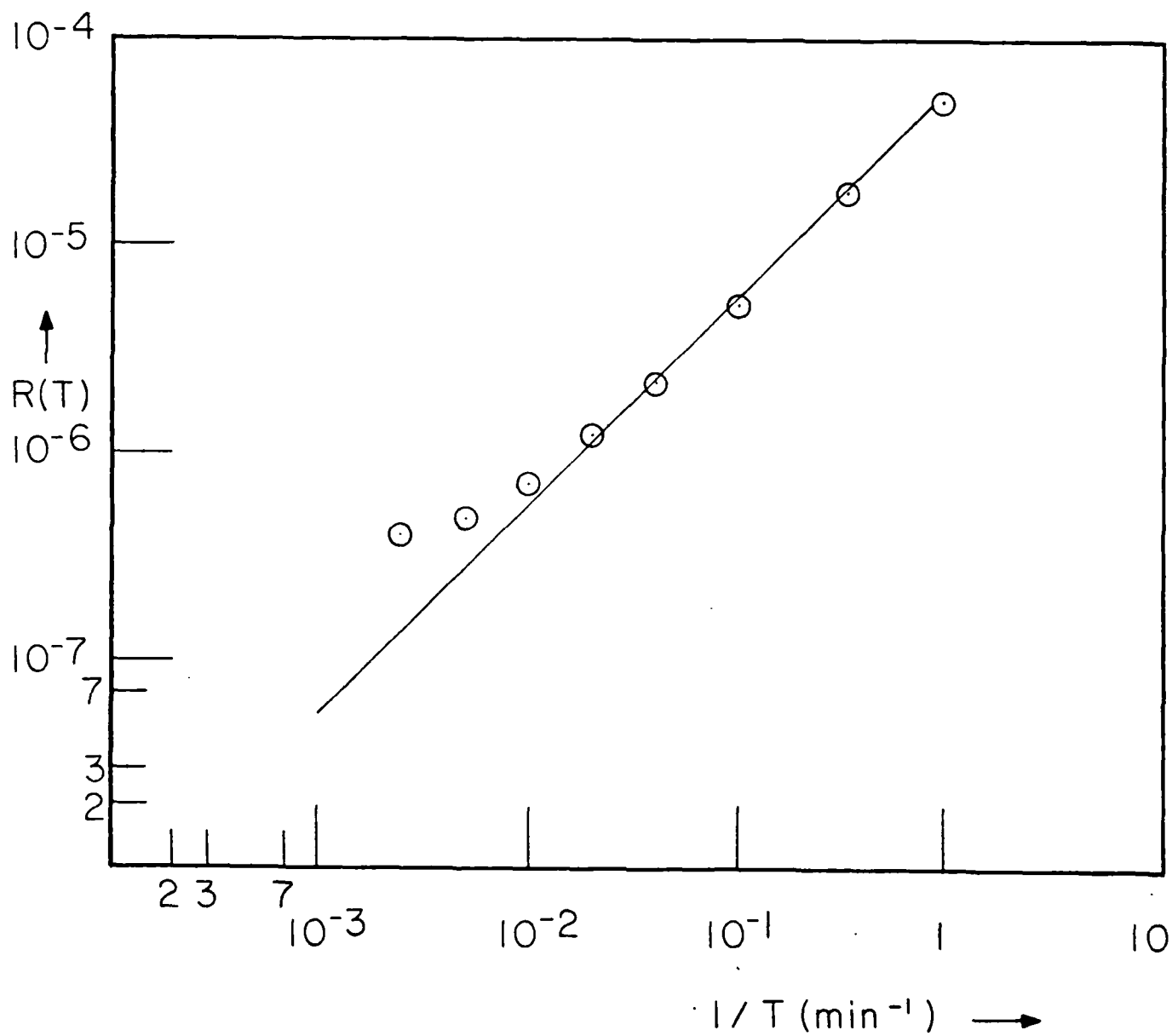


Figure 15. Averaged $R(T)$ vs. $1/T$. The straight line is Poissonian noise; the deviation is due to $1/f$ noise.

Δ $\sigma_{M_T}^2$ (Normal Variance)

\circ $\sigma_{M_T}^{A^2}$ (Allan Variance)

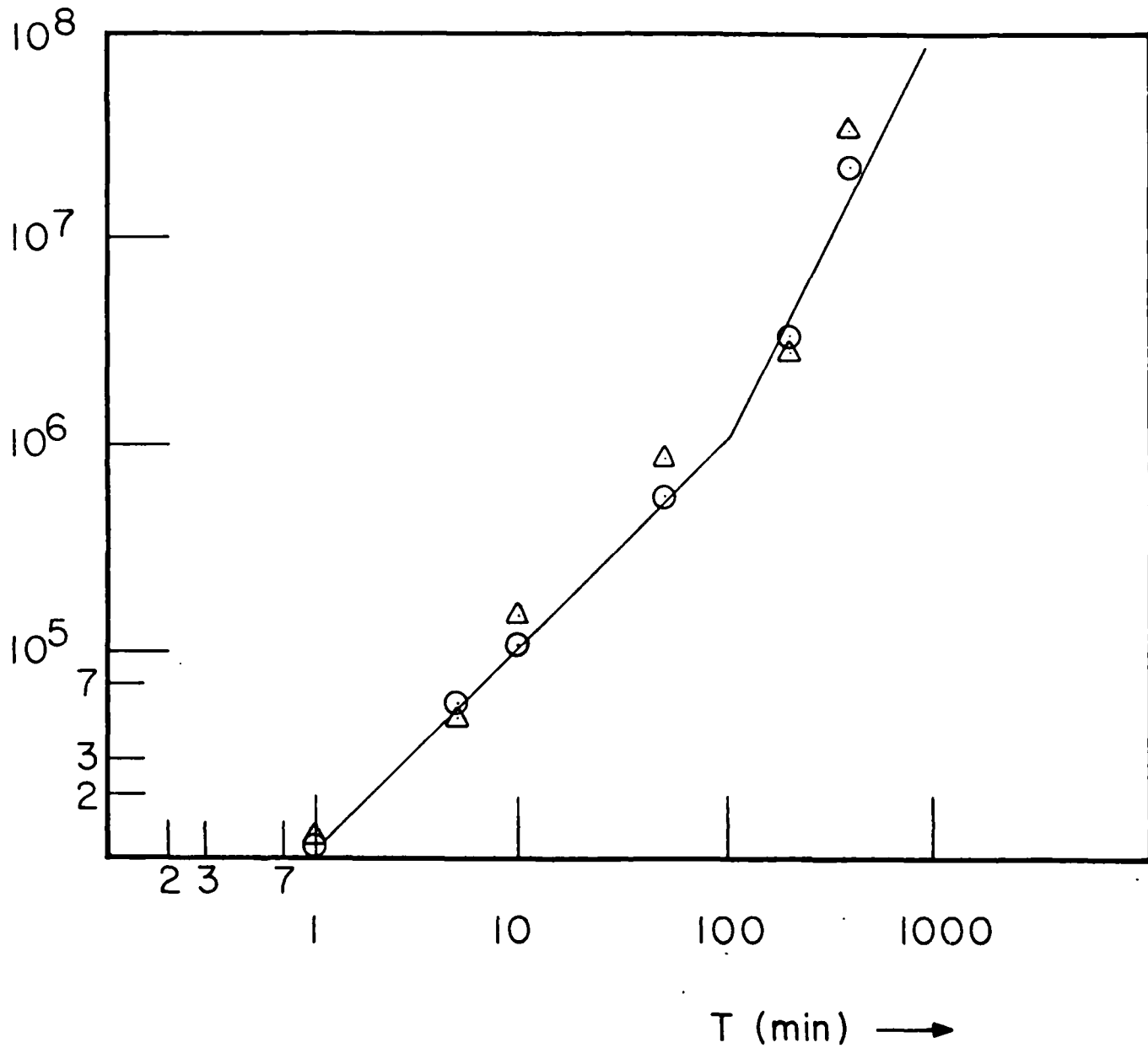


Figure 16. The variance ($\sigma_{M_T}^2$) and the Allan variance ($\sigma_{M_T}^{A^2}$) vs. T.

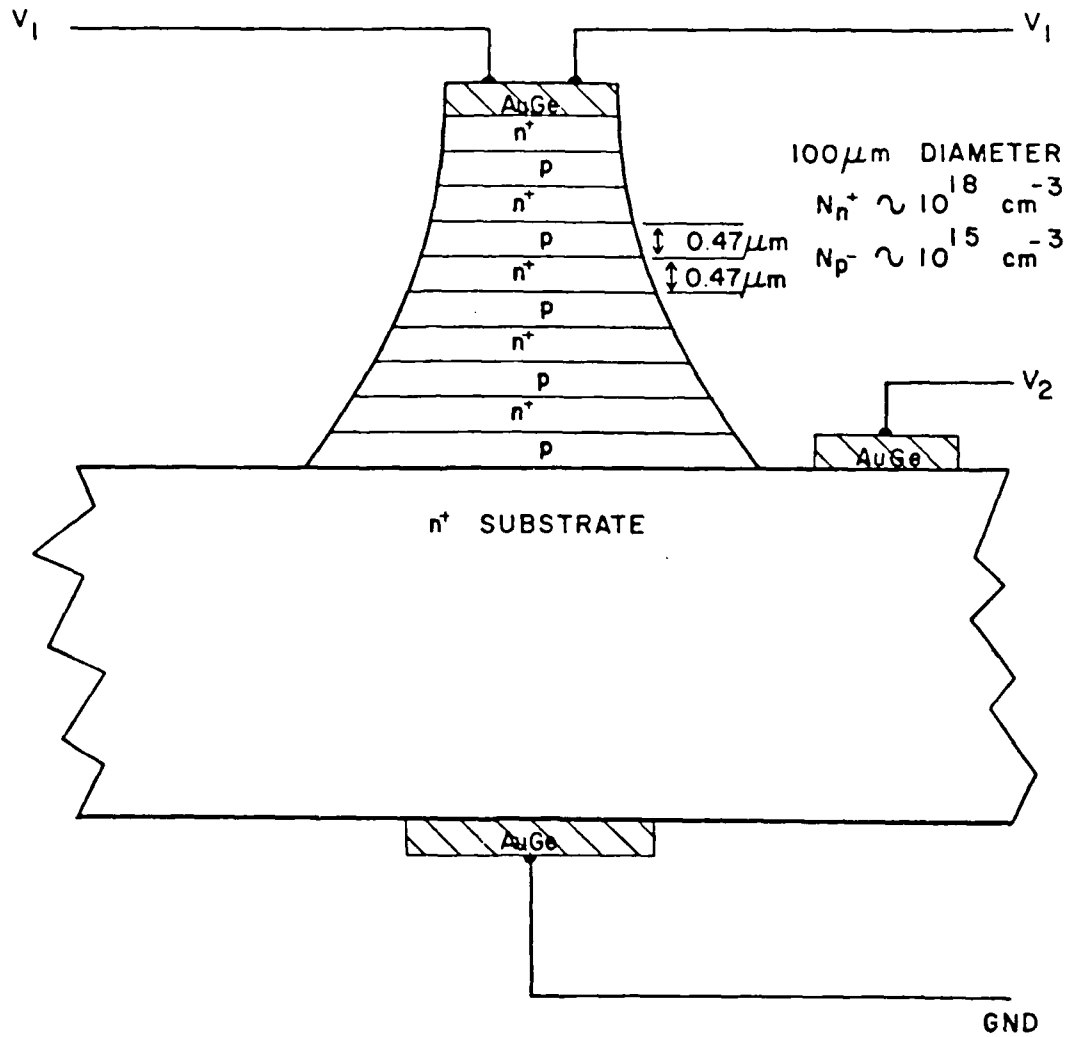


Figure 17. P-type near-ballistic mesa structure.

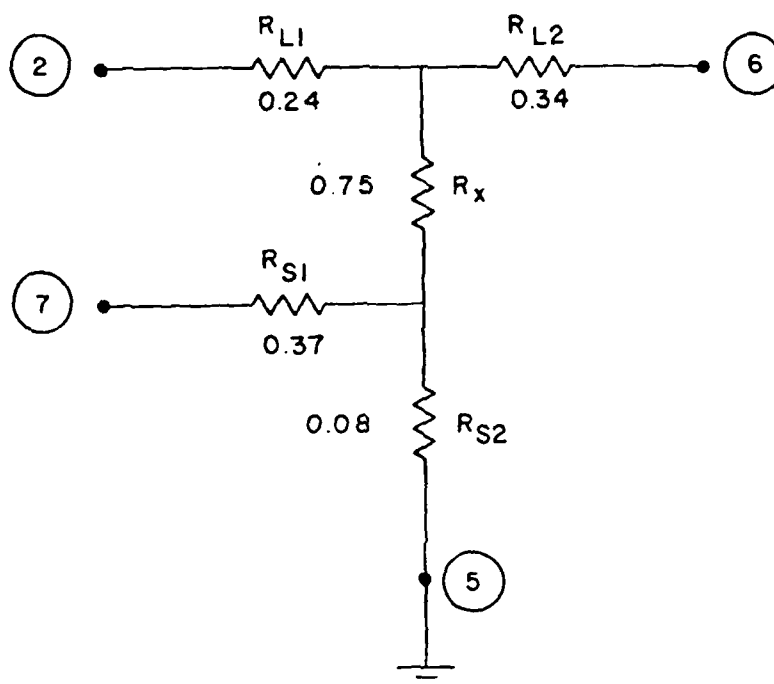


Figure 18. Equivalent circuit of n^+nn^+ structure, showing parasitic elements. R_{L1} , R_{L2} are lead resistances, R_{S1} is the lateral substrate resistance, while R_{S2} is the bulk substrate resistance. R_x is the device resistance. Terminals 2 and 6 are connected with the top of the mesa, terminal 7 is connected with the top of the substrate, while terminal 5 is connected with the bottom of the substrate.

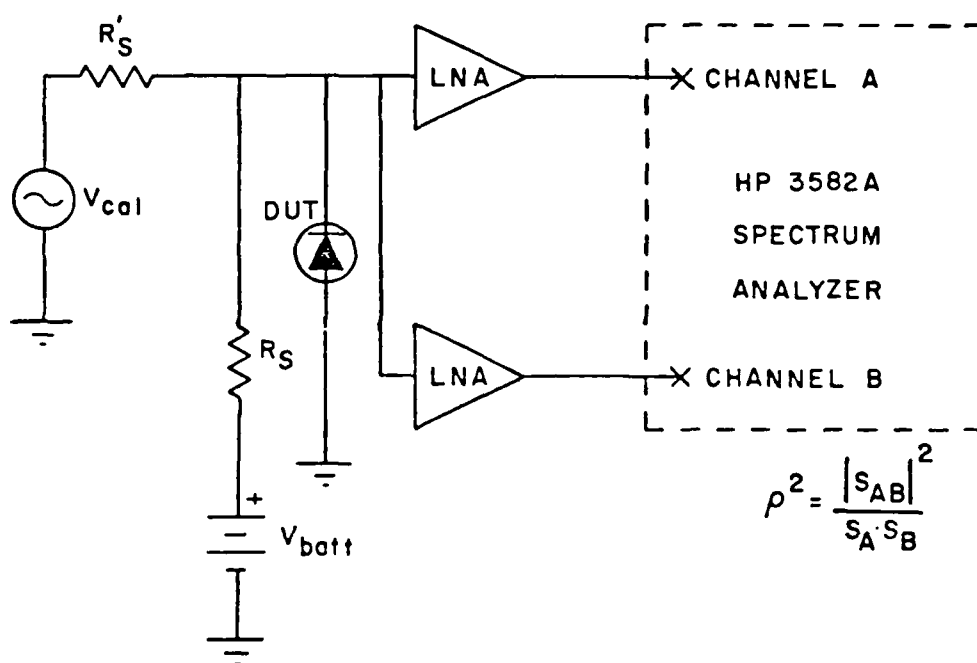


Figure 19. Correlation measurement setup.

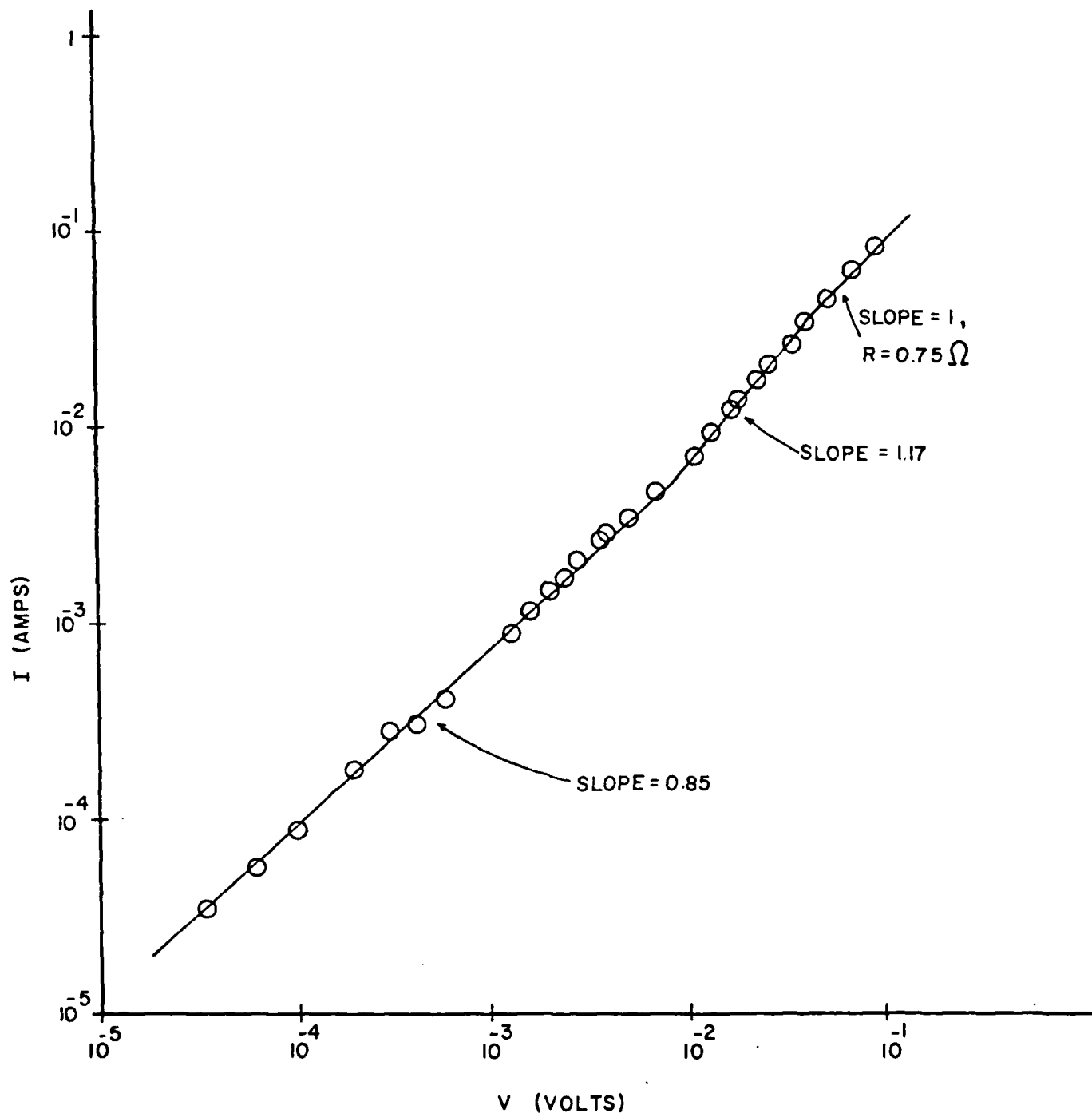


Figure 20. I-V characteristic n^+nn^+ device.

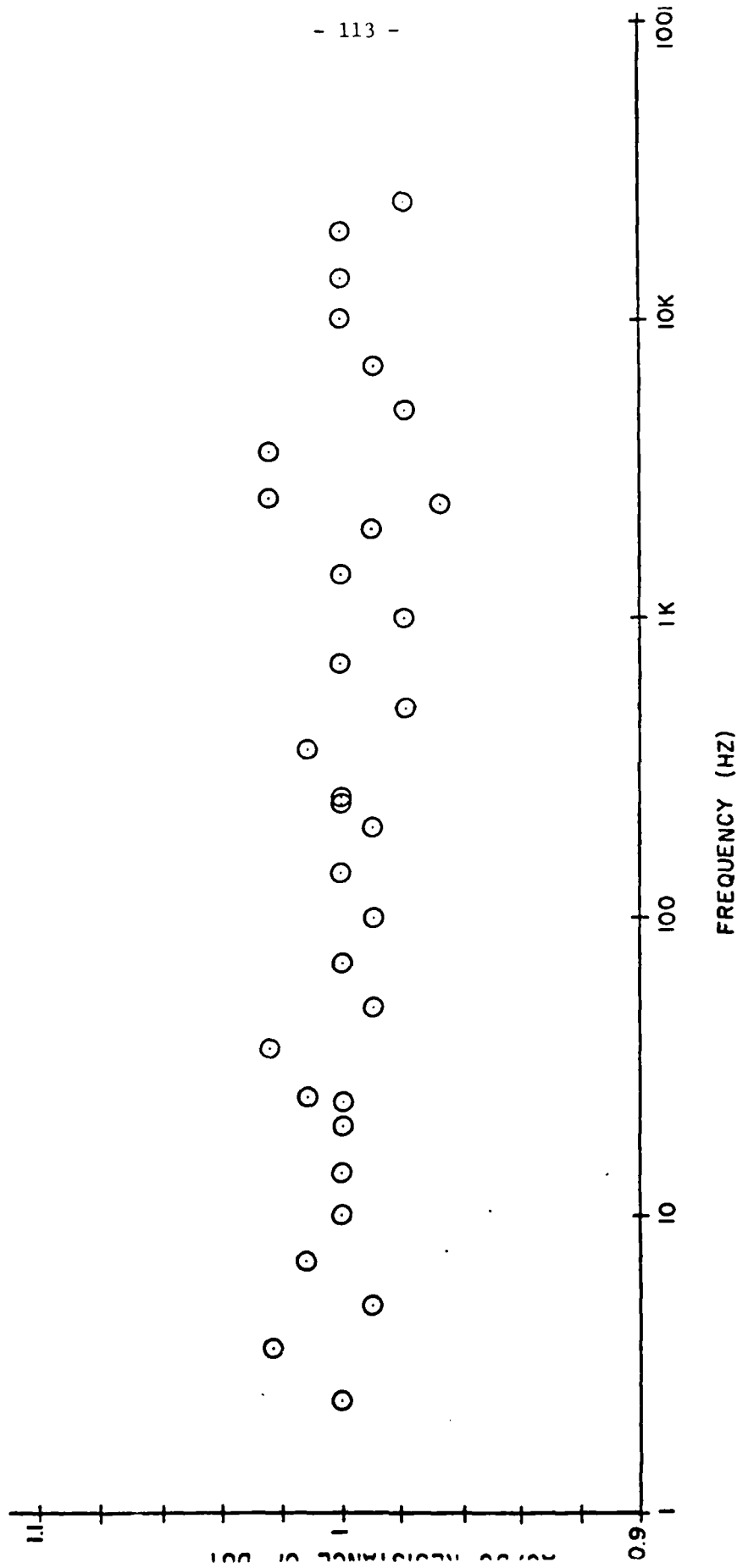


Figure 21. A.C. resistance of n n⁺ device versus frequency.

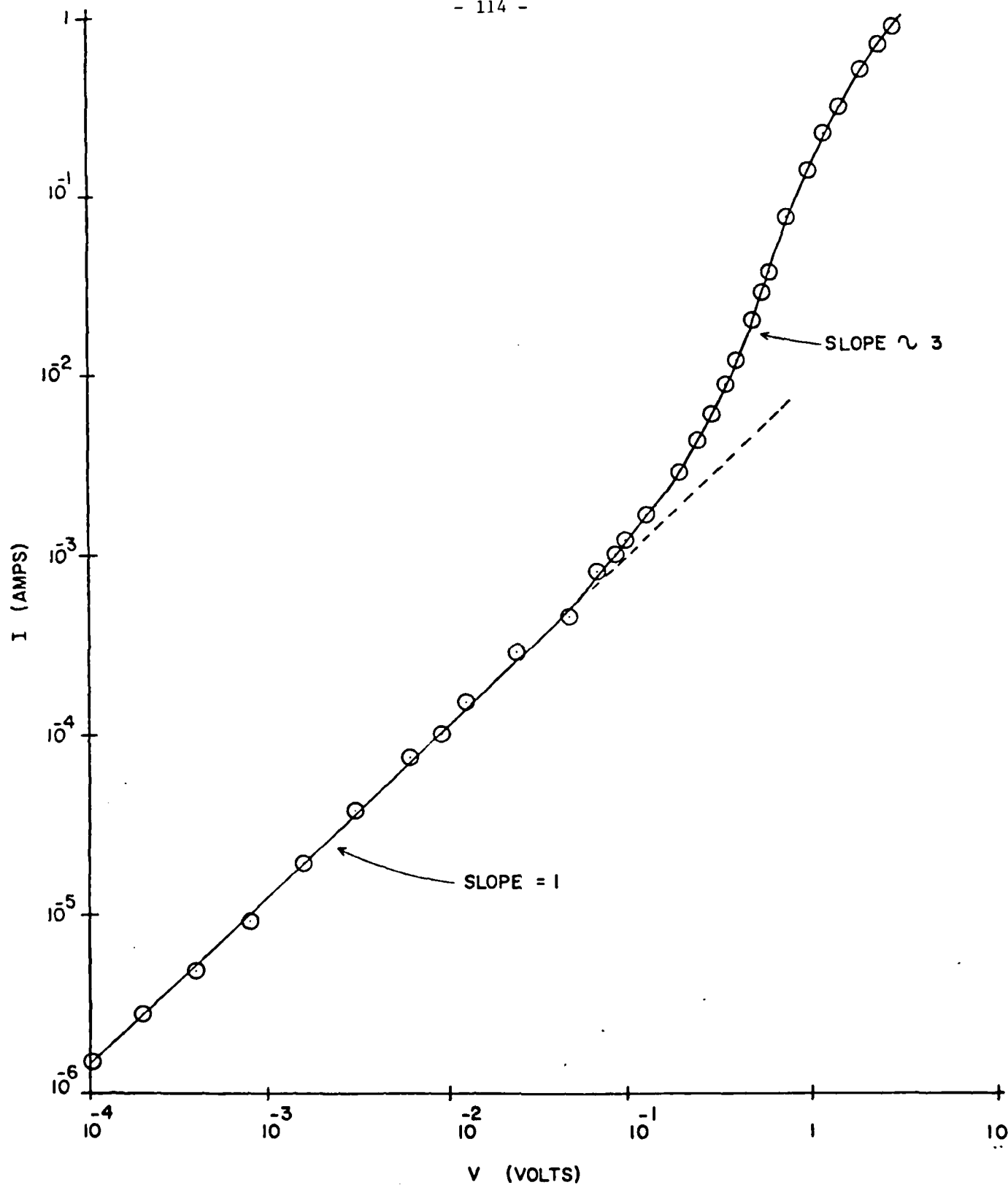


Figure 22. I-V characteristic of n^+pn^+ device.

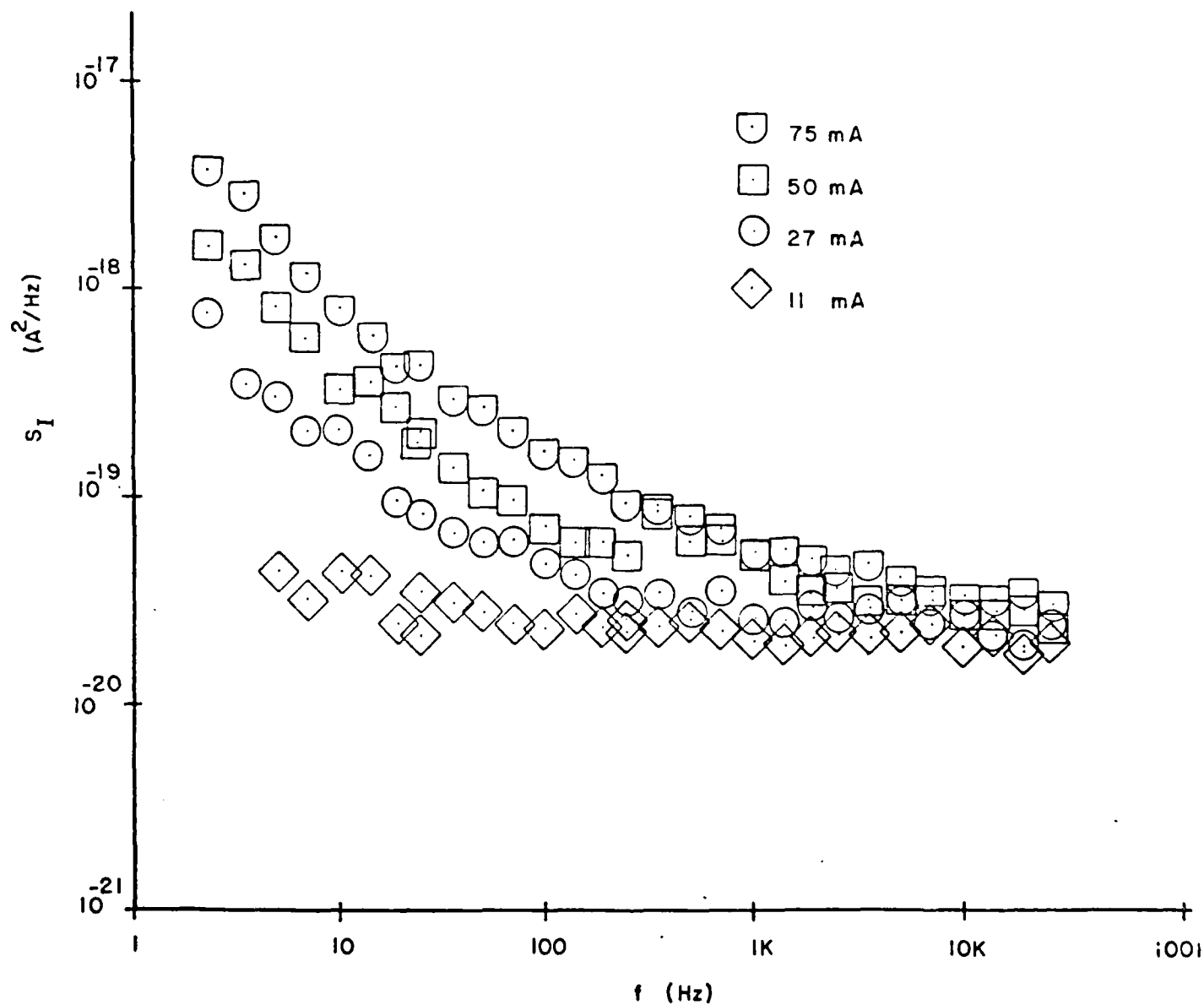


Figure 23. Noise spectra for n^+nn^+ device.

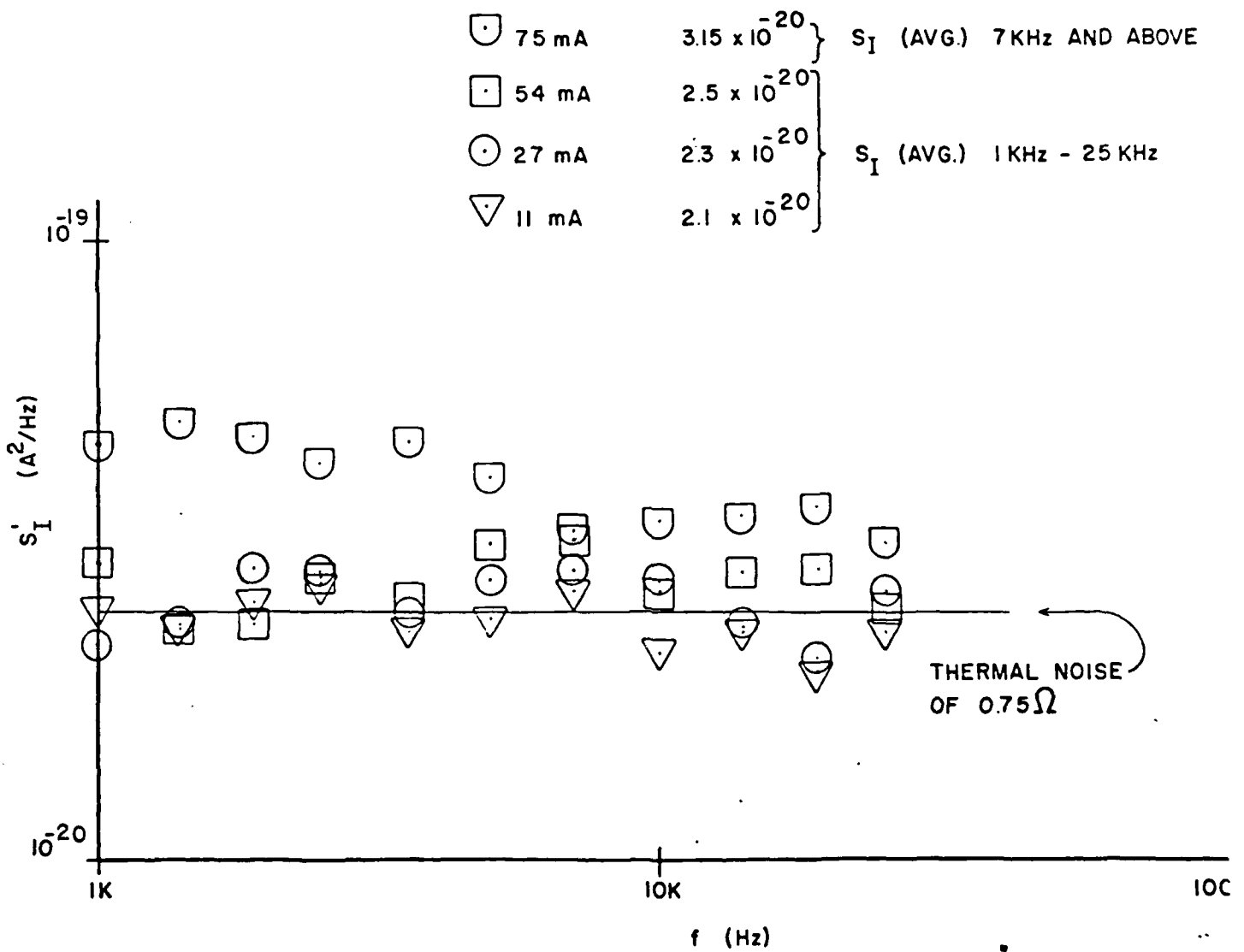


Figure 24. Thermal (-like) noise for $n^+ n n^+$ device.

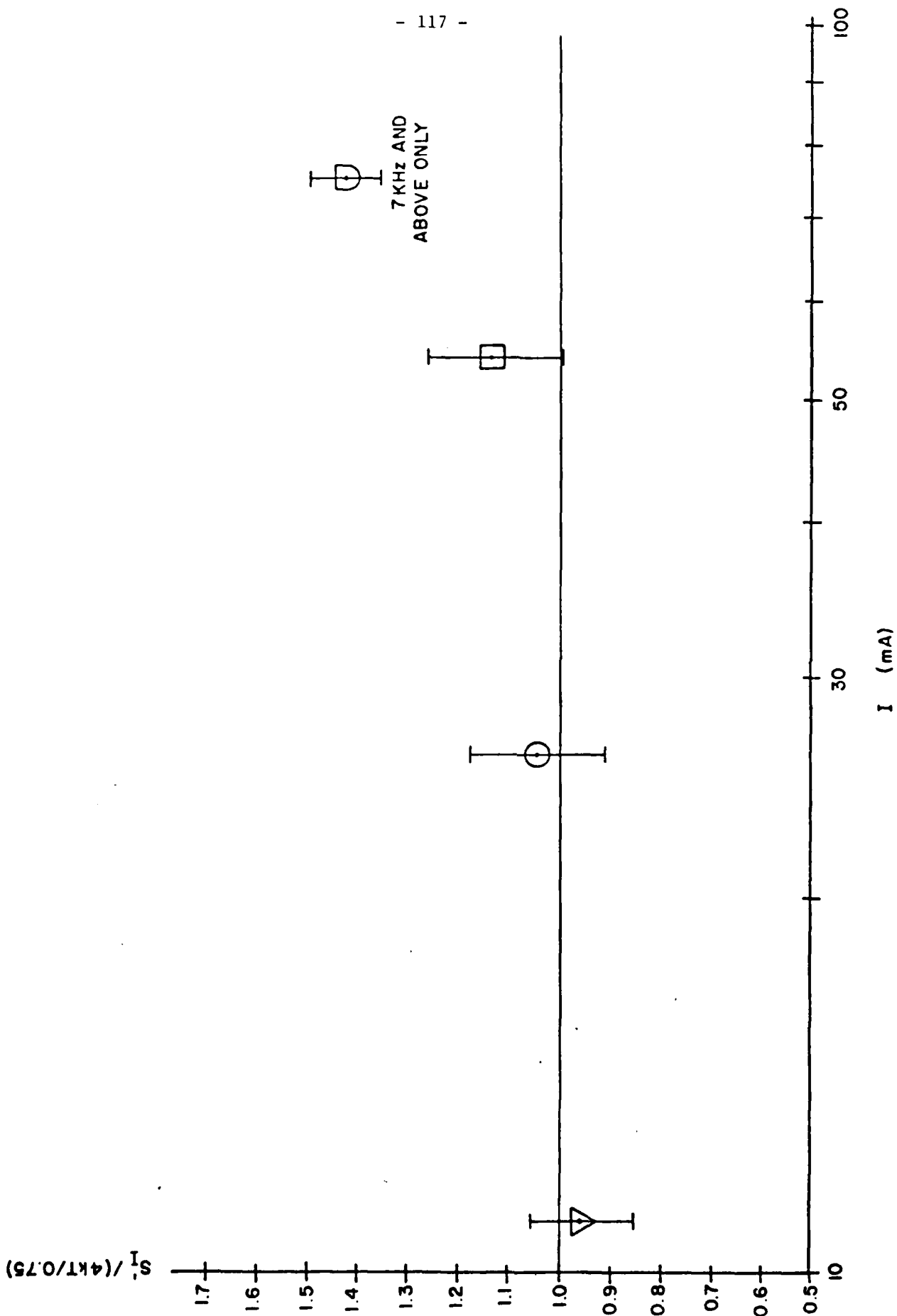


Figure 25. Plot of thermal (-like) noise of n^+n^+ diode versus diode current.

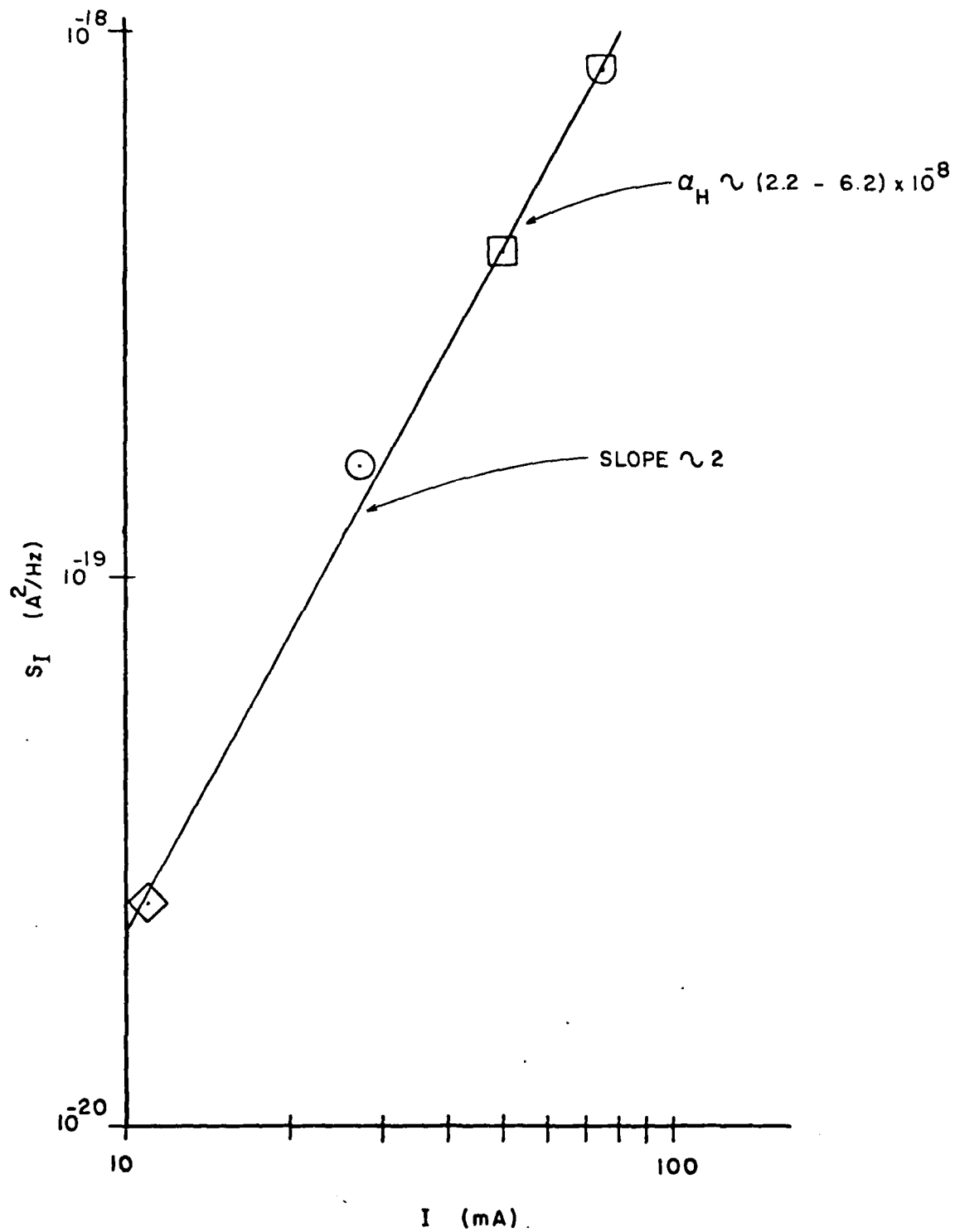


Figure 26. 1/f noise of n^+nn^+ diode versus current.

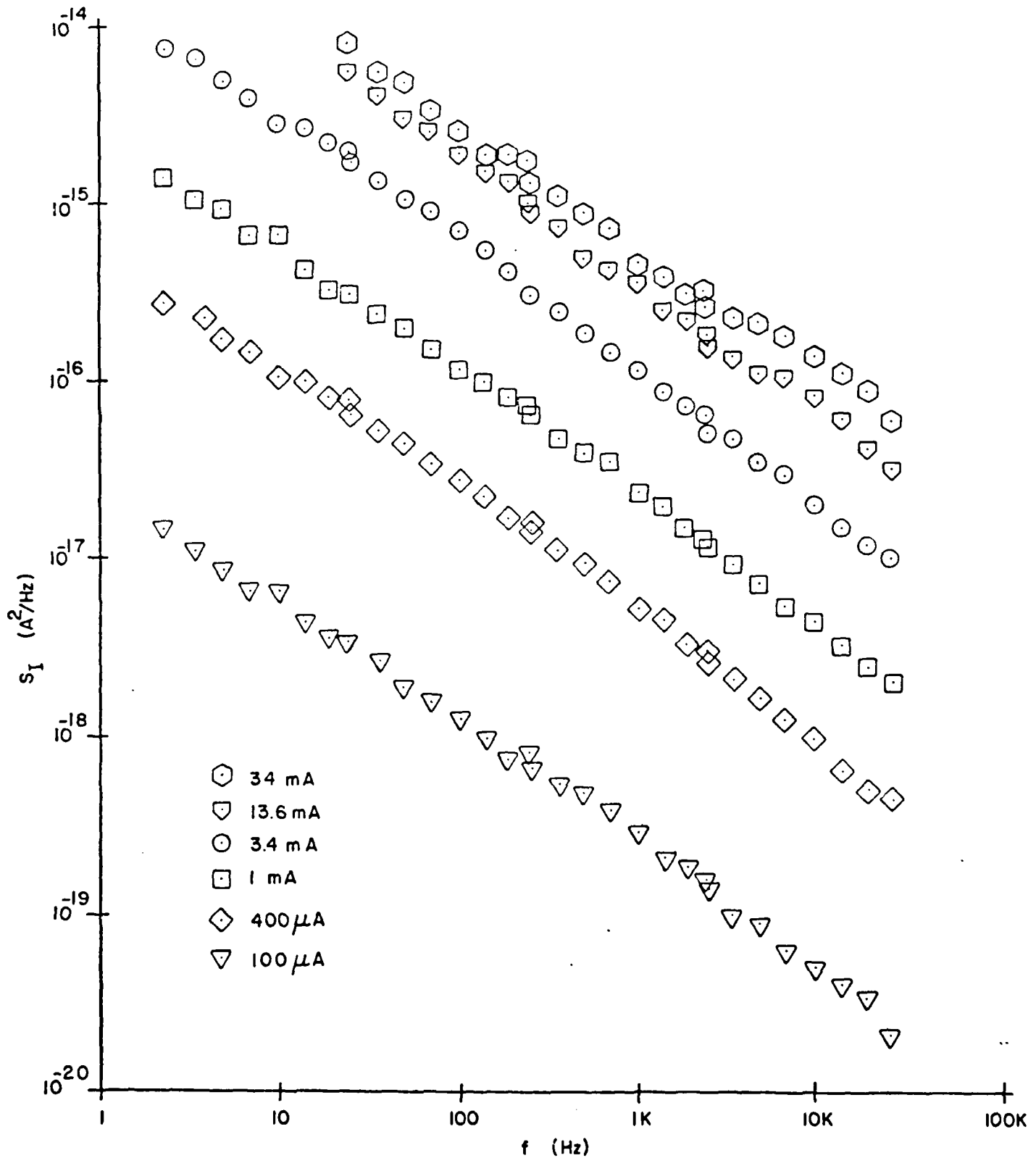


Figure 27. Noise spectra for $n^+p n^+$ device.

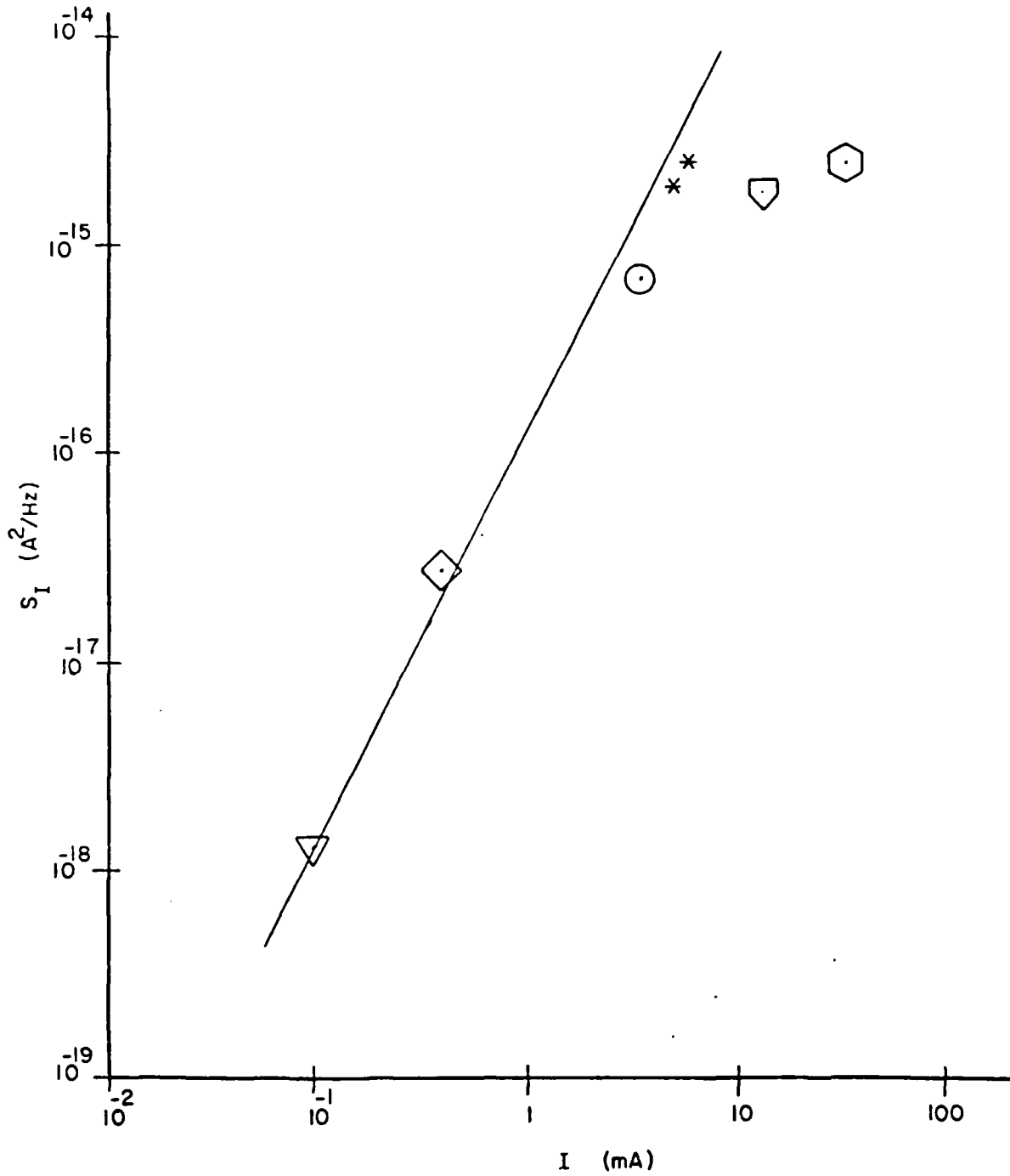


Figure 28. Noise at 100 hz of $n^+p n^+$ device versus current. (The ** points are obtained from ∇ and \hexagon points if the abscissa denotes only the punch-through current.)

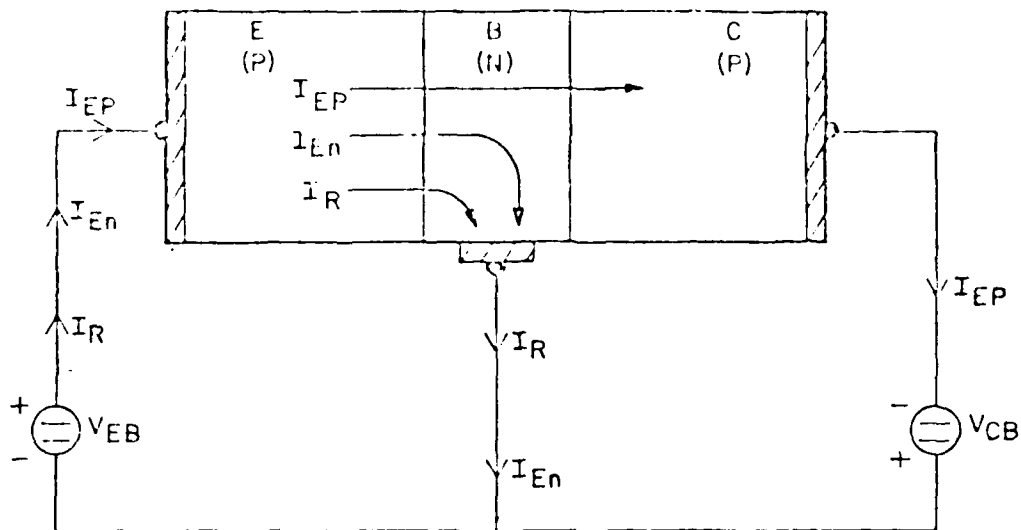


Figure 29. a) Current flow in a p^+-n-p transistor.

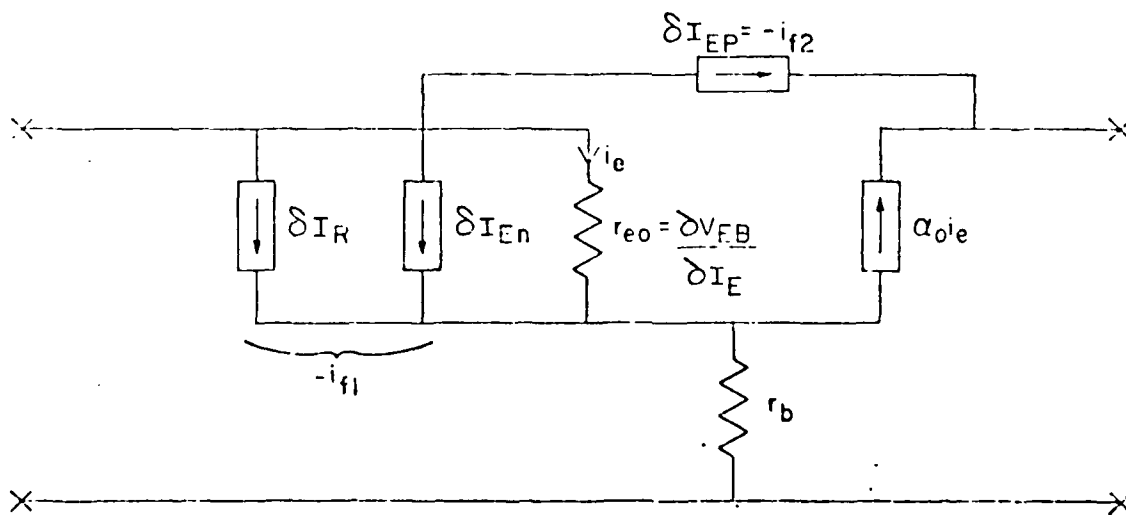


Figure 29. b) Equivalent circuit for the fluctuating current generators.

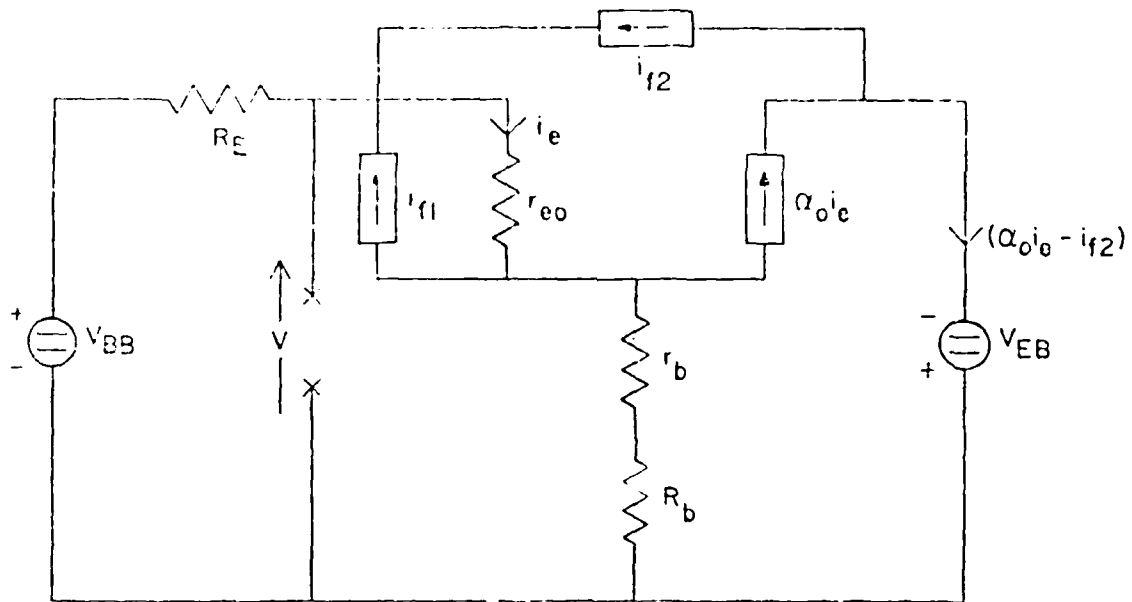


Figure 30. Plumb-Chenette schematics for discriminating between i_{f1} and i_{f2} .

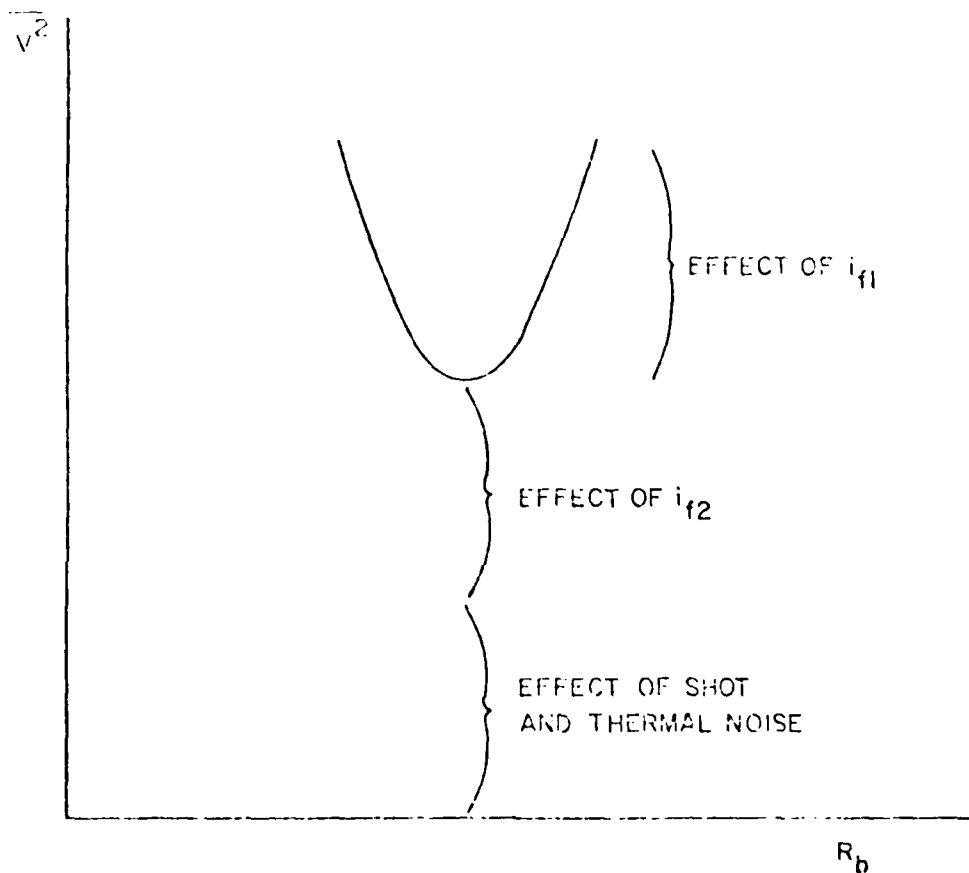


Figure 31. Splitting $\overline{v^2}$ into component parts representing the effects of i_{f1} , i_{f2} and of shot and thermal noise.

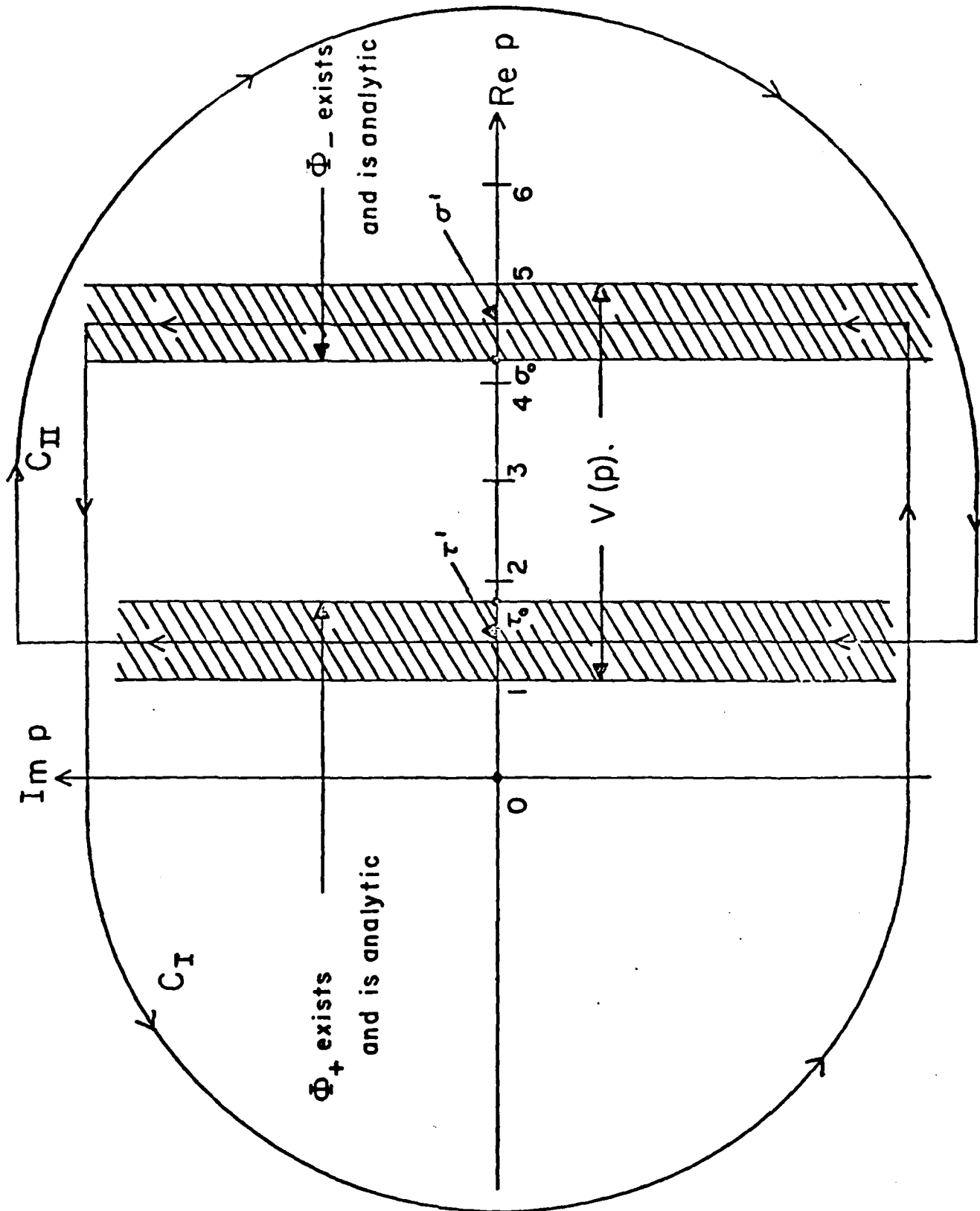


Figure 32. Contour integration for inverse Mellin transforms. Shaded area is domain of analyticity for the transformed equation (4.7). Case $\tau_0 < \sigma_0$.

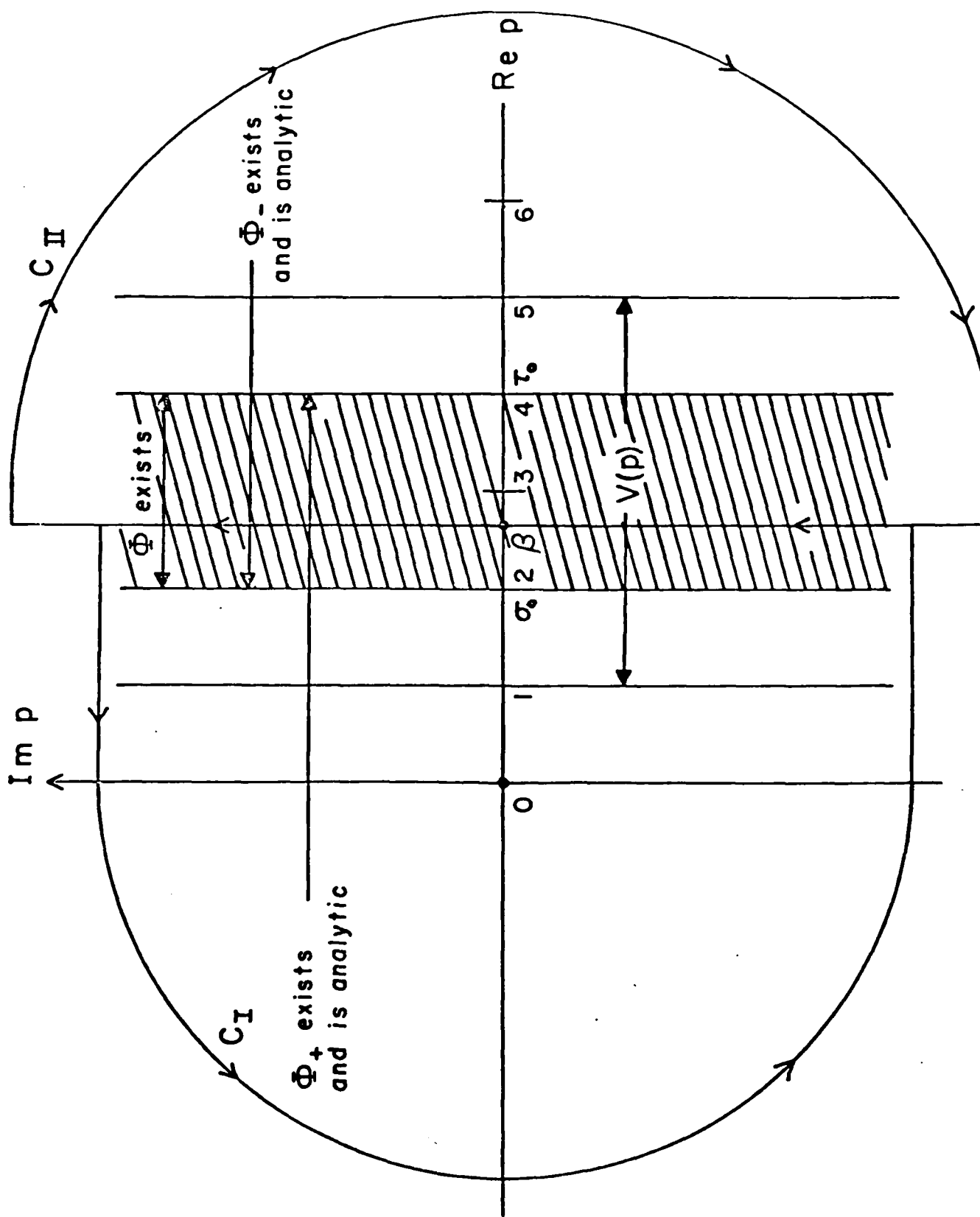


Figure 33. Contour integration for inverse Mellin transform. Shaded area is area of existence for $\phi(p)$. Case $\sigma_0 < \tau_0$.